REAL TIME ANALYSIS
OF
PROTEIN ADSORPTION

REAL TIME ANALYSIS OF PROTEIN ADSORPTION

By

RENA MARIE CORNELIUS, B. Eng.

A Thesis
Submitted to the School of Graduate Studies
in Partial Fulfilment of the Requirements
for the Degree
Master of Engineering

McMaster University

September 1988

MASTER OF ENGINEERING (1988) McMaster University
(Chemical Engineering) Hamilton, Ontario

Title:	Real Time Analysis of Protein Adsorption
Author:	Rena Marie Cornelius, B. Eng. (McMaster University)
Supervisor:	Professor J. L. Brash
Number of Pages:	xvi, 153

Abstract

An experimental method for monitoring the adsorption of proteins in real time has been developed and is the topic of this thesis.

Proteins were radioactively labeled using ^{125}I and injected at a constant flow rate into a well stirred glass cell containing buffer and the adsorbing surface in particle form. The buffer contained in the cell was gradually displaced by the protein solution. NaI(Tl) detectors, coupled to a multichannel analyzer and high voltage power supply, were placed at the exit of the cell to monitor the radioactivity of the bulk solution. Adsorption of the protein was determined by depletion of protein in the bulk solution.

A process to treat the surface of the cell and the glass tubing so as to prevent adsorption was developed and implemented prior to the flow experiments. This procedure involved exposing the cell and glass tubing to a 1 mg/mL fibrinogen solution for two hours at room temperature. The cell and tubing were then placed in an oven for 10 minutes at 70° C. This procedure (referred to as the thermal treatment procedure) resulted in a non-adsorbing protein layer that appeared, from extensive experiments, to be irreversibly attached to the surface of the cell and tubing.

The adsorption of fibrinogen from a single component system, as well as from plasma, was studied using the experimental arrangement described above. Concentrations of fibrinogen in isotonic Tris, for the single component system, ranged from 40 mg/mL to 300 mg/mL. It was found from these

experiments that an initial, fairly rapid, adsorption of protein took place. Later the adsorption of protein slowed significantly.

The adsorption and subsequent desorption of fibrinogen from diluted plasma was also studied. Dilutions ranged from 1% to 20%. The results from these experiments are consistent with the model proposed by Vroman for plasma surface interactions.

ACKNOWLEDGEMENTS

The author of this thesis greatly appreciates the advice and guidance supplied by J. L. Brash. Appreciation is also extended to P. ten Hove and S. Mulzer for their technical discussions relating to this work.

Finally, a very special thanks to my husband B. J. Cornelius for his support and patience.

TABLE OF CONTENTS

LIST OF FIGURES

LIST OF TABLES

1.0 Introduction and Objectives

The adsorption of proteins to solid surfaces is important in any situation where solids are in contact with protein-containing fluids. These include food processing, where surfaces tend to become fouled by the deposited biofilm; biotechnology requiring mass culturing of cells on surfaces with an intervening protein "glue"; new delivery methods for protein drugs (e.g. insulin, human growth hormone, tissue plasminogen activator) in which the proteins are in contact with polymeric matrices; and implant situations of all kinds such as dental, ophthalmologic, orthopedic and cardiovascular. Protein adsorption occurring during blood contact is the particular interest of the present work. Such adsorption occurs within a few seconds of contact and is the first observable event. It is believed to provide the trigger for thrombus formation, a phenomenon which limits the usefulness of any device involving contact with blood. Thus it is believed that an understanding of protein adsorption is essential to the understanding and control of surface-induced thrombosis. Knowledge of protein adsorption will also be useful in the other fields mentioned above.

The purpose of this research project was to develop an experimental method for monitoring the adsorption of plasma proteins in real time. " Real time " refers to the on-line continuous monitoring of the adsorption of the protein as the process occurs. Most previous studies of adsorption by other researchers have involved exposing surfaces for a designated length of time to a protein solution, rinsing, and then determining the amount of adsorbed protein bound to the surface (often via protein radiolabeling). This type of experiment

may be described as "off-line" or "non real-time" and suffers from two major disadvantages. First, the time resolution is low: successive time intervals of less than about 30 seconds are difficult to accommodate. Thus more rapidly occurring events cannot be detected. Second, the requirement to rinse the surface prior to measuring adsorption introduces uncertainties since variable amounts of loosely bound protein may be lost.

The approach to real time in situ adsorption measurements used in the present work is based on the "serum replacement" process. Proteins were radioactively-labeled using ^{125}I and injected at a constant flow rate into a well stirred cell containing buffer and the adsorbing surface in particle form. By "serum replacement" the buffer is gradually replaced by the protein solution and the concentration of protein increases within the cell. At the same time adsorption of protein to the surface of the particles reduces the protein concentration in the cell. Application of a protein mass balance across the cell along with continuous measurement of protein concentration at the exit (assumed equal to the concentration within the cell on the basis of perfect mixing) allows determination of the kinetics of adsorption in situ and in real time. The resolution of the kinetic data is limited only by that of the measurement technique.

The glass tubing and the cell itself were coated with a thermally treated non-adsorbing protein layer that appeared, from extensive experiments, to be irreversibly attached to the surface. Thus changes in protein concentration within the cell were due only to mixing and adsorption to the particles. Moreover the measurement of solution radioactivity in a tubing segment at the cell exit was not compromised by adsorption to the walls of the tubing.

The main advantage of the experimental approach discussed in this report is that it allows for virtually continuous, real time measurements. In particular, measurements over very short time intervals can be made which could not, due to obvious physical limitations, be conducted using the more conventional off-line techniques. Detection of very rapid adsorption phenomena thus becomes possible. In addition the elimination of the rinsing step enables the determination of the true in situ adsorption, probably a combination of reversibly (loosely) and irreversibly (tightly) bound proteins.

The experimental method developed in the present work has proven particularly useful in the study of the rapid transient adsorption of fibrinogen from plasma, known as the Vroman effect. It is hoped that in the future this method can be used in the study of different aspects of the interactions of materials that come in contact with protein containing fluids.

2.0 Background

In order to understand and appreciate the importance of protein adsorption and the role it plays in blood compatibility, one must first have a general understanding of the normal haemostatic mechanism. This section of the report gives an outline of haemostasis with particular emphasis on blood coagulation. A more detailed discussion of protein structure and protein adsorption, with particular reference to the Vroman effect, is also given. Since radioiodinated proteins were used extensively to monitor the adsorption of proteins in real time, an overview of the principles of radiation dosimetry as well as a discussion of the protein iodination procedures currently used is provided.

2.1 Blood Material Interactions

It is well established that one of the first readily observable events occurring when blood comes into contact with a foreign surface is protein adsorption(1-3). Subsequent interactions of the blood with the adsorbed protein layer lead to blood coagulation, thrombus formation, and embolization. These are potentially catastrophic events resulting in heart attacks or strokes. Indeed, complications arising from blood surface interactions are responsible for many of the failures in vascular grafts, external arteriovenous shunts for blood access in haemodialysis, prosthetic heart valves, artificial heart assist devices and artificial hearts.

An outline of the processes that occur when blood comes into contact with a foreign surface is shown in Figure 1. The various pathways and the interactions between them are distinguished. It is of particular importance to note the role that protein adsorption plays in the coagulation process. Although

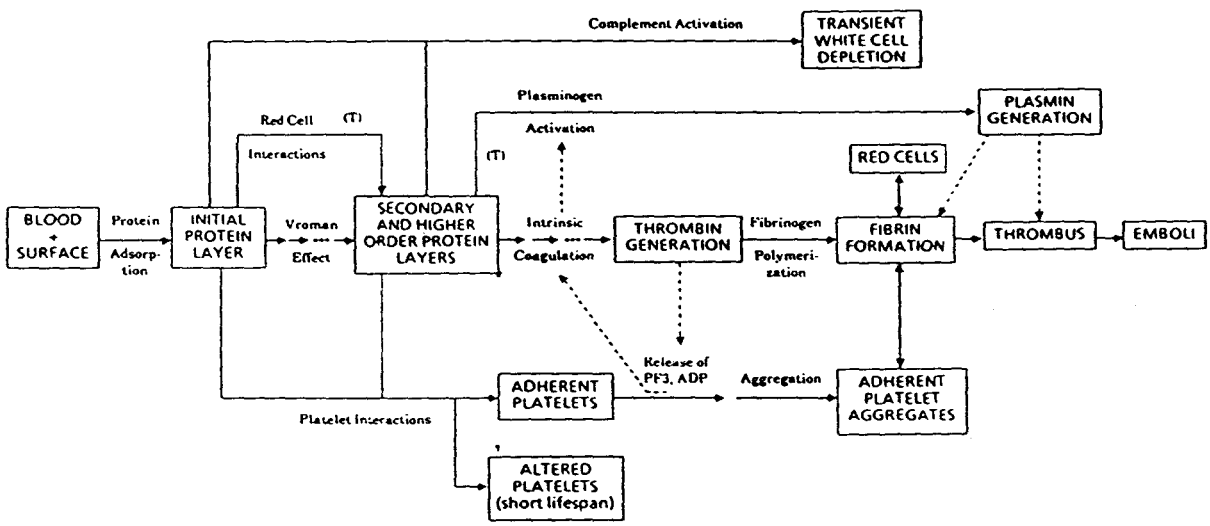

Figure 1. Schematic representation of the sequence of events that occur during blood material interactions(4).

the effects of white cells and platelets are not addressed in the present work, the importance of their role in the interactions of blood with a foreign surface should be recognized. Many of the other interactions, as shown in Figure 1, are discussed in the following pages of this report.

Protein adsorption and the subsequent events that occur lead to potentially serious problems when blood comes into contact with an artificial surface. This is particularly true of blood coagulation. However blood coagulation plays an essential role in the function of the normal haemostatic mechanism to arrest bleeding from an injured blood vessel, and to prevent blood loss from intact vessels (5,6). Injury to a vessel results in constriction of the vessel wall followed by the formation of a platelet plug at the injured site. The platelet plug provides a surface upon which blood coagulation occurs. Blood flow, natural plasma coagulation inhibitors and fibrinolysis prevent uncontrolled growth of the plug. When tissue repair is complete, fibrinolysis takes place resulting in the dissolution of the fibrin clot. In summary, haemostasis is achieved through the interactions of the vessel wall, platelets,and coagulation.

Blood coagulation, whether initiated by contact with an artificial surface or vessel injury, is a complex series of steps which ends in the formation of a fibrin clot (5,6). The series of steps occurs in a chain-like reaction which is often likened to a waterfall or cascade. Coagulation factors, platelets and calcium are required for coagulation to proceed. The coagulation process can occur via two pathways; the intrinsic pathway, which is a relatively slow process, and the extrinsic pathway, which is a much faster process (5,6) (see Figure 2).

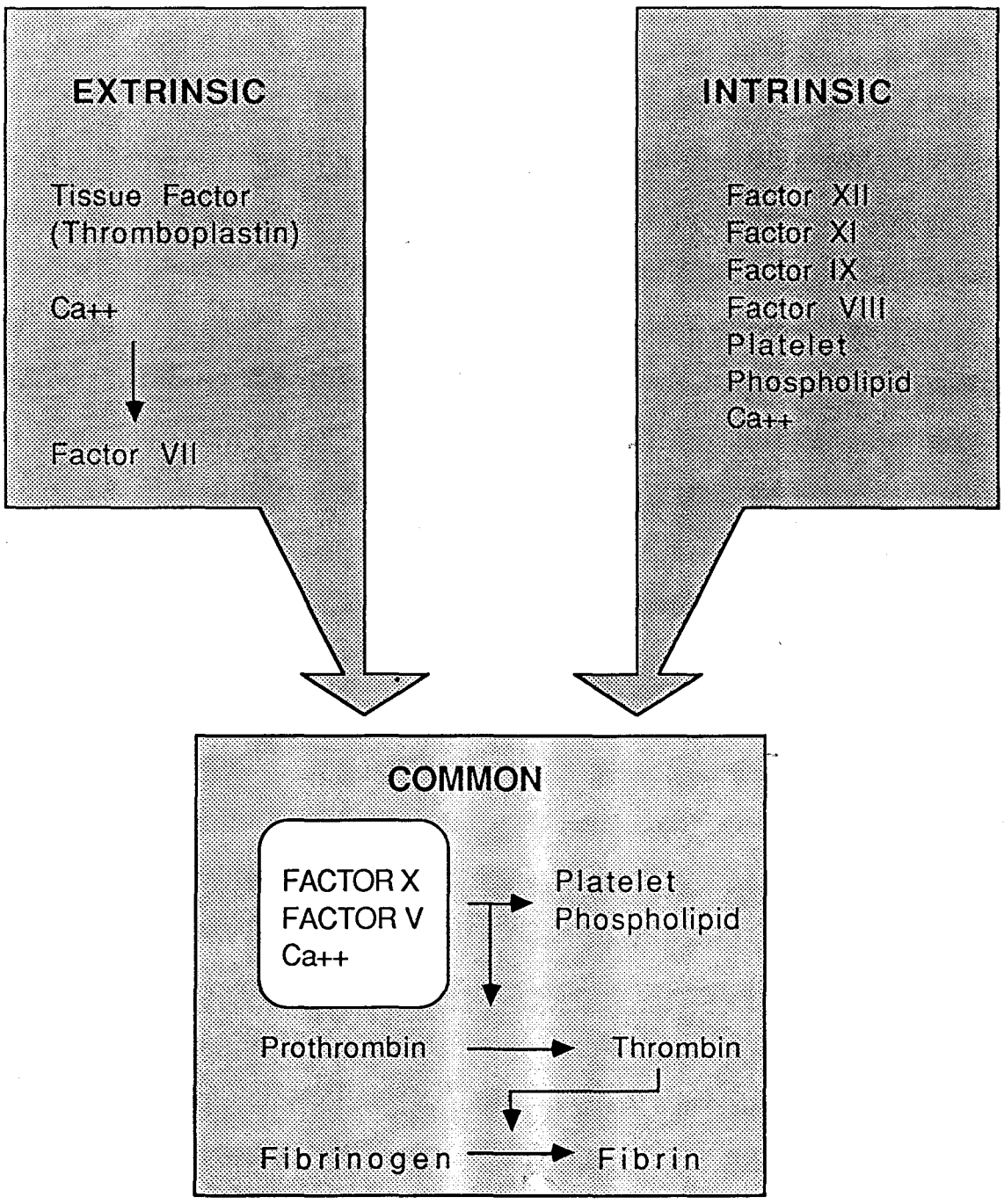

Figure 2. The Blood coagulation pathway(5).

The intrinsic pathway is initiated by the reactions of zymogens at a solid surface (6-8), such as a damaged vessel or prosthetic device. When blood vessels are damaged, collagen and other subintimal components are exposed(6). The proenzyme factor XII is adsorbed to the surface and is converted to its enzyme form, XIIa (see Figure 3). This contact phase reaction does not require calcium. Activated factor XII in turn converts the zymogen factor XI to the enzyme factor XIa, a reaction which is again calcium independent. Activated factor XI (XIa), in the presence of calcium , cleaves a small peptide from factor IX , thus converting it to its activated form (IXa). Factor IXa forms a complex with calcium, phospholipid, factor VIII and factor X to generate factor Xa.

The extrinsic pathway is activated when cell damage or alterations to the cell membrane release a lipoprotein tissue factor known as thromboplastin (5,6). Thromboplastin interacts with factor VII, in the presence of calcium, to form VIIa. Factor VIIa then activates factor X to Xa. The presence of thromboplastin allows the by-passing of a number of the early time consuming steps in the intrinsic pathway. Thus the extrinsic pathway is relatively rapid. However the intrinsic pathway , although slower, is probably the major contributor to the coagulation process occurring in response to blood-foreign surface contact.

Factor X is activated by either the intrinsic or extrinsic pathway. Xa forms a complex with platelet phospholipid, factor V and calcium. This complex in turn converts prothrombin (factor II) to thrombin (IIa). Thrombin is a proteolytic enzyme with the amino acid serine at its centre which cleaves two pairs of

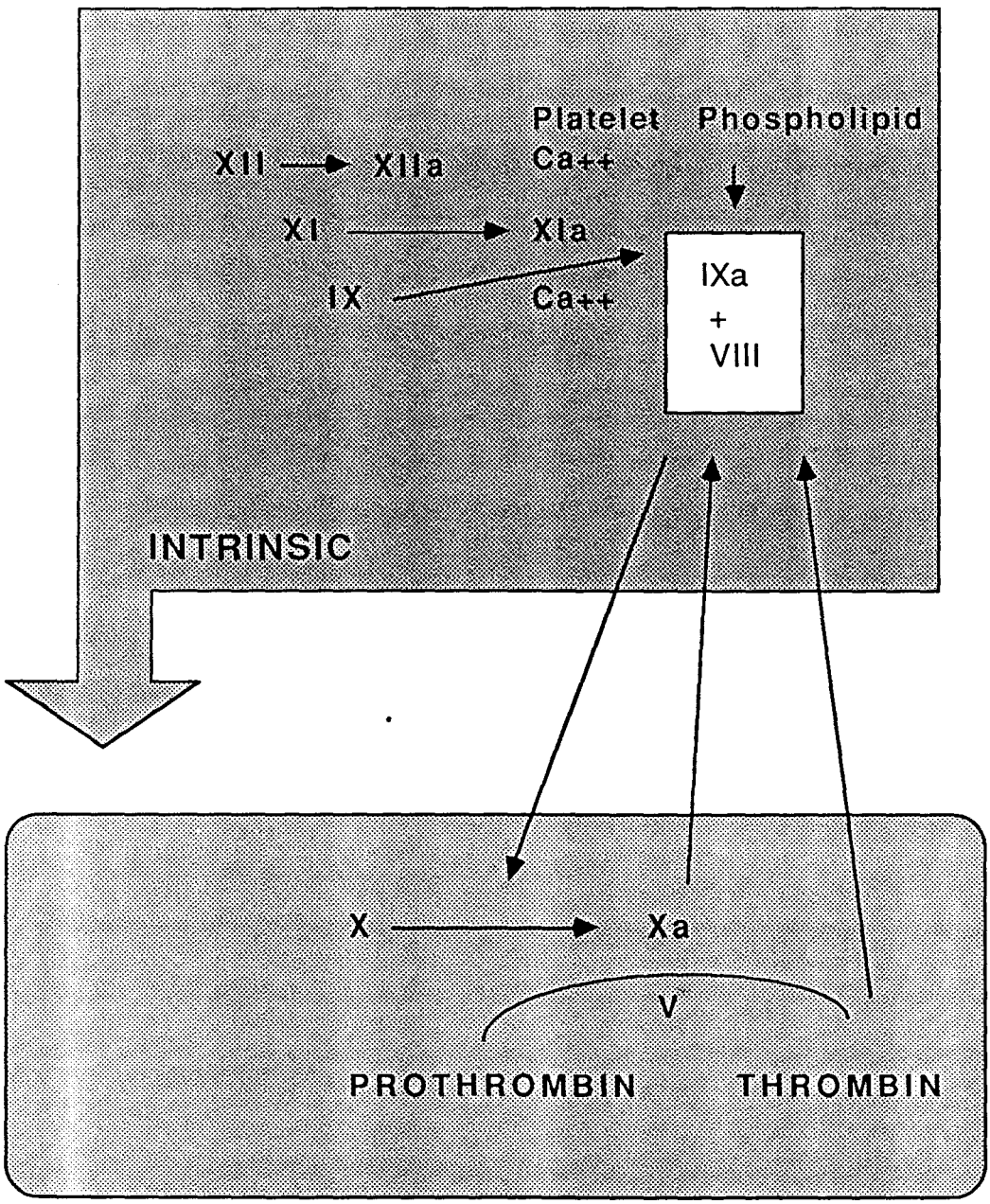

Figure 3. The intrinsic pathway(5).

arginine-glycine bonds in fibrinogen releasing the fibrinopeptides, and converting it to fibrin monomer. Fibrin monomer then undergoes spontaneous polymerization to form fibrin polymer which is initially cross-linked by hydrogen bonds. The fibrin polymer chains are further cross-linked via covalent bonds in the presence of factor XIII, thrombin and calcium.

Blood coagulation is thus a complex process which requires three primary components: coagulation factors, platelets, and calcium. The blood coagulation proteins circulate as zymogens and upon initiation of the blood coagulation cascade, for example in response to blood-surface contact, the proteins are sequentially converted to active enzymes or cofactors. The final product is the enzyme thrombin which converts fibrinogen to fibrin. The initiating event in relation to blood-surface contact is protein adsorption.

2.2 Proteins and Protein Adsorption

The word " protein " is derived from the Greek word *proteious*, meaning "the first ", and proteins are essential to life. Proteins have complex structures and functions and are found in all living things. This section of the report includes a general discussion of protein structure, as well as a more detailed discussion of the blood coagulation protein fibrinogen and its adsorption characteristics.

2.2.1 Protein Structure

A protein is a polymer made up from relatively simple monomeric units (1,9-11). These monomers are the amino acids, and there are 20 common amino acids found in proteins. Proteins have an exact sequence of amino acids and a precise length of polypeptide chain. Nineteen of the 20 amino acids used to build the proteins have the general structure (11):

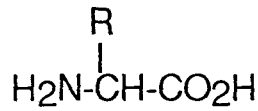

The amino acids differ from one another in the chemical nature of the side chain R. Amino acids are assembled into proteins by linking them together through peptide bonds. A typical linear polypeptide chain is formed by linkage of 50 to 1,000 amino acids.

Primary Structure

All proteins have the simple basic structure discussed above, differing only in the number of amino acid residues linked together, the amino acid composition, and the sequence in which the amino acids occur. This amino acid sequence identifies a particular protein and distinguishes it from all other proteins, even those, if any, that have the same composition. The sequence also determines the chemical and biological properties of the protein. The sequencing of the amino acids in the protein is the most basic level of structuring and is thus referred to as the "primary structure " (10-12). Higher levels of structure refer to the three dimensional orientation of the molecule in space.

Secondary Structure

The secondary structure of a protein is the local arrangement of the polypeptide backbone (11,12). In 1951, Pauling and Corey (13) proposed the α-helical structure as one of the secondary structures that should occur in nature because of its inherent stability. The α-helix is a spiral arrangement of the polypeptide chain, with the chain winding around a central axis, and each amino acid residue rising along the spiral in a uniform manner (see Figure 4a).

Another type of secondary structure, also proposed by Pauling and Corey in 1951, is the β sheet structure. This conformation results in a number of polypeptide chains being aligned side by side in close contact, and stabilized by intermolecular hydrogen bonding. The length of the β sheet polypeptide is shorter than that of a fully extended polypeptide chain due to the bonds between chains. Thus, the polypeptide backbone appears puckered and resembles a pleated sheet. In this β-sheet structure, the side chains (R groups) are located above and below the plane of the sheet, with the direction alternating from one residue to the next (see Figure 4b).

Different secondary structural elements are frequently connected by sharp turns, particularly at the surface of a molecule. These turns are referred to as β turns (or reverse turns, or β bends). They generally have distinctly recognizable conformations. The general consensus on the definition of a turn by a number of researchers, is in terms of four residues, connected by three peptide linkages, stabilized by a hydrogen bond between the carbonyl of the first and amide of the fourth residues (14).

On the basis of secondary structure, proteins have been subdivided into four classes: (α) having only α helices; (β) having primarily β-sheet structure; (α+β) having both helices and sheets but in separate parts of the structure; and (α/β) where both helices and sheets interact and often along the polypeptide chain (11).

Tertiary and Quaternary Structure

The tertiary structure of a protein refers to the overall 3-D architecture of the molecule resulting from chain folding (11,12). The quaternary structure is the specific way in which the individual polypeptide chains in a multichain

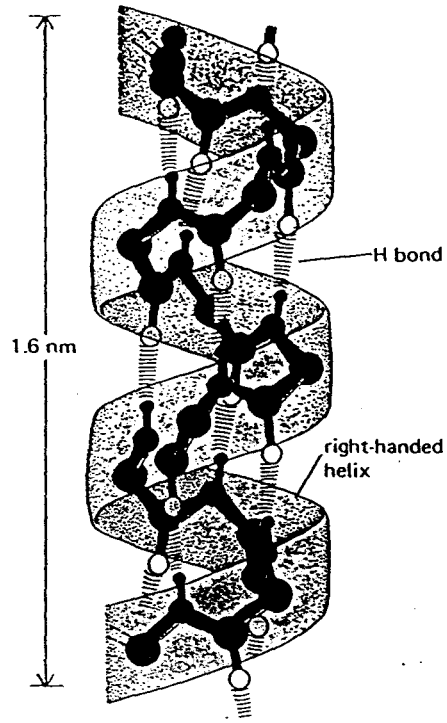

Figure 4a. α-Helical structure(15). Every peptide bond is hydrogen bonded to its neighbour. The side chains on each amino acid have been omitted for clarity. They protrude radially along the outside of the helix (see below).

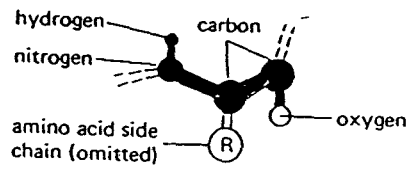

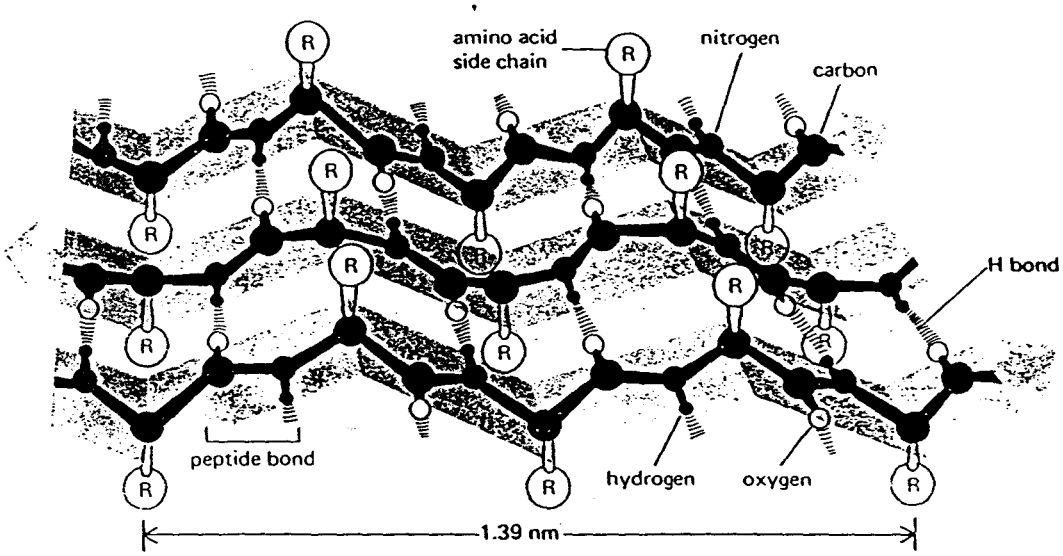

Figure 4b. β sheet structure(15). Every peptide chain is hydrogen bonded to its neighbour.

protein are combined to produce the final protein. Thus, the shape of a protein molecule which consists of only one polypeptide chain is determined by the tertiary structure, while proteins which consist of two or more polypeptide chains have shapes determined by both tertiary and quaternary structures.

Fibrinogen Structure

The protein fibrinogen was used extensively in the experimental work performed in this research and thus will be used to demonstrate some of the aspects of protein structure discussed above. The properties and adsorption behaviour of fibrinogen will however be discussed in a later section.

Fibrinogen is a soluble blood plasma protein which is modified during the blood coagulation process to give the product clot material fibrin. The fibrinogen molecule has a molecular weight of 340,000 and is made up of two identical halves each containing three different polypeptide chains designated Aα and Bβ and γ (see Figure 5) (12,16,17). The molecule contains almost 3,000 amino acids with 610 in the α chain, 461 in the β chain and 411 in the γ chain (18,19). Table 1(19) outlines the amino acid composition of fibrinogen, and its polypeptide chains. The complete amino acid sequence of the three fibrinogen chains (i.e. the primary structure) has been determined (18,20,21).

Each of the polypeptide chains has a different amino (NH_2) terminal end and a different carboxy (COOH) terminal end. The polypeptide chains α, β and γ, are held together in each molecular half by disulphide bonds forming a disulphide ring. In the amino terminal part, all six chains are interconnected by the so-called disulphide knot (17,22,23). The human fibrinogen molecule, in its entirety, has 26 more negative than positive charges (16). There is an excess of 8 negative charges on the central or D domain, and 4 on each of the terminal or

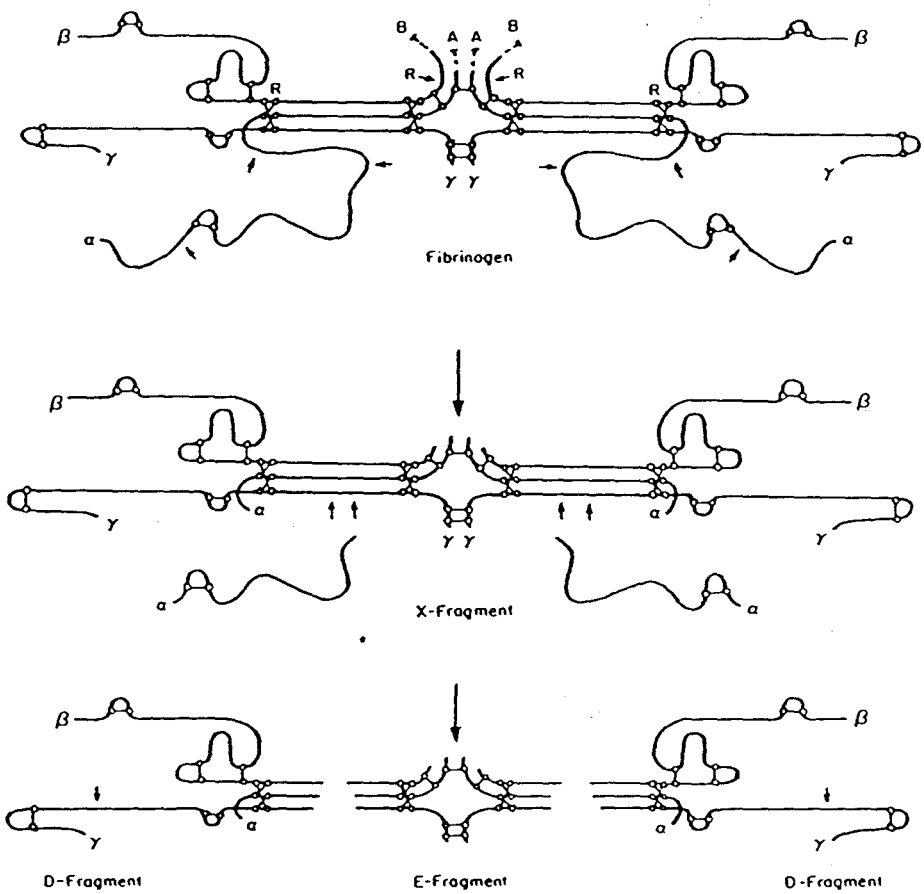

Figure 5. Schematic representation of the chemical structure of fibrinogen, and its fragments obtained by enzymatic degradation(17). Arrows indicate sites of preferential cleavage of chains by proteolytic enzymes. R, disulphide ring according to Doolittle(23). A and B, fibrinopeptides released by thrombin.

Table 1

Amino Acid and Carbohydrate Composition of Fibrinogen (19)

	Fibrinogen	Aα-Chain	Bβ-Chain	γ-Chain
Amino acids				
Asp	190	35	28	32
Asn	168	29	32	23
Thr	196	48	22	28
Ser	284	86	31	25
Glu	192	44	30	22
Gln	136	18	26	24
Pro	138	35	23	11
Gly	292	69	42	35
Ala	142	22	23	26
Cys	58	8	11	10
Val	134	28	25	26
Met	66	10	15	8
Ile	116	17	16	25
Leu	166	29	28	26
Tyr	100	9	21	20
Phe	94	19	10	18
Lys	208	39	31	34
His	64	15	7	10
Arg	154	40	27	10
Trp	66	10	13	10
Sum	2964	610	461	411
Carbohydrates				
N-Acetylgluocsamine	16	-	4	4
Galactose	8	-	2	2
Mannose	12	-	3	3
N-Acetylneuraminic	4-8	-	1-2	1-2
Molecular Mass	338162	66161	54375	48545

E domains. Removal of the fibrinopeptides results in the central domain assuming a net positive charge of +5. This is compatible with each terminal domain having a complementary electrostatic interaction with a positively charged central domain during polymerization (16).

Enzymatic digestion of the fibrinogen molecule by plasmin during fibrinolysis first leads to splitting in the large carboxy terminal portion of both α-chains, leading to the formation of the X fragment, as shown previously in Figure 5. Further degradation splits the X fragment into three large portions: fragment E, which originates from the central portion of the molecule, and two identical fragments, D, which originate from the terminal portions.

The secondary structure of fibrinogen has been studied by a number of researchers (24,25). The α–helix content of the native fibrinogen molecule in solution has been estimated by optical rotary dispersion to be about 33%(24,25). However, this is reduced to approximately 20% in the acid-, alkali- and urea-denatured molecule and is further reduced to a level close to zero in 5M guanidine-HCl (25). Other researchers report that fibrinogen eluted from a glass surface showed a 50% reduction of α-helicity relative to native fibrinogen (26) suggesting that forces sufficient to disrupt α-helices are involved in the bonding of fibrinogen to glass.

The only significant regions of α–helical structure in any of the chains of the native fibrinogen molecule appear to be those between the disulphide rings. This connector region is largely composed of supercoiled α–helices (coiled coils), with a relatively unstructured stretch in the centre of each connector (16). The carboxy-terminal halves of the beta and gamma chains appear to be highly folded compact regions that make up the bulk of the terminal D domains.

However, the carboxy terminal ends of the alpha chains are unfolded and highly polar (16).

The three dimensional shape of the fibrinogen molecule in solution has been thoroughly studied (27-30). The trinodal structure (see Figure 6) proposed in 1959 by Hall and Slater from electron microscopy data(27), although initially controversial, is now generally accepted (22,28,29). The molecule measures 475 Å in length. The terminal or D domains measure 65 Å, and the central or E domain measures 50 Å. The connector regions have a lateral dimension of about 15 Å.

2.2.2 Principles of Protein Adsorption

A number of factors are important in the adsorption of a protein to an interface. These include mass transport, and the adsorption process itself including kinetics and thermodynamics.

Mass Transport

The adsorption of a protein requires the transport of the protein molecule to the interface. There are four major transport mechanisms(1):

1. Diffusion
2. Thermal Convection
3. Flow (convective transport)
4. Coupled transport (convective / diffusion processes)

During the initial stages of the protein adsorption process, when the fractional coverage of the surface is low, the rate of adsorption may be transport controlled: every molecule that comes to the interface sticks and adsorbs. Thus, all molecules near the interface will be rapidly adsorbed resulting in

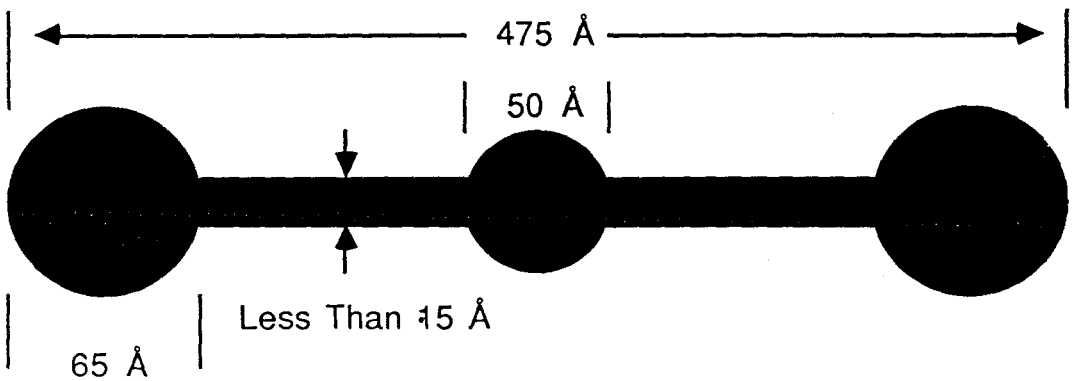

Figure 6. Trinodular structure of the fibrinogen molecule (16).

depletion of solute in the undisturbed fluid adjacent to the interface, often referred to as the boundary layer.

For static systems, the transport of molecules to the surface is by diffusion alone. Thus, a depletion in concentration in the boundary layer results in a concentration gradient resulting in diffusion from the bulk solution towards the boundary layer during the initial stages of protein adsorption. Under these conditions, the rate of adsorption is equal to the rate of diffusion, and can be described by Equation 1. Integration of this equation gives the total number of molecules, n, adsorbed in an elapsed time, t (Equation 2).

$$\frac{dn}{dt} = C_o \sqrt{\frac{D}{\pi t}} \qquad [1]$$

$$n = 2C_o \sqrt{\frac{D\,t}{\pi}} \qquad [2]$$

Where

n = number of adsorbed molecules

C_o = bulk solution concentration

D = diffusion coefficient

t = time

A stirred solution, such as in the experimental procedure used in this report, may incorporate most or all of the transport processes listed above. Mass transport occurs only by diffusion in the layer of undisturbed fluid assumed to exist adjacent to all solid interfaces. However, the thickness of the layer depends on such factors as temperature, stirring conditions and the interface itself.

Following transport of the protein molecule to the interface, molecular adsorption takes place at the solid wall. When an interface is partially covered with adsorbed protein, the rate of adsorption may fall below the rate of diffusion. This suggests that there is an energy barrier to adsorption and some of the molecules which reach the interface may diffuse back into solution.

Models of Protein Adsorption

Protein adsorption from single component systems has been studied by a number of researchers and several models of protein adsorption have been proposed.

The Langmuir theory for gas adsorption is often applied to the adsorption of protein molecules from solution (31,32) (see Figure 7a). When a solution is contacted with a solid adsorbent, molecules of adsorbate transfer from the fluid to the solid until the concentration of adsorbate in solution is in equilibrium with the adsorbate on the solid. The equilibrium data at a given temperature are usually represented by an adsorption isotherm which is the relationship between the quantity adsorbed and the concentration of adsorbate in solution. The equilibrium Langmuir adsorption isotherm is given by Equation 3.

$$\theta = \frac{Kc}{1+Kc} \qquad [3]$$

Where

θ = fractional coverage

c = bulk concentration

K = equilibrium constant for adsorption

Plots of adsorbed amount vs bulk concentration at equilibrium are well defined and show a plateau. A good deal of protein adsorption data found in

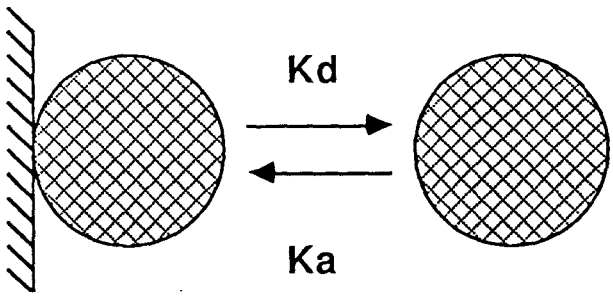

Figure 7a. Langmuir model for reversible adsorption.

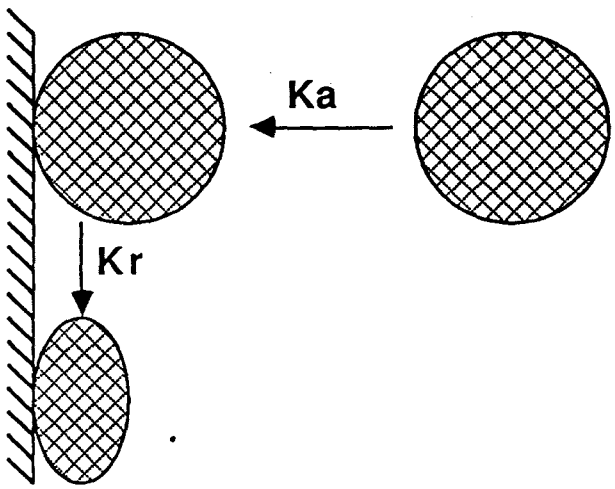

Figure 7b. Lundstrom model for irreversible adsorption.

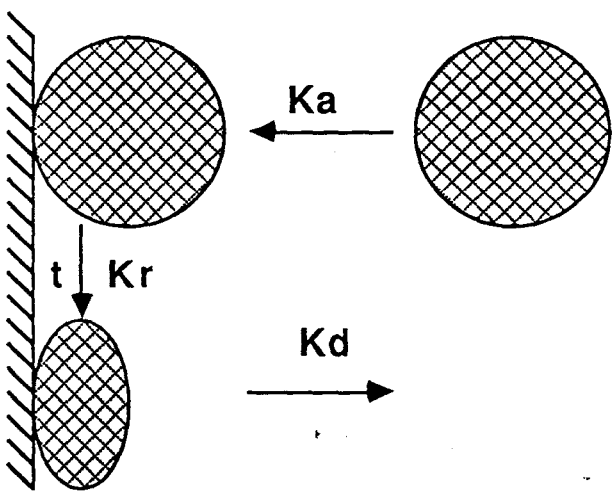

Figure 7c. Lundstrom model allowing for desorption.

the literature fits reasonably well to the Langmuir adsorption isotherm given in Equation 3. For example the isotherm for adsorption of fibrinogen to glass exhibits the shape of a high affinity Langmuir isotherm with a well defined plateau of 0.7 $\mu g/cm^2$ (33). A number of simplifying assumptions are made in deriving the Langmuir model. These assumptions are listed below:

1. only one molecule can be adsorbed per site (monolayer).
2. one type of site is present (homogeneous surface).
3. adsorption of one molecule does not affect the adsorption of adjacent molecules (no lateral interactions).
4. reversible adsorption.

The adsorbed amounts of protein at saturation are often in the range corresponding to a close packed monolayer. For fibrinogen this range is from 0.2 $\mu g/cm^2$ (side on orientation) to 1.8 $\mu g/cm^2$ (end on orientation). Thus, a surface concentration of 0.7 $\mu g/cm^2$, representing the limiting capacity of glass for fibrinogen, is within the range corresponding to a monolayer. Others of the Langmuir assumptions may however not be true in many situations. For example, the adsorption of many proteins is essentially irreversible. The agreement of experimental data with the Langmuir model for protein adsorption must be considered fortuitous in most cases.

Other more complicated models have been proposed such as that of Lundstrom(34). The Lundstrom model (see Figure 7b) also assumes that the transport of protein to the surface is not rate limiting, and thus the process is surface reaction limited. This model allows for conformational change following adsorption. The protein is assumed to adsorb with a rate constant k_a into state 1. Some of the protein in state 1 may then undergo a conformational change to

occupy state 2 with a rate constant k_r. The equations for the Lundstrom model (Equations 4,5,6) are shown below.

$$\frac{dn_1}{dt} = (k_a C_o - k_r n_1)(1 - a_1 n_1 - a_2 n_2) \quad [4]$$

Where

n_i = number of molecules in state i

a_i = surface area fraction occupied by molecules in state i

C_o = bulk solution concentration

$$\frac{dn_2}{dt} = k_r n_1 (1 - a_1 n_1 - a_2 n_2) \quad [5]$$

$$n_2 = \frac{k_a C_o}{k_r} \ln\left(\frac{k_a C_o}{k_a C_o - k_r n_1}\right) - n_1 \quad [6]$$

Although not discussed here, Lundstrom has also developed a model allowing for desorption (see Figure 7c).

Other models such as Beissinger and Leonard's model (35) and Sevastianov's model (36) have been used to describe protein adsorption. These models are more complex than those already discussed but even so certain simplifying assumptions which may not always be justified are made.

Thermodynamics of Protein Adsorption

The feasibility of protein adsorption at constant temperature and pressure is determined by the Gibbs energy of adsorption, ΔG. ΔG must be negative for the adsorption process to occur spontaneously according to Equation 7:

$$\Delta G = \Delta H - T\Delta S < 0 \qquad [7]$$

Where

ΔG = change in free energy

ΔH = change in enthalpy

ΔS = change in entropy

The Gibbs energy, ΔG, is related to the equilibrium constant by the following equation:

$$\Delta G = -RT \ln K \qquad [8]$$

Where

R = gas constant

T = Temperature

K = equilibrium constant

For a reversible process ΔS and ΔH can be obtained from the temperature dependence of ΔG as follows:

$$\frac{\partial \Delta G}{\partial T} = -\Delta S \qquad [9]$$

$$\frac{\partial \Delta G/T}{\partial T} = -\frac{\Delta H}{T^2} \qquad [10]$$

However, it can be argued that the above thermodynamic relations cannot be applied to the overall adsorption process since it is not completely reversible. In particular the determination of ΔG and ΔH from isotherms at different temperatures may not be a valid procedure.

Norde and Lyklema (37,38) have determined ΔH values using calorimetric methods. In order to calculate ΔH for the overall adsorption process, Norde and Lyklema subdivided the process into components

processes (37). The main components involved in protein adsorption according to Norde and Lyklema are redistribution of charge, changes in state of hydration, and rearrangement of the protein structure. More recent work of Norde and Lyklema (38) indicates a very striking dependence of ΔH on pH for the system human plasma albumin adsorption from aqueous solution on finely dispersed hematite particles. Under most conditions studied by Norde and Lyklema (38) the adsorption was endothermic, thus implying a positive entropy change, $\Delta S > 0$. At pH away from the isoelectric point (i.e.p.), the interaction between the protein and the surface is weak, and is enthalpically more favourable than at the i.e.p. (38). It appears that protein molecules may change their conformation at different pH values, thus modifying the interactions between the protein and the interface.

Conformational change induced by surface protein interactions may also take place leading to a surface-protein interaction of higher affinity. The protein molecule at the surface may increase the number of contacts and rearrange its structure in order to optimize interactions with the surface. These structural changes may contribute to the adsorption free energy. If this occurs, the desorption process is not simply the reverse of adsorption. Recent work by Norde et. al. (39) indicates structural rearrangements in molecules desorbed from different surfaces. In particular, a reduced α-helix content in samples desorbed from different surfaces indicated the occurrence of structural perturbation upon adsorption (39).

The thermodynamics of protein adsorption is thus relatively complicated due to the potentially complex nature of the process. The thermodynamic analysis by Norde and Lyklema discussed above indicates that protein

adsorption is entropically driven. The increase of entropy on adsorption is likely to be due mainly to conformational changes and hydrophobic interactions involving dehydration of the interacting surfaces.

Protein adsorption is affected by a number of surface properties such as hydrophobicity. Protein adsorption is generally considered to be greater and to involve stronger binding on hydrophobic than on hydrophilic surfaces. In addition, adsorption is more readily and more rapidly reversible on hydrophilic surfaces. However, other surface properties such as electrical charge may also play a role. It has been suggested that a negative surface charge would provide a good environment for blood based on the observation that normal endothelium is negatively charged. Most proteins have a negative charge at blood pH, thus it has been hypothesized that they should be repelled from a negatively charged surface. It is also widely believed that a positive surface will promote adhesion and aggregation of the negatively charged platelets thus leading to thrombus formation. A negatively charged surface is believed to promote activation of the Factor XII. Norde and Lyklema, as discussed earlier, indicate that structural perturbations resulting in the redistribution of charge may occur on adsorption. Thus, negative-negative or positive-positive interactions are possible.

2.2.3 Properties and Adsorption Behaviour of Selected Plasma Proteins

The number of proteins in plasma is of the order of 200. The functions of these plasma proteins span a wide range and include: maintaining colloid osmotic pressure, pH and electrolyte balance; transport of metal ions, fatty

acids, steroids, and hormones; regulation of cellular activity, as well as haemostasis. Many of the proteins have, as yet, no known biological function.

The clotting protein fibrinogen was used extensively in the experimental work performed in this thesis. This section of the report therefore discusses the properties and adsorption behaviour of fibrinogen from a single component system. In addition, numerous experiments were performed in developing a thermally treated fibrinogen layer that was non-adsorbing for a variety of proteins. Thus, the thermal transitions that occur in the fibrinogen molecule will also be discussed. Since adsorption studies were also performed using the proteins IgG and albumin, the properties of these two proteins are briefly discussed.

Fibrinogen

Fibrinogen is an abundant plasma protein, synthesized in the liver, that is an essential component of blood clots. The normal concentration of fibrinogen in human plasma is 2 to 4 mg/mL (40-42). Various physico-chemical parameters, as determined for human and bovine fibrinogens, are summarized in Table 2 (42).

The major function of fibrinogen is to serve as a " glue " in the formation of platelet plugs, thus enabling aggregated platelets to stay at a site of vessel wall injury. Fibrinogen binds to platelets through fibrinogen receptors, although firm adherence of fibrinogen molecules to one another requires the conversion.of fibrinogen to fibrin, thus rendering a platelet plug stable. Three general reactions can be used to describe the conversion of fibrinogen to fibrin(43):

1. Proteolytic activation of fibrinogen with cleavage of fibrinopeptides;

Fibrinogen $\xrightarrow{thrombin}$ *Fibrin Monomer + Fibrinopeptides*

2. Linear association of fibrin monomer to form long double stranded protofibrils;

Fibrin Monomer —— *Fibrin Polymer*

3. Lateral association of protofibrils to form fibrin fibres of varying diameters.

Fibrin Polymer $\xrightarrow{Ca++\ XIII}$ *Cross Linked Fibrin Polymer*

Table 2

Physico-chemical Parameters of Fibrinogen (42)

Molecular Weight (MW)	340,000 ±20,000
Sedimentation Coefficient ($S_{20,w}^{\circ}$)	7.9 S
Translational Diffusion Coefficient ($D_{20,w}$)	2.0×10^{-7} cm^2 sec^{-1}
Rotary Diffusion Coefficient ($_{O20,w}$)	40,000 sec-1
Intrinsic Viscosity	0.25 dl/gm
Partial Specific Volume (v)	0.71-0.72
Frictional Ratio (f/f_o)	2.34
Extinction Coefficient (at neutral pH)($E_{1\%cm,280}$)	15-16
Isoelectric Point (i.e.p)	5.5
Percent alpha-helix	33

In the presence of thrombin, fibrinogen is converted to fibrin monomer via release of the fibrinopeptides A and B from the Aα and Bβ chains respectively. Fibrinopeptide A consists of 16-19 amino acid residues, and fibrinopeptide B consists of 14-21 amino acid residues (43). Thus, a total of 60-80 amino acid

residues are released on exposure of fibrinogen to thrombin. Following the release of the fibrinopeptides from fibrinogen, the molecule can be regarded as fibrin monomer. The fibrin monomer polymerizes linearly as well as laterally to form fibrin polymer.

The adsorption characteristics of fibrinogen from single protein systems have been thoroughly studied (33,43,44). For example in previous studies in this laboratory (43,44), borosilicate glass tubing was exposed to a pure fibrinogen solution containing radioiodinated fibrinogen in 0.05M Tris, at a pH of 7.35, under static conditions. The tubes were exposed for a designated length of time at several different concentrations. The tubes were then rinsed extensively, cut into measured lengths, and counted for bound radioactivity using a NaI(Tl) detector. The surface concentration was estimated by comparing solution radioactivity to surface radioactivity. The results indicated that a limiting surface concentration of approximately 0.70 ± 0.05 $\mu g/cm^2$ is reached under these conditions of ionic strength and pH (43). The dependence of adsorption on fibrinogen concentration is shown in Figure 8.

The dependence of fibrinogen adsorption to glass on shear rate and Tris concentration has also been studied (43,44,). It was found that shear rate does not significantly affect fibrinogen adsorption at relatively high concentrations. However, the effect of increasing Tris concentration (pH 7.35) is to cause a decrease in adsorption, as is shown in Figure 9 (44).

Thermal Transitions of Fibrinogen

When the temperature of an aqueous fibrinogen solution is raised above 37°C thermal transitions take place. These transitions have been studied by a number of researchers (17,45,46).

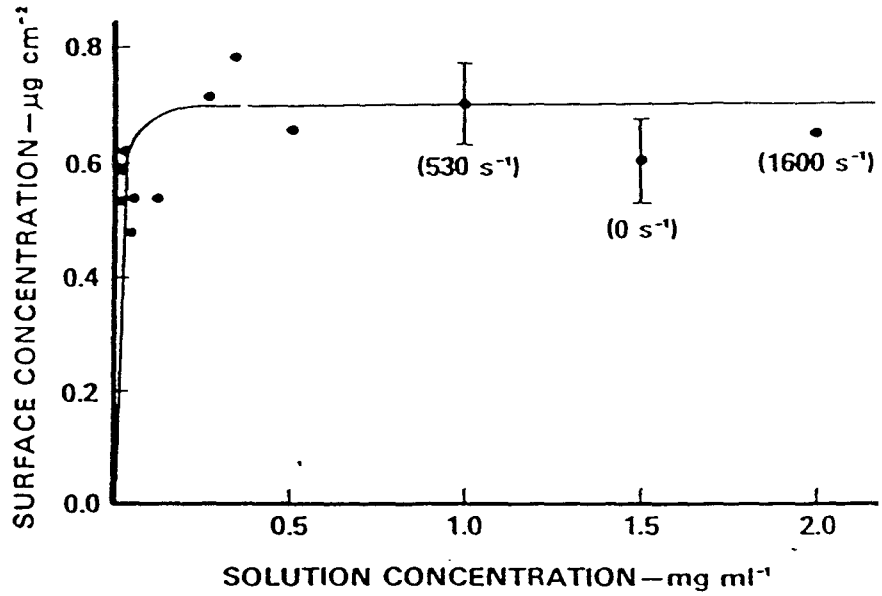

Figure 8. Dependence of fibrinogen adsorption to glass (single component system) on bulk solution concentration(44).

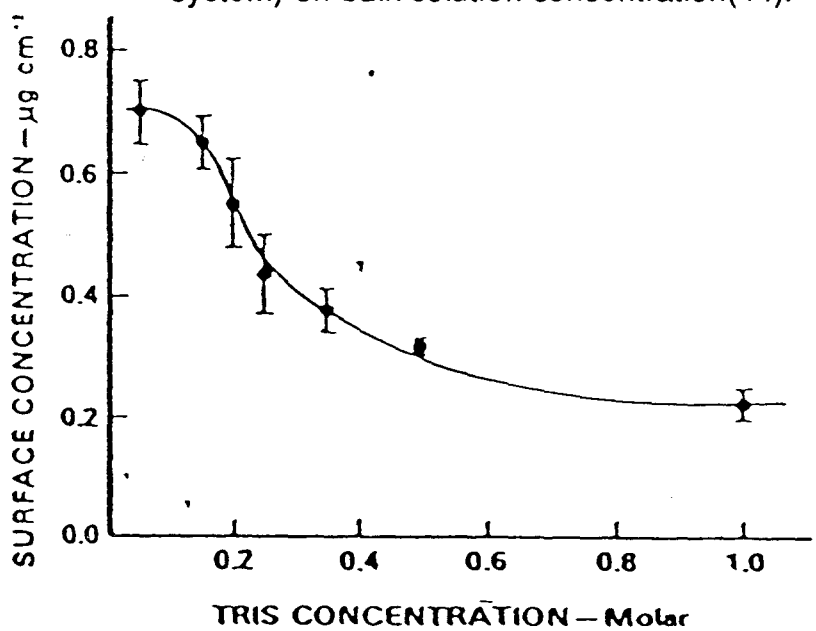

Figure 9. Dependence of fibrinogen adsorption to glass (single component system) on Tris concentration(44).

Solutions of fibrinogen, when heated in a differential scanning calorimeter (DSC), show two main endothermal transitions (17,46) occurring at temperatures close to 60°C and 97°C (46). Similar transitions were observed for mixtures of fragments D and E that were obtained by the limited proteolysis of fibrinogen (46). However, isolated fragment E showed only a single transition at the higher temperature (46) as shown in Figure 10. Thus portions of the fibrinogen molecule undergo thermal transitions separately.

The independent thermal transitions of the fibrinogen molecule support the trinodular model (27) proposed by Hall and Slater (as discussed earlier). The two transition temperatures of intact fibrinogen, and of the D and E fragments respectively, are nearly identical suggesting that the D and E domains exist independently as subunits in fibrinogen and in essentially the same conformation as in the proteolytically released fragments.

A more recent calorimetric study of the thermal transitions of fibrinogen and its fragments has shown that parts of the fibrinogen molecule are removed at an early stage of its degradation by proteolysis (47). This phenomenon has a small but noticeable heat effect which is largely obscured by much more pronounced heat effects in other parts of the molecule (47). The transition that is screened corresponds to a change in the C terminal part of the Aα chain. This transition is accompanied by a distinct heat capacity increase which is an indication that the process proceeds with structural unfolding and the exposure of non-polar groups to water (47).

It has been found that the thermal transition of the D fragment, which occurs at approximately 60°C, is irreversible in nature (47,48) whereas the transition of the C-terminal part of the A α chains is reversible. These properties

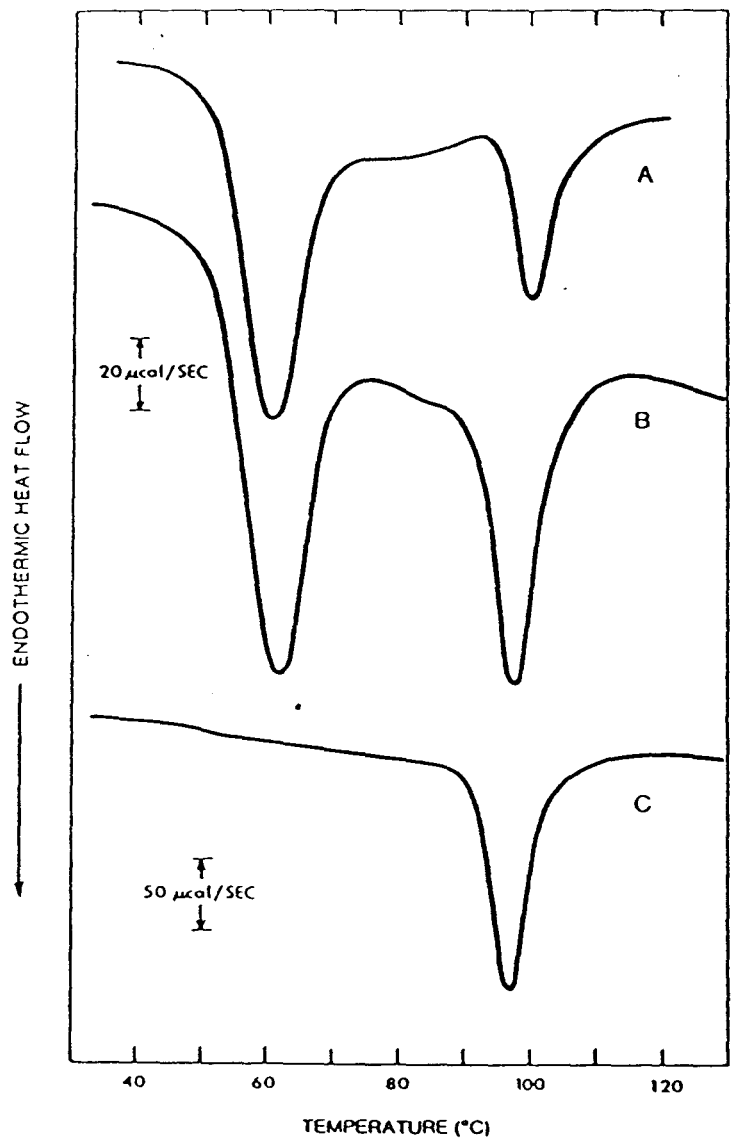

Figure 10. Thermal denaturation of the D and E subunits of fibrinogen(46) (A) Native fibrinogen, (B) Mixture of D and E fragments, (C) E fragment.

enabled researchers to isolate and study the C-terminal part of the Aα-chain by pre-exposure of the sample at an increased temperature (47,48).

The thermal transitions of fibrinogen that occur around 60°C correspond to "melting" of the terminal D-domains. Parts of these terminal nodules are able to anchor the molecule strongly to a glass surface, possibly via hydrophobic interactions (45). Above 70°C molecules anchored to an interface seemed to be "glued" onto it. This indicates a very large free energy of adsorption for each individual molecule or possibly the existence of some interfacial polymerization due to multiple attachments between molecules.

The turnover properties of an adsorbed radioactively labeled fibrinogen layer which had been previously maintained for 15 minutes at 75°C have been studied (45). When unlabeled solutions of either fibrinogen or albumin were incubated with the surface layer, no release of radioactivity was observed. Thus, the thermally treated fibrinogen layer was concluded to be irreversibly attached to the interface (45). It was also shown that this layer provided an essentially non-adsorptive surface. This finding is of particular interest to the experimental work reported in this thesis, since a thermal treatment procedure similar to that discussed above, was used to prevent adsorption from occurring on the experimental apparatus (i.e. cell and glass tubing) during experiments.

It should perhaps be noted that proteins that show more than one distinct stage of denaturation are not common (46). Intermediates that have been documented previously (49), for other proteins, were obtained by variations in the pH or denaturant concentration. Presently, fibrinogen appears to be the only known protein having stable intermediates, such as molecules with denatured D subunits and a native E subunit.

Other Plasma Proteins

Of particular importance to the topic of this report, in relation to the adsorption characteristics of fibrinogen from plasma, are the proteins prekallikrein and high molecular weight kininogen (HMWK). These two proteins are important in the activation of the contact phase of coagulation. Prekallikrein and HMWK interact with factor XII in the initiation of the intrinsic coagulation pathway by activation of factor XI (50).

Prekallikrein is present in plasma at concentrations of 20 to 40 μg/mL (50), and circulates as a precursor to the enzyme kallikrein. It is known that about 25% exists as prekallikrein, while approximately 75% is bound to HMWK (51-53). Prekallikrein, when run in reduced polyacrylamide SDS gel electrophoresis shows two subunits: a heavy chain with a molecular weight of 55,000 and a light chain with a molecular weight of 33,000 (50). Recent evidence suggests that HMWK binds to kallikrein through the heavy chain.

The kininogens are proteins in plasma from which vasoactive peptides (kinins) are released. Two forms of purified human kininogens exist (50,54). There is a high molecular weight form (HMW) with a molecular weight of 120,000, and a low molecular weight form (LMW) with a molecular weight of 60,000 (50,54,55). 5 to 25% of the total plasma kininogen is HMW kininogen. HMWK is present in plasma at concentrations of 70 to 82 μg/mL. Despite its low plasma concentration, HMWK has been shown to be highly surface active and to be extensively adsorbed from plasma especially to hydrophilic surfaces like glass (53).

Plasma kallikrein cleaves HMWK, producing bradykinin and a disulphide linked molecule containing a heavy (MW 64,000) chain and a light (MW

46,000) chain (53,55,56). The light chain of the HMWK molecule appears to possess the portion of the molecule which has coagulant activity. This cleaved form of the HMWK molecule appears to bind to a greater extent to activating surfaces than does the intact molecule (53). Another function of HMWK and its light chain is that it appears to decrease the inactivation rate of kallikrein and factor XIa by C1 inhibitors and alpha-1-antitrypsin respectively.

Prekallikrein, as mentioned previously, circulates as a complex with HMWK. The main role of HMWK in prekallikrein activation is to place the prekallikrein on the surface in an optimal position for its interaction with factor XII. In the absence of HMWK, much less prekallikrein is bound to the surface, and activation of factor XII and prekallikrein do not proceed at a normal rate (53).

The role that HMWK plays in blood-surface interactions is of particular relevance to the work performed in this thesis. As mentioned earlier, HMWK has been shown to be extensively adsorbed on some surfaces. In achieving its dominant surface concentration, it seems likely that HMWK is capable of displacing other more abundant proteins, such as fibrinogen, known to be transported to the surface more quickly.

Other proteins of relevance to this thesis are albumin and IgG. Albumin is a relatively simple plasma protein, synthesized in the liver, consisting only of amino acid residues and contains no carbohydrate (57,58). It is a single polypeptide chain with 580 amino acid residues (58,59). Albumin has a molecular weight of 66,240 (58-60) and is present in plasma at a concentration of 35 to 55 mg/mL (60,61). Albumin thus represents about 60% of the total

protein found in plasma and is the principal agent responsible for the osmotic pressure of the blood and for the transport of fatty acids and bilirubin.

IgG, or immunoglobulin G, is a protein found in plasma at concentrations of 8 to 18 mg/mL (61). IgG has a four chain polypeptide structure which consists of a pair of heavy chains disulphide bonded to a pair of light chains (62). IgG differs from other classes of immunoglobulins (i.e. IgA, IgM, IgD, IgE) by the nature of its heavy chain. The total molecular weight of IgG is 160,000 daltons (62).

2.2.4 The Vroman Effect

The adsorption of a protein from a single component system is relatively well understood. However, adsorption from plasma is considerably more complex since many proteins are present and are competing for the same surface sites. The Vroman Effect is the terminology used to describe the transient adsorption of proteins from plasma, and is named after Leo Vroman, who first reported it (63). Vroman (63-65), as well as other researchers (66-69), have shown that high concentration proteins dominate the surface at short time exposures. At longer times exchange processes occur and proteins with higher affinities should dominate the surface. At very long times only the highest affinity proteins should be present on the surface.

Fibrinogen adsorption from plasma, under static conditions, has been studied in detail (66,67,69). Fibrinogen adsorption is found to increase with plasma concentration and then to decrease, with a maximum occurring around 1% plasma, as shown in Figure 11. This behaviour is in general agreement with the model proposed by Vroman (65), that in plasma-foreign surface interactions the initially adsorbed fibrinogen is displaced by proteins of lower

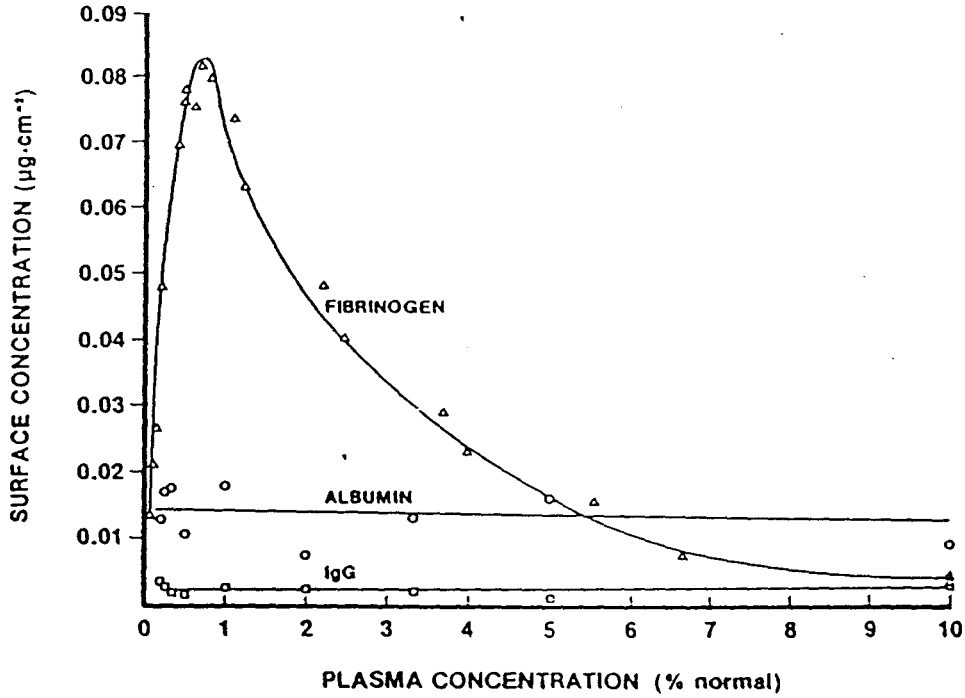

Figure 11. Fibrinogen adsorption onto glass as a function of plasma concentration(67).

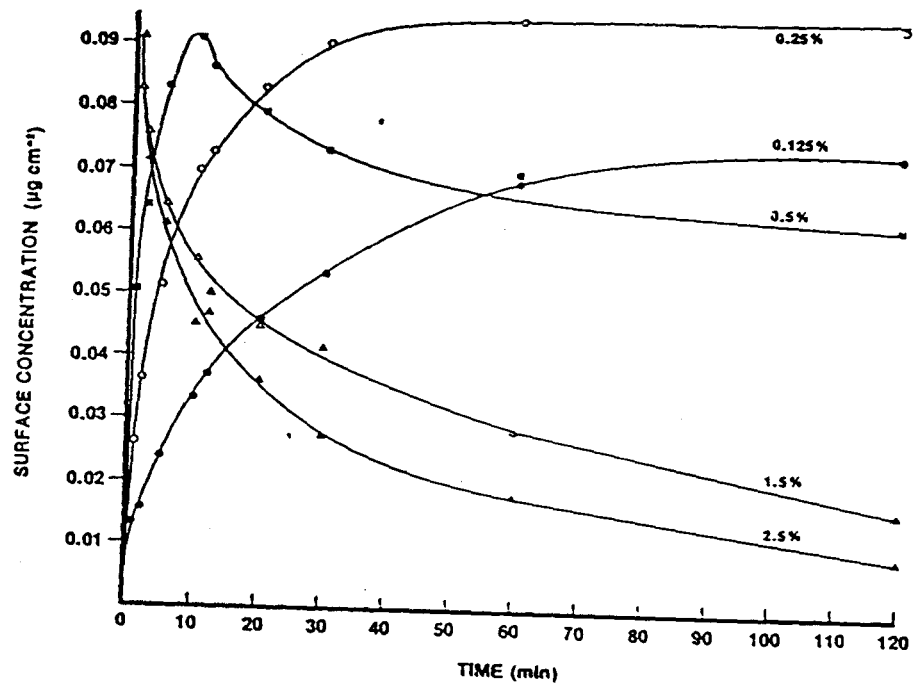

Figure 12. Fibrinogen adsorption onto glass as a function of time at various plasma dilutions(67).

concentration and higher surface affinity. Kinetic data (see Figure 12) at high dilution support this interpretation as they do not show maxima indicating that the concentration of the higher affinity protein is insufficient to cause displacement of fibrinogen. Vroman has also suggested that fibrinogen is displaced principally by HMWK, based on observations that fibrinogen adsorbed from HMWK-deficient plasma is not displaced , or is displaced more slowly (63).

Other researchers have shown quantitatively that proteins other than fibrinogen may be subject to the Vroman effect (66,68,70,71). These proteins include albumin, IgG, hemoglobin and fibronectin.

2.3 Principles of Radiation Dosimetry

The adsorption of proteins can be studied using a radioactive tracer technique involving attachment of a radioisotope to the protein. This approach necessitates the use of a counting system to monitor the radioactivity levels. The choice of a particular counting system is dependent on a number of factors such as the type of radiation to be measured, the need to match dosimeter to medium, the precision required, the size of detector required, the spatial resolution required, the convenience, the cost and the ruggedness.

The radioactive isotope used in this experimental work was ^{125}I, which emits characteristic gamma rays. This section of the thesis gives a brief overview of the fundamentals of gamma radiation, and discusses some of the factors listed above as they pertain to the dosimetric system used in the present work.

2.3.1 Fundamentals of Gamma Radiation

Gamma radiation is an electromagnetic wave radiated as photons of energy which travel at the velocity of light. The energy of a photon can be calculated from the relationship $E=h\upsilon$ where E is the energy in ergs, h is Planck's constant (6.624×10^{-27} erg sec) and υ is the frequency in Hertz. There are three principal mechanisms by which gamma rays interact with matter resulting in the partial or complete transfer of the photon energy to electron energy.

1. Photoelectric Effect (PE)
2. Compton Scattering
3. Pair Production (PP)

The photoelectric effect (see Figure 13a) is the inelastic collision of the photon with an orbital electron, resulting in the complete ejection of the electron and the production of an ion pair. This effect occurs primarily when the photon energy is low (i.e. <0.1 MeV).

Compton scattering involves a collision between a photon and an electron in which part of the energy of the photon is imparted to the electron. The photon emerges from the collision in a new direction with a reduced energy, as is depicted in Figure 13b. The energy of the electron and the scattered photon can be related to the scattering angle (θ) as is shown in the following equations (72):

$$E\gamma = E_o\left(1+\left(\frac{E_o}{mc^2}\right)(1-\cos\theta)\right)^{-1} \qquad [11]$$

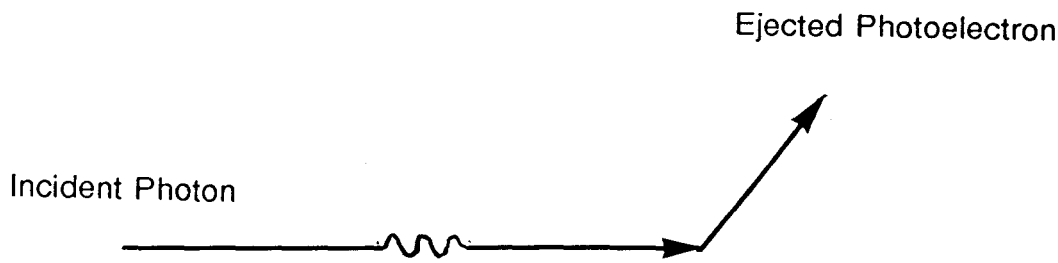

Figure 13a. Photoelectric effect.

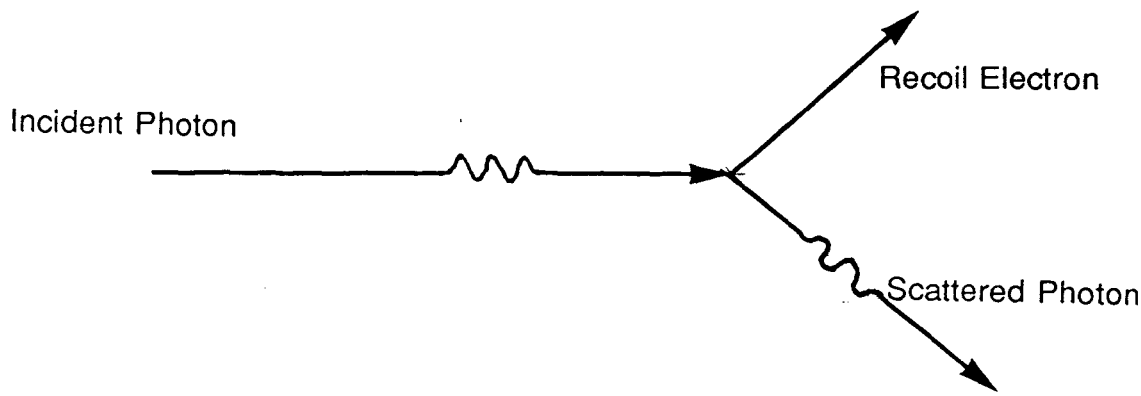

Figure 13b. Compton scattering.

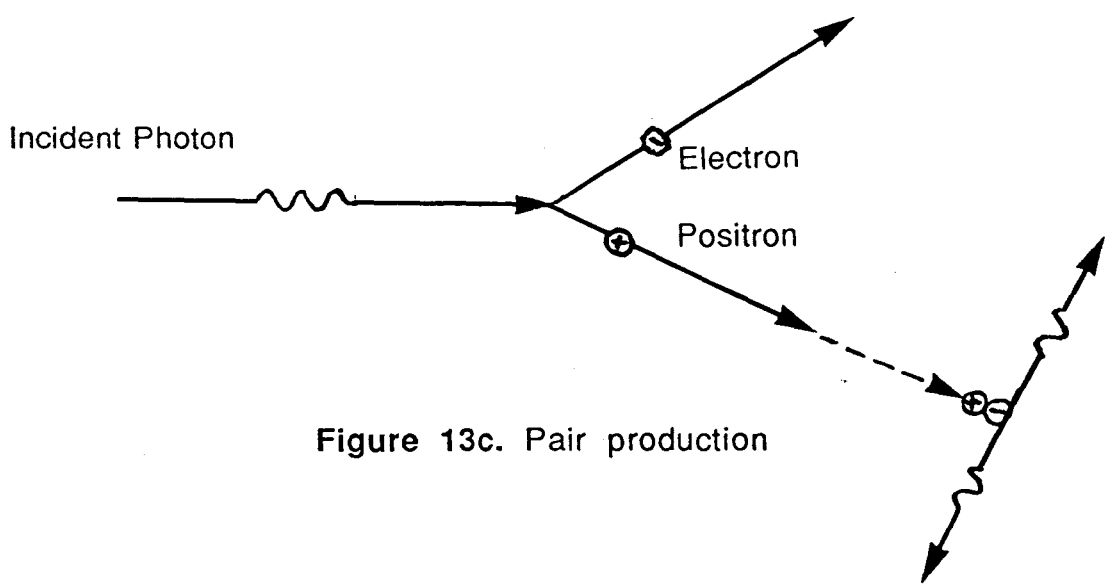

Figure 13c. Pair production

$$E_e = E_o - E\gamma = E_o \left(\frac{\left(\frac{E_o}{mc^2}\right)(1-\cos\theta)}{1+\left(\frac{E_o}{mc^2}\right)(1-\cos\theta)} \right) \qquad [12]$$

Where

E_o = incident photon energy

$E\gamma$ =scattered photon energy

E_e = electron energy

m = electron mass

c = velocity of light

θ = angle between incident and scattered gamma ray directions

The maximum energy loss by the photon is reached when a head on collision occurs (see Equation 13).

$$E_o - E\gamma = \frac{E_o}{\left(1+\frac{mc^2}{2E_o}\right)} \qquad [13]$$

Generally, the Compton effect is particularly important for gamma rays of medium energy, in the range of 0.5 to 1.0 MeV.

Pair production occurs only with gamma rays having energies greater than 1.022 MeV. The energy of the gamma ray is converted to an electron and a positron in the region of a strong electromagnetic field, as in the field of the nucleus. The creation of the antimatter positron can be viewed as ejecting an electron from a negative energy state into a positive energy state, thus leaving a hole (the positron) in a region normally filled with negative energy states (see Figure 13c). There is a gap of $2mc^2$ between the two energy regions. Thus, as

mentioned earlier, the energy required to create the positron must be at least 1.022 MeV.

Sodium iodide scintillators were used for the detection of gamma radiation during the experimental work discussed in this thesis. Figure 14 shows the typical relative contributions of the gamma ray absorption processes, discussed above, for NaI. The X and Y axes of Figure 14 correspond respectively to the energy of the incident radiation (MeV), and the mass absorption coefficient (cm^2/g). An absorption coefficient refers to the rate of decrease in the intensity of a beam of radiation as it passes through matter. The mass absorption coefficient is the fractional decrease in beam intensity per unit of surface density(73). In sodium iodide, the iodine (Z=53) is mainly responsible for the photoelectric absorption that results in effectively complete absorption of the gamma ray energy and hence in a light pulse whose amplitude is a measure of the gamma ray energy(73). The radioactive isotope used extensively during the experimental work performed in this thesis was ^{125}I which has a low gamma ray energy (35.4 keV). Thus, the predominant process that occurs, as depicted in Figure 14, is the photoelectric effect.

2.3.2 Scintillation Counting Systems

A scintillation counter consists of a scintillation detector, in the form of a solid, liquid or gas, which produces a flash of light upon excitation by ionizing radiation. The scintillator is optically coupled to a photomultiplier tube which converts the incident photons into electrical impulses whose magnitude is proportional to the intensity of the initial flash. In turn, this is proportional to the total energy deposited by the gamma ray quanta in the detector. The

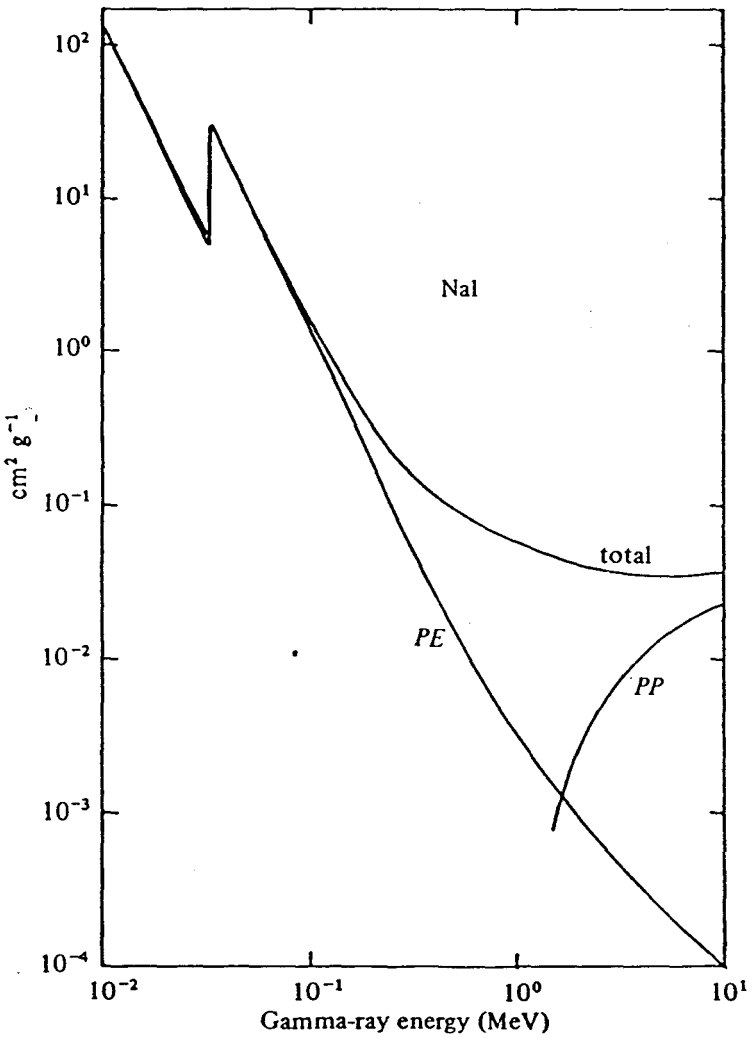

Figure 14. Relative contributions of the gamma ray absorption processes for NaI (72).

photomultiplier pulses may be analyzed in terms of pulse height to generate an energy spectrum, or counted to provide a measure of radiation intensity.

A distinct advantage of solid scintillation detectors, such as those used in this work, is that the density of the solid is such that gamma ray quanta with energies in the MeV range are stopped in a scintillator only a few millimeters thick. Furthermore, the detection of gamma rays can be accomplished with much higher efficiency than is possible with many other types of detectors. Scintillation counters are also found to have a very fast response to ionizing radiation. Thus solid scintillation counters are particularly useful for sources with fast counting rates.

Crystal Scintillators

Theoretically, any substance that can undergo luminescence can be used as a scintillator. Organic crystals are available commercially and are relatively inexpensive. However, the inorganic crystals, although more expensive, have a greater density (e.g. 3.67 g/cm^3 for NaI(Tl)) and stop a greater percentage of the gamma radiation. Thus, the detection of gamma radiation at the highest possible efficiency is obtained by using a solid inorganic scintillator.

The inorganic scintillators that are most widely used are the alkali halides, and in particular the alkali iodides. Generally, a scintillator is in the form of a single crystal. This is necessary in order to achieve maximum density, optical transparency, and uniform activation. Crystals that have been prepared are LiI, KI, RbI, CsI and NaI. LiI and NaI are hygroscopic and occur in both the hydrated and the anhydrous form. The hydrated material must be converted to the anhydrous state. This is accomplished by slow heating in a vacuum.

Growth of the crystal can be accomplished by a number of techniques, two of which are the Kyropoulos method and the Bridgman-Stockbarger method. Activation of the alkali-halide crystal is generally carried out by mixing the activator impurity, in the form of a salt with the starting material prior to growth. Thallium is frequently used as an activator and is added to alkali iodides in the form TlI. This is necessary to increase the probability for photon emission and to reduce self absorption. The activator provides states in the energy gap and the light emission takes place between the activator states. This is discussed in more detail later.

Of particular interest to the work reported in this thesis are the characteristics of thallium-activated sodium iodide (see Table 3). Large ingots, containing 10^{-3} mole fraction of thallium can be grown from high purity sodium iodide. As mentioned earlier NaI(Tl) is hygroscopic and will deteriorate due to water absorption upon exposure to air. Thus it must be sealed in airtight containers. Aluminum, a weak absorber of gamma radiation, is generally used for this purpose. A notable property of NaI(Tl) is its excellent light yield, which is the highest of any scintillation material (73). Its response to gamma rays is close to linear over most of the significant energy range. NaI(Tl) crystals are available in a wide assortment of shapes and sizes. However, the crystal is somewhat fragile and can be easily damaged by mechanical or thermal shock. In addition, the dominant decay time of 0.23 μsec is long for high counting rate applications. Nonetheless, NaI(Tl) has become accepted as the standard scintillation material used in gamma ray spectroscopy. Its extraordinary success stems from its extremely good light yield, excellent linearity and the high atomic number of its iodine constituent(73,74).

Table 3

Characteristics of a NaI(Tl) Scintillator (74)

Scintillation Efficiency	13%
Wavelength of maximum emission(nm)	410
Decay Constant(μsec)	0.23
Index of Refraction (at 410 nm)	1.85
Specific Gravity(g/cm^3)	3.67
Other Properties	Available as large clear crystals, which are hygroscopic and must be sealed in an airtight environment. Easily damaged by shock.
Principal Uses	Gamma ray detection

Mechanism of the Scintillation Process

The physical events responsible for the luminescence of inorganic solids, and in particular of activated alkali halides, are primarily caused by the presence of the activator at low concentrations. Gamma rays interact with a crystal in essentially three distinct steps (75):

1) The gamma ray quantum is slowed down and loses its energy primarily to electrons of the crystal, resulting in ionization and excitation of the constituents of the crystal lattice.
2) The energy deposited by the gamma ray quantum migrates to an activator centre or to a trapped centre and is stored there.
3) Energy is emitted in the form of a photon or via a nonradiative transition resulting in thermal excitation of the lattice.

In the ground state of a crystal, the filled bands are completely occupied. Ionization results when passage of a gamma ray quantum supplies the electrons with sufficient energy to be raised to the conduction band. The electron vacancy remaining in the valence band is known as a hole, and in the case of ionization is no longer bound to the electron (see Figure 15). Thus, both electron and hole are free to wander independently through the lattice, and each may contribute to the electrical conductivity in the crystal (73).

Another event, excitation, may occur such that the energy imparted to an electron in the filled band is not sufficient to raise it to the conduction band. Thus, it remains bound to the hole in the valence band. The resulting electron-hole pair is referred to as an exciton and does not contribute to the electrical conductivity in the crystal as it has no net charge.

The above discussion leads to the concept of an exciton band whose upper limit is the bottom of the conduction band, and whose lower limit is the exciton ground state. This is depicted in Figure 15.

The reason for the presence of the thallium activator in the crystal is to provide a number of impurity centres distributed through the lattice. Tl^+ ions occupy random sites normally held by the alkali metal ions. The existence of these impurity centres gives rise to localized electronic energy levels in the forbidden band below the conduction band. The impurity centre may be raised to an excited state by the capture of an exciton or by successive capture of an electron and a hole.

To summarize, the sequence of events leading to a scintillation are as follows. Passage of a gamma ray quantum through a crystal results in the formation of excitons, and electrons in the conduction band, and holes in the

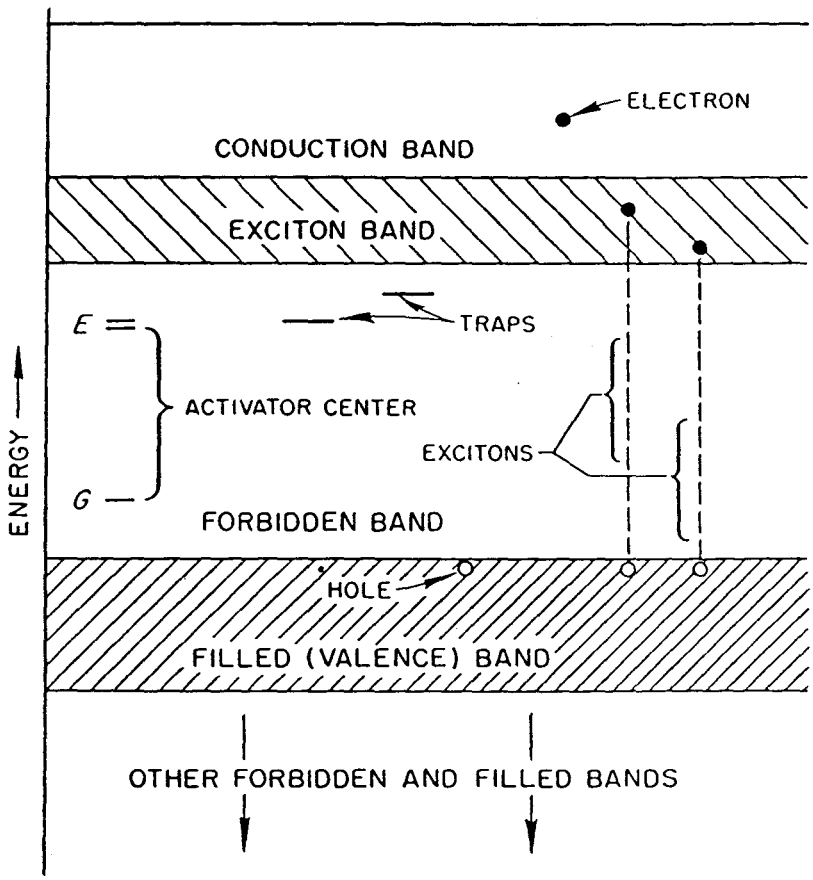

Figure 15. Electronic energy band diagram of an ionic crystal (74).

valence band. Each is considered free to wander through the crystal lattice. Energy lost by an incident quantum migrates from the immediate vicinity of the its path and is deposited at an activator site or trapping centre. This occurs via the process of exciton capture or by electron hole capture. The activator centre will be raised to an excited state. A transition occurs between the excited state and the ground state and a photon is emitted. The scintillation efficiency (ratio of emitted photon energy to incident particle energy) for NaI(Tl) is approximately 13% which represents one of the highest scintillation efficiencies for inorganic crystals. The absorption of 1 MeV of energy yields about 1.3×10^5 eV in total light energy. The wavelength of light emitted for thallium activated alkali halides occurs in the visible or near ultraviolet region.

Photomultiplier Tubes

The photomultiplier tube performs the important function of converting the light flashes from the scintillator into current pulses. In order that optimum results be obtained the photomultiplier must serve as a fast linear amplifier of high gain and low noise, with a minimal spread of the output pulse per incident photon and a minimum spread in transit time of the photoelectrons.

The basic components of a photomultiplier are the photocathode which converts a fraction of the incident photons into electrons, and a series of diodes which amplify the initial photoelectron pulse by secondary emission. The photocathode material used in most commercial photomultipliers is an intermetallic compound of cesium and antimony.

As mentioned previously, the photomultiplier tube is coupled to a high voltage power supply. The size of the electrical pulse produced by each gamma ray entering the NaI(Tl) crystal is proportional to the energy dissipated

by the gamma ray in the crystal. As the power supply voltage is increased, amplification of the pulses is proportionally increased. The largest pulses, representing the most energetic gamma rays are detected first. A further increase in voltage results in further amplification of the smaller pulses representing less energetic gamma rays which are then detected and counted. Continued increase in voltage eventually results in all pulses being detected and recorded including small noise pulses produced in the photomultiplier tube. A typical plot of the count rate versus voltage, often referred to as an integral spectrum, depicts the effect of increasing the voltage of the power supply, and is shown in Figure 16 (73). Preliminary experiments performed to establish the integral spectrum of the photomultiplier tube used in the experimental work in this thesis indicated that the high voltage level could not exceed 1000 volts. Beyond this level a significant number of noise pulses were detected. The operating voltage generally used was 900 volts.

Analyzer

The pulses generated in the detector are transmitted to a multichannel analyzer which performs the essential functions of collecting the pulses, providing a visual monitor, and storing the output (raw data) for later analysis. There are essentially two ways in which a multichannel analyzer can be used: (1) in pulse height analysis mode, (2) in multichannel scaling mode.

Pulse height analysis mode, as its name implies, analyzes or sorts the pulses according to their height. The amplitudes of the pulses are proportional to the energies of the incident radiation that was absorbed by the detector. The number of pulses of each height are counted, stored in separate channels, and a histogram is formed.

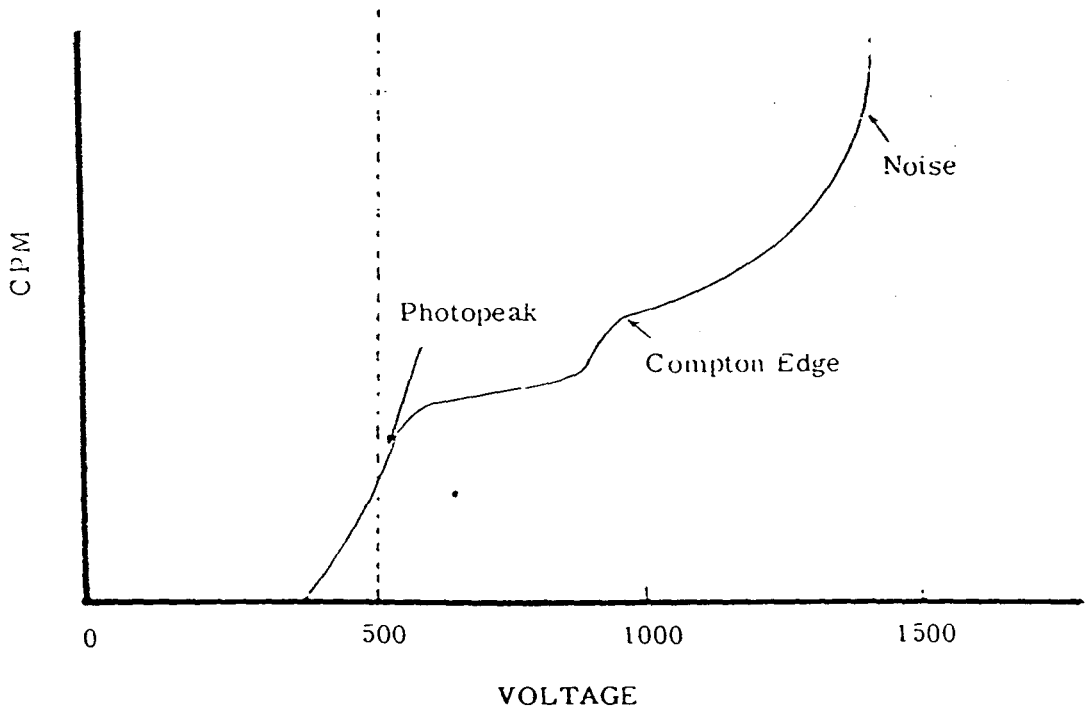

Figure 16. Typical integral spectrum for a scintillation detector (73).

When a multichannel analyzer is used in the multichannel scaling mode, as in the present work, a histogram representing number of events versus time is obtained. Used in this mode the multichannel analyzer does not register the amplitude of the pulses, but simply counts the total number of pulses received in a given time period, and stores them in the current memory channel. At the end of that time period, referred to as the dwell time, the multichannel analyzer advances to the next memory channel and pulses are now counted into this channel. Thus, each channel represents the summation of all counts within the given time period. The dwell time can range from μsec to hours thus allowing the monitoring of very rapidly or slowly evolving events.

A summary of the process that occurs in a scintillation system (see Figure 17) such as the one used in the present work, is as follows. The energy of the incident radiation is converted into a flash of light in a scintillator. The scintillator light enters a photomultiplier tube and impinges on a photocathode to produce electrons. The photomultiplier tube amplifies the number of electrons through secondary emission through a series of diodes producing a pulse. The pulse is then transmitted to an analyzer and recorded.

2.3.3 Radioiodination of Proteins

The radioactive source used in this work consisted of ^{125}I labeled proteins. The isotope ^{125}I has a characteristic gamma ray energy of 35.4 keV, and a half life of 60.2 days.

In recent years, radioactively labeled proteins have been used widely in biomedical research. In particular, the radioiodination of fibrinogen has been studied very thoroughly (77-79). In general, fibrinogen radioiodinates readily and at relatively high efficiencies regardless of the technique used. Methods

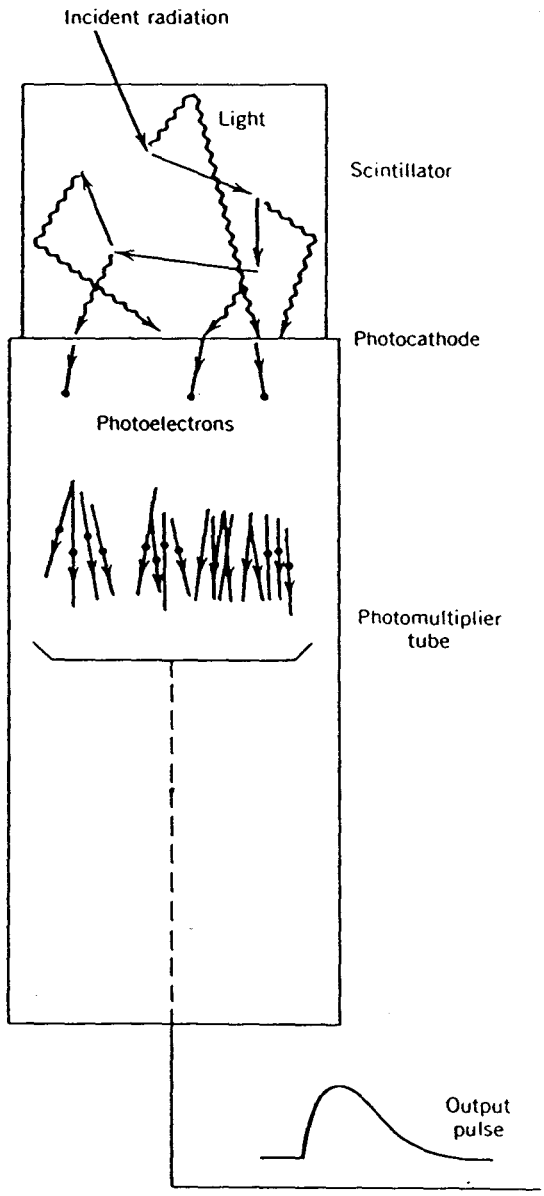

Figure 17. The basic processes in a scintillation detector(76).

that are currently used in the labeling of fibrinogen are the iodine monochloride (ICl) method (77,80,81), the lactoperoxidase (LP) method (79,82,83), and the thyroid peroxidase (TP) method (79,83). Two of these methods (ICl and LP) were used extensively in the experimental work reported in this thesis. Thus, a discussion of these methods is given in some detail.

The ICl method is generally efficient in its use of radioiodine when used for trace labeling. However, it cannot be used effectively to iodinate proteins to high specific activities. The basic method involves the mixing of ^{125}I in the form of iodide ions with the protein solution to be iodinated at an alkaline pH. An appropriate quantity of ICl, in a weakly acidic NaCl solution, is stirred rapidly with the protein-NaI mixture. Radioactive iodide, ^{125}I, is converted to ^{125}ICl by a rapid chemical exchange with non-radioactive ICl. The iodination of the protein, mostly in tyrosine residues, takes place according to the following reactions (80):

$$ICl + NaOH \longrightarrow HOI + NaCl$$

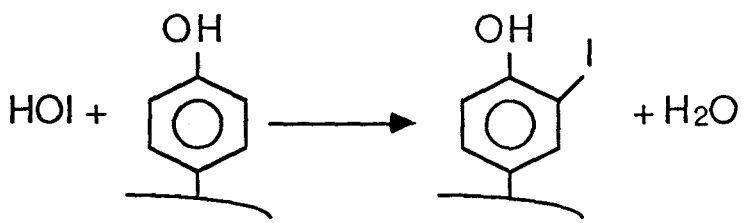

It should be emphasized that it is important to carry out ICl iodinations in such a way that an appropriate molar ratio of ICl to protein is used, since ICl is an oxidizing agent that may damage the protein if used in excess. It has been suggested that the number of iodine atoms that should be incorporated into a labeled protein should not exceed one iodine atom per 40000 Daltons (80). Thus, for a molecule such as IgG (MW 160,000), 4 iodine atoms per molecule of

IgG would be acceptable. However, there is reported evidence that some proteins, such as fibrinogen, are damaged under these conditions (80). One iodine atom per molecule of fibrinogen is considered to be the maximum acceptable level (81). Thus, to reemphasize, serious consideration must be given to the fact that the number of iodine atoms incorporated into, and the chemical damage done to the labeled protein by the iodination conditions can seriously affect the behaviour of the protein.

The lactoperoxidase labeling method is generally considered to be more gentle than the ICl method and gives labeled proteins of higher specific activity(79,82-84). This method involves the use of a reagent which consists of immobilized preparations of lactoperoxidase and glucose oxidase carefully blended to provide optimal enzymatic activity. Such reagents are available commercially.

The basic method involves the addition of glucose to a suspension of immobilized enzyme particles, $Na^{125}I$ and protein. Under these conditions the immobilized glucose oxidase generates small, steady amounts of hydrogen peroxide. The lactoperoxidase catalyzes the peroxide oxidation of labeled iodide to iodine. The labeled iodine is then incorporated into the tyrosine residues of the protein to produce radioiodinated protein.

Problems with the lactoperoxidase technique may arise when too much (or too little) H_2O_2 is liberated from the immobilized enzyme preparation (84). Some evidence suggests that sensitive proteins may be damaged by excess peroxide.

Another method that is frequently used in labeling proteins is the thyroid peroxidase (TP) method. This method is also an enzymatic method; however,

fibrinogen labeled with TP shows modifications in the Aα chain. Until this modification can be explained, labeling fibrinogen using this technique seems inappropriate.

Tables 4 and 5 show data obtained by Ardaillou and Larrieu on the properties of fibrinogen labeled by the three different methods described above (79). The yield of iodination, as indicated in Table 4 is clearly higher for the LP method than for the ICl method (90% vs 50% respectively). 98% of the ^{125}I was bound to the TCA precipitable protein. Thus the concentration of free iodine after dialysis, irrespective of the labeling technique employed was < 2%. Table 4 also shows that 86% (ICl) and 85% (LP) of the label was recovered in the fibrin clot after addition of thrombin to the fibrinogen preparations. 94% (ICl) and 96% (LP) of the radioactivity was
recovered in the fibrinogen peak when labeled protein was subjected to gel filtration. Thus, with the exception of the yield of iodination, the properties of fibrinogen labeled by the ICl method or the LP method were similar in the hands of these investigators.

It should also be noted that the substitutions occur in the three chains in roughly the same proportions for each labeling method as indicated in Table 5. Approximately 50% to 54% of the substitutions occur in the Bβ chain, and the rest are shared equally by the Aα and γ chains. The numbers of tyrosine residues in the α, β, and γ chains are 9, 21, and 20 respectively. Thus it appears that the α and β chain label proportionally to their tyrosine content while the γ chain tyrosines are much less reactive. As noted previously the substitutions occur in roughly the same proportions irrespective of the labeling

Table 4

Properties of Fibrinogen Labeled by three Different Methods (79)

Test	ICI	L.P.	T.P.
Iodination Yield	50%	90%	80%
Free Iodine After Dialysis	<2%	<2%	<2%
Clottable Radioactivity	86%	85%	75%
Sepharose 48 Gel Filtration			
- Radioactivity in the fibrinogen peak	94%	96%	86%
- At the top of the column	<2%	<2%	<5%

Table 5

Recovery of ^{125}I in Fibrinogen chains in Polyacrylamide Gel Electrophoresis(79)

	Radioactivity in Fibrinogen Line (%)	Radioactivity in Different Chains		
		Aα	Bβ	γ
ICI Method	95.6±0.92	19.7±0.7	53.7±2.89	21.1±2.42
Lactoperoxidase Method	89.4±2.66	21.5±1.24	50.0±6.09	19.7±1.63
Thyroid Peroxidase Method	85.5±2.64	18.7±3.7	52.5±5.38	20.4±1.82

technique employed, thus suggesting that the same labeling reactions are occurring.

Figure 18 shows the results obtained from a clotting study of fibrinogen labeled by the ICI, LP, and TP methods. The in vitro clotting activity of ICI labeled fibrinogen does not appear to be significantly different from that of unlabeled fibrinogen. However, the polymerization behaviour of fibrinogen labeled by the TP technique appears to be significantly altered, thus indicating that modification of the protein is occurring due to labeling.

To summarize, fibrinogen labeled by the ICI and LP techniques behaves in vitro similarly to unlabeled fibrinogen (79). However, the lactoperoxidase technique results in fibrinogen of much higher specific activity.

2.3.4 Methods of Studying Protein Adsorption using Radiolabeled Proteins

Protein adsorption can be studied using radioactive tracers. This section of the report outlines a few of the methods currently used in the study of protein adsorption using radioactive labels.

As mentioned previously most adsorption studies, using radioactively labeled proteins, have involved exposing surfaces for a designated length of time to the protein solution, followed by rinsing. The surface concentration of protein is determined by comparing the bulk solution radioactivity to the surface radioactivity. This technique, as briefly described above, was used in the present work to study the adsorption characteristics of a thermally treated protein layer. The disadvantages of this method are that short time studies are not feasible, and the rinsing procedure may result in the removal of some of the protein bound to the surface. However this classical, off-line, non-real time

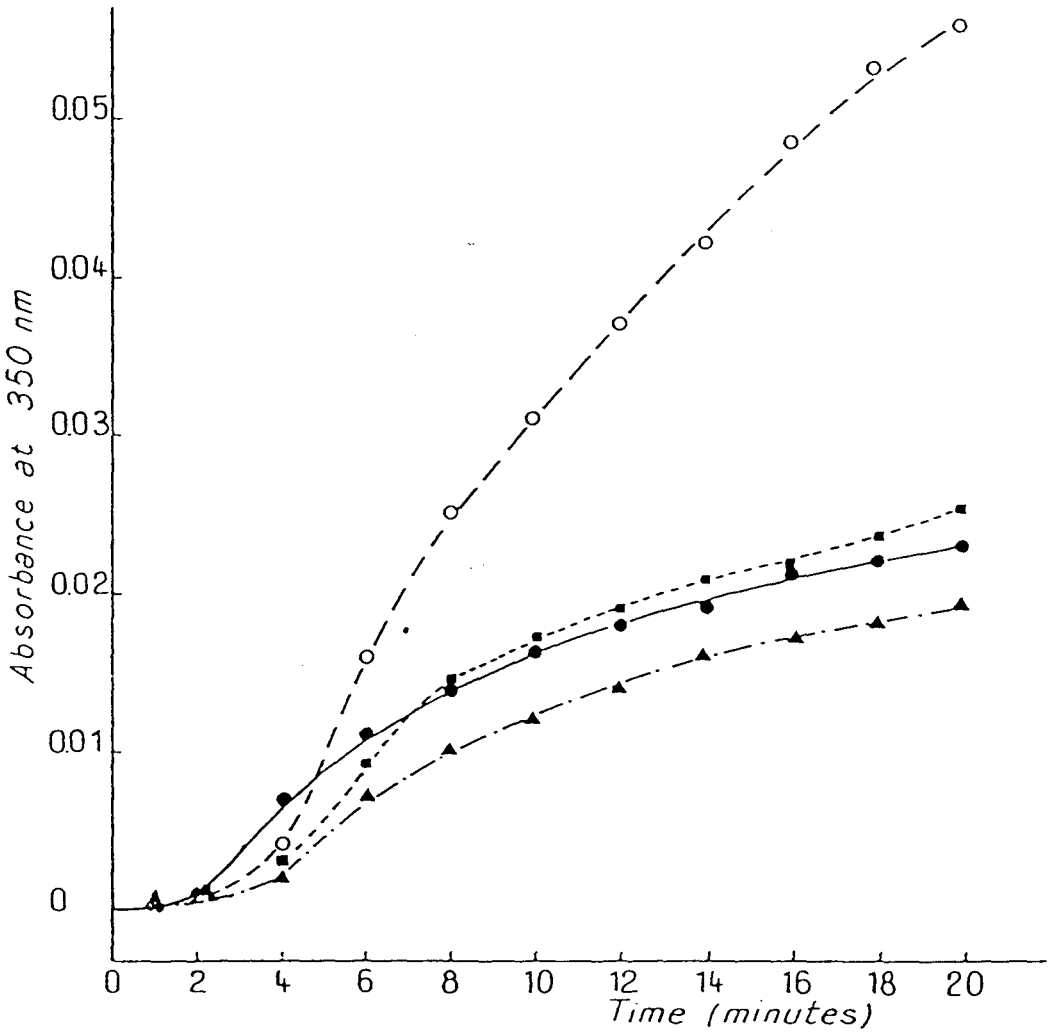

Figure 18. Polymerization studies of fibrinogen after addition of thrombin. •----• unlabeled, ■- - -■ LP, ▲-·-·-▲ ICI, o- -.-o TP (79).

method is the one that has been used in the vast majority of adsorption studies using labeled proteins reported thus far.

Recent work by Baszkin et al (85) involved measurements of the accumulation of radiolabeled protein bound on an adsorbing surface in situ as a function of time. This adsorption/desorption technique was based on the use of ^{14}C-labeled proteins and enabled the distinction to be made between irreversibly and reversibly bound proteins. ^{14}C emits characteristic β rays which have a mean free path in aqueous solution of 0.16 mm. Thus if a detector is placed near a surface in contact with a solution, radioactivity from a thin layer of solution as well as from protein adsorbed to the surface will be measured. In order to distinguish between adsorbed and solution protein, two experimental runs were performed. The first run was carried out in the presence of the adsorbing protein. The radioactivity recorded during this run was due to adsorbed and solution protein. The second run was carried out under the same geometrical conditions but using a ^{14}C-labeled, non-adsorbing solute. Thus, the radioactivity levels recorded during this run originated solely from the solution close to the interface. The data from the second run could be subtracted from those of the first to give the radioactivity of the adsorbed protein and the surface concentration could then be calculated. The distinct advantage of this technique is that it allows for continuous measurements of adsorption over time under static conditions. Such a technique cannot, however, be used with γ-emitting isotopes since the range of γ rays is much greater. Radioactivity from the entire solution would reach the detector. Since the solution radioactivity is then much greater than the adsorbed radioactivity, adsorption

cannot be measured by such a "difference" method when γ-emitting isotopes are used.

The radiolabeling based technique described in this report involves the real time in situ analysis of protein adsorption under flow conditions. The experimental approach is based on a variation of the method of solution depletion and is similar to the technique described by Pefferkorn for studying the adsorption of synthetic polymers(86). Recent work using a similar method has been performed by Aptel and Voegel to study the adsorption of human albumin onto hydroxyapatite powder (87). The method used in the work reported in this thesis is described in detail in the next chapter.

3.0 Experimental

In this chapter a brief overview of the general approach and technique employed to study protein adsorption in real time is given. The materials used in the experimental work and their sources are indicated and a detailed account of the experimental methods used is also given.

3.1 General Approach and Technique

Protein adsorption has been studied extensively in the last few years, and data have been obtained using several different experimental techniques. Quantitative data have been obtained using methods such as radiolabeling (67), total internal reflection infrared spectroscopy (88), immunochemical labeling (63), ellipsometry, total internal reflection fluorescence (88), and electron microscopy. Many of these methods require the rinsing away of the protein solution prior to measurement of the surface. Rinsing almost certainly removes at least a part of the reversibly bound protein, leaving only the irreversibly adsorbed protein on the surface. The exact amount of reversibly bound protein lost will also vary depending on the rinsing method, thus introducing an element of arbitrariness into the measurement.

The experimental approach developed in this report involves the monitoring of protein adsorption using the method of solution depletion modified so that data are obtained continuously in real time. The technique employed is similar to that used by Pefferkorn to study the adsorption of polyacrylamide on solid surfaces(86). More recently, Aptel and Voegel have used the method of solution depletion to study the adsorption of human albumin onto hydroxyapatite powder(87).

A protein solution containing a radioiodinated tracer protein is injected at a constant flowrate into a well stirred cell containing the adsorbing surface under study in particle form. The adsorption can be determined from its effect on the depletion of protein in the bulk solution. Thus the continuous measurement of solution radioactivity as adsorption proceeds allows the corresponding in situ adsorption to be determined. A distinct advantage of this procedure is that it enables short time intervals to be studied, thus allowing the researcher to study the " real time" course of events however rapidly they may be occurring. Another advantage is the elimination of the rinsing step, thus enabling the determination, in situ, of both the reversibly and irreversible bound proteins.

In developing the method it was found that adsorption on surfaces contacted by the protein solution other than that of the particles being studied needed to be minimized. An effective method of doing this by thermal treatment of a layer of adsorbed fibrinogen was developed. In brief, this procedure involved exposing the surfaces to a 1 mg/mL fibrinogen solution for two hours at room temperature followed by treatment in an oven at 70°C for ten minutes. This procedure appeared to minimize adsorption on the glass tubing and cell surfaces of the experimental system.

3.2 Materials and Equipment List

The following is a list of materials and equipment used in the experimental work of this thesis:

1. Pooled citrated human blood plasma- Source: Canadian Red Cross (courtesy of Dr. George Adams)
2. Human fibrinogen- Source: Kabi, Stockholm, Sweden

3. Pyrex glass tubing (0.1 cm I.D., 0.17 cm O.D.)- Source: Corning Glass
4. Glass beads- Source: Cataphote Division, Ferro Corporation, Jackson, Mississippi.
5. Three way teflon valves- Source: Pharmaseal, Toa Akta, Puerto Rico
6. Tygon tubing (1/32" I.D., 3/32" O.D. and 3/32" I.D., 5/32" O.D.)- Source: Fisher Scientific, Pennsylvania
7. 60 mL plastic syringes- Source: Becton- Dickinson, Rutherford, California
8. Gamma counter- Source: Beckman, Fullerton California
9. Model 802-3 NaI(Tl) chrome plated scintillation detectors (2)- Source: Canberra Industries Inc., Meriden, Connecticut
10. Model 3002 multichannel analyzer- Source: Canberra Industries Inc., Meriden, Connecticut
11. Tris (hydroxymethyl) amino methane- Source: Boehringer Manheim, GmbH , West Germany
12. ^{125}I (10 mCi/mL)- Source: ICN Biomedical Canada Ltd., Montreal, Quebec
13. ^{125}I (100 mCi/mL)- Source: Amersham Laboratories, Buckinghamshire, England
14. Enzymobead radioiodination reagent- Source: Biorad, Richmond, California
15. Chromerge- Source: Manostat, New York, New York

16. Glycine- Source: Biorad, Richmond, California
17. D-glucose- Source: BDH Chemicals, Toronto, Ontario
18. Na_2HPO_4 $7H_2O$- Source: BDH Chemicals, Toronto, Ontario
19. Analytical grade anion exchange resin AG 1-X4 - Source: Biorad, Richmond, California
20. NaOH- Source: BDH Chemicals, Toronto, Ontario
21. Speed adjustable syringe pump- Source: Harvard Apparatus, Millis, MA.
22. Eppendorf centrifuge- Source: Brinkmann Instruments, Rexdale, Ontario
23. Sodium Dodecyl Sulphate (SDS)- Source: Biorad, Richmond California
24. Labquake Shaker- Source: Labindustries Incorporated, Berkeley, California
25. Immune Serum Globulin (Human)-Source: Connaught Laboratories Limited, Willowdale, Ontario
26. Albumin (Human)-Source: Behringwerke AG, Marburg, W. Germany

3.3 Experimental Methods

The experimental methods involved in the preparation of buffers, the protein labeling procedures, the surface preparation, and the adsorption studies are detailed in this section of the report.

3.3.1 Preparation of Isotonic Tris Buffer

Isotonic Tris buffer was prepared by dissolving 48.8 g electrophoretically pure Tris in distilled water and making up the volume to 1000 mL in a volumetric flask. 27 mL 0.4 N HCl solution was mixed with distilled water and the volume brought up to 500 mL. The two solutions were added to 881 mL distilled water. The pH was adjusted to a point between 7.35 and 7.40 by the addition of small amounts of concentrated HCl solution. The resulting buffer was sealed in a plastic bottle and stored at room temperature.

3.3.2 Preparation of ICl

A stock iodine monochloride solution was prepared by dissolving 150 mg NaI in 8 mL 6N HCl, and 108 mg $NaIO_3$ H_2O in 2 mL distilled water. The solutions were then mixed and brought to a volume of 40 mL with distilled water. This mixture was shaken with 5 mL CCl_4 until a pink colour was no longer visible in the organic phase. Residual CCl_4 was removed by aerating for approximately one hour. The resulting solution was made up to 45 mL with distilled water to form stock ICl solution. The stock solution, kept in a glass stoppered cylinder at 2 to 4°C, can be drawn on for several years with no loss in iodine value (84).

One part of the stock solution was mixed with 9 parts 2 M NaCl solution to give a 0.0033 M ICl solution in 1.8 M NaCl. This solution was then used in the ICl labeling process.

3.3.3 Preparation of Glycine Buffer

75 g glycine and 58.5 g NaCl were dissolved in distilled water . The volume was brought up to 500 mL to form a 2M glycine solution in 2M NaCl. 2.0 N NaOH was added to the resulting solution until a pH of 8.8 was reached.

3.3.4 Iodine Monochloride Labeling Procedure

Fibrinogen was labeled using the iodine monochloride technique initially described by McFarlane (77). This procedure results in a substitution of iodine in the aromatic rings of the tyrosine residues. The biological activity of the labeled fibrinogen has been shown to be unaffected provided that less than 1 iodine atom per molecule of protein is incorporated (77-79).

The amount of fibrinogen labeled for each experiment varied, although the labeling procedure was essentially the same. Typically, 0.467 mL fibrinogen solution (approximately 10 mg/mL in 0.05M Tris buffer, pH 7.35) was prepared for labeling by the addition of 70 µL glycine buffer (pH 8.8). 35 µL glycine buffer was added to 0.1 mL ICl solution (0.0033M) immediately prior to labeling. 5 µL $Na^{125}I$ was mixed with the ICl for two minutes. The fibrinogen solution was then carefully mixed with the ICl, avoiding air bubbles as much as possible. The unbound ^{125}I was then removed by passing the preparation through a 3 mL column containing a strong anion exchange resin that had been previously equilibrated with isotonic Tris buffer. The column was rinsed with approximately 5 mL Tris buffer and the rinse fluid added to the labeled fibrinogen solution. For experiments that required a large amount of fibrinogen, two to three labeling reactions were performed as described.

3.3.5 Preparation of 0.2M Phosphate Buffer

62.5 g NaH_2PO_4 $7H_2O$ was dissolved in distilled water and the volume brought up to 2,000 mL. Concentrated NaOH was added until a pH of 7.2 was obtained. The buffer was stored in a glass flask at room temperature for a length of time not exceeding one week.

3.3.6 Preparation of 1% Beta-D-Glucose

0.5 g α-D-glucose was dissolved in a small amount of distilled water and the volume brought up to 25 mL. The mixture was placed in a refrigerator at 2-4°C overnight to allow it to mutarotate. The glucose thus prepared could be stored for a period of up to 1 week at 2-4°C.

3.3.7 Lactoperoxidase Labeling Procedure

The lactoperoxidase labeling technique is an enzymatic method which involves oxidation of the iodide by peroxide and incorporation of the resulting iodine into the protein tyrosine residues (79,82,83). The enzymatic reaction is more desirable than the chemical methods of iodination since it is mild and minimizes changes in the labeled protein (79). The yield of iodination is higher for the lactoperoxidase method than for the ICl method (e.g. 90 vs 50% respectively) (79).

Enzymobead reagent was rehydrated with 0.5 mL distilled water and separated into 50 µL aliquots at least one hour before use. The aliquots not used were frozen at -40°C for future use. 200 µL 0.2M phosphate buffer (pH 7.2) was added to 50 µL Enzymobead reagent. 50 µL protein (10 mg/mL) dialyzed overnight into phosphate buffer was added to the reagent followed by 8 µL $Na^{125}I$ (100 mCi/mL) and 50 µL beta-D-glucose. After mixing the reagents, the iodination was allowed to proceed for 30 minutes at room

temperature. The reaction was "quenched" by centrifugation (3200 g for 1 minute) to remove the Enzymobead reagent from the mixture. The supernatant was then passed through a column containing AG-1X4 anion exchange resin which had been previously equilibrated with isotonic Tris(pH 7.35). This step removed any unbound ^{125}I. The column was then rinsed with 5 mL of Tris buffer.

3.3.8 Surface Preparation for Adsorption Studies

Glass Tubing: Glass tubing (0.17 or 0.10 cm I.D.) was cut into 20 cm lengths and placed in Chromerge for one hour. It was then thoroughly rinsed with distilled water and equilibrated overnight in isotonic Tris buffer, pH 7.35.

Glass Beads: The glass beads (mean diameter 41.01 μm) were placed in Chromerge overnight and then rinsed extensively with distilled water. The pH of the wash water was monitored in order to ensure sufficient rinsing had taken place. The glass beads were then dried in an oven overnight at 50°C. Before an experiment the required amount of beads were weighed and equilibrated overnight in isotonic Tris buffer, pH 7.35.

3.3.9 Static Adsorption Experiments Using Glass Tubing

Static experiments involved the attachment of 3 way valves to each end of the glass tubing segments. A side arm was attached to the inlet valve so that air bubbles could be removed from the system and prevented from entering the tubing segment. A drain tube was attached to the outlet valve. As mentioned previously, the tubes were filled with isotonic Tris buffer, and allowed to equilibrate overnight to ensure that water uptake and ion exchange, if any, was complete.

Labeled protein solution was taken up into a syringe and injected into the buffer-filled tubing segments at a rate of 3 to 4 mL per second. A total of 20 tube volumes of solution was used to displace the buffer. Care was taken beforehand to ensure that any leading air bubbles were removed through the inlet side arm (see Figure 19). Upon reaching the end of the required adsorption time the tube was rinsed with approximately 20 volumes of isotonic Tris buffer injected at a rate of 3 to 4 mL per second. After a 5 minute interval the tube was rinsed a second time and drained. The three way valves were then removed. The tube was cut up into 5 cm lengths and placed in scintillation vials for counting. All tubing specimens, and appropriate calibrating solutions, were counted for ten minutes. Using an average surface area, the quantity of adsorbed protein per unit area of surface was calculated.

Thermal Treatment of Adsorbed Fibrinogen Layers and Related Procedures

Tubes similar to those used for static adsorption experiments were exposed to a fibrinogen solution at a concentration of 1 mg/mL for a minimum of two hours. They were then placed in an oven at a given elevated temperature for a designated length of time (thermal treatment procedure). The tubes were then rinsed extensively, and exposed to a labeled protein solution for a minimum of 2 hours, as described above, to determine whether adsorption would occur. The tubes were then rinsed with 20 volumes of isotonic Tris. After a 5 minute period the tubes were again rinsed and then cut into 5 cm lengths. The tubes were counted for ten minutes.

Variations on the above procedure were performed in order to establish the optimum thermal treatment procedure that would minimize adsorption on the cell and tubing walls during flow experiments. These include:

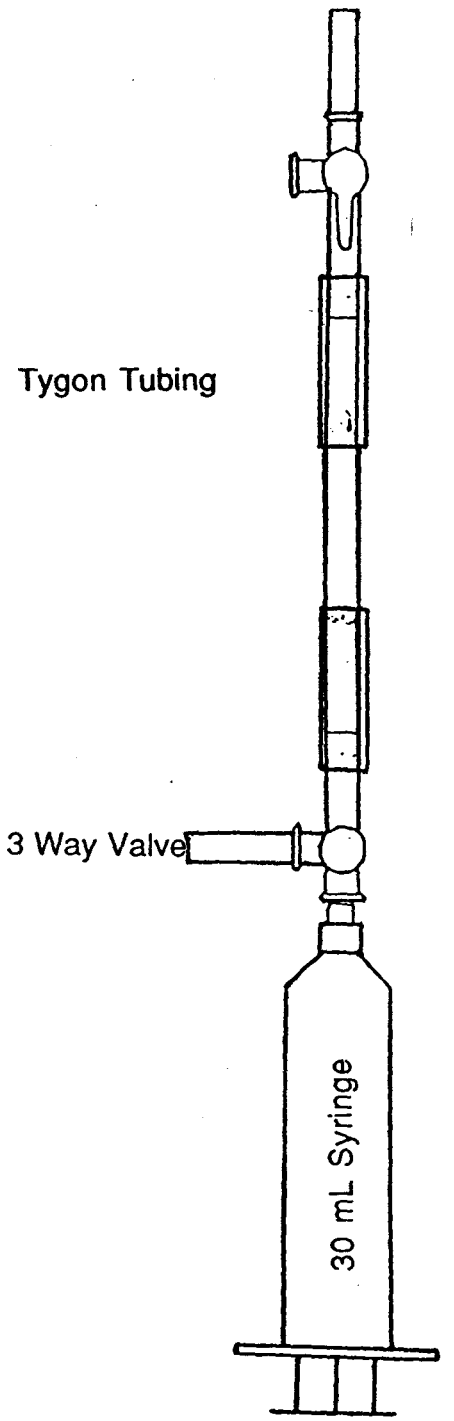

Figure 19. Experimental set-up for static adsorption experiments.

1) Varying the fluid contained in the tubes during heating (buffer, fibrinogen solutions, or empty tube).
2) Varying the heating time.
3) Varying the heating temperature.
4) Application of initial adsorbed fibrinogen layer using labeled protein.
5) Varying the pH of the adsorbing fibrinogen solution.

Experiments were also carried out on the thermally treated fibrinogen layer to determine how firmly it was attached to the glass surface. These experiments involved:

1) Exposure to unlabeled fibrinogen under static conditions.
2) Exposure to plasma under static conditions.
3) Exposure to fibrinogen and plasma solutions at different flow rates.
4) Exposure to salt solutions of different concentrations.
5) Exposure to SDS solutions.

Based on the results obtained from these experiments, a thermal treatment procedure was chosen which resulted in a layer that was firmly attached to the interface, and which provided a reasonably non-adsorptive surface. This procedure was used to treat the tubing and cell surfaces prior to in-situ experiments to minimize adsorption onto these surfaces.

Off-line Adsorption Experiments using Glass Beads

The chemical composition of the glass beads used in this work is given in Table 6, from which it is seen that the beads are essentially of soda-lime glass. The range of diameters quoted by the supplier was 37 to 44 μm. Studies

performed by the Ontario Research Foundation Fine Particle Laboratory indicated that the glass beads had a mean diameter of 41.01± 1.16 μm, and an average surface area of 611.56 cm^2/g (Coulter counter analysis). In order to study the adsorption characteristics of the glass beads, a number of solution depletion experiments were performed off-line. The information from these experiments was intended for use in designing the "on-line" in-situ adsorption experiments. The procedure followed is outlined here.

Table 6

Chemical Composition of Glass Beads*

Component	% Composition
SiO_2	72
Na_2O	15
CaO	7.0
MgO	4.2
Fe_2O_3	0.37
Al_2O_3	0.3
Pb	0.2
K_2O	0.2
B_2O_3	trace

* The glass beads are manufactured from high grade glass compounds and have an excellent resistance to most common acids. The composition is of a type to resist wear and fracture. The approximate diameter was 37 to 44 μm and the beads contain no more than 2% irregular shaped particles.

Measured quantities of glass beads (approximately 100 mg) were placed in 1.5 mL Eppendorf tubes and clamped in a Labquake shaker. Isotonic Tris was added, and the glass beads were equilibrated overnight with the shaker in continuous operation.

The Eppendorf tubes containing the glass beads were then centrifuged for 1 minute at 3,200 g, and the Tris buffer removed. A protein solution containing the radioactively labeled protein under study was then added to the glass beads and the Labquake shaker started. The glass beads were equilibrated with the protein solution for a minimum of 2 hours. The shaker was then stopped and the tubes centrifuged for 1 minute at 3,200 g.

Measured samples of the supernatant contained in the Eppendorf tubes were taken and placed in scintillation vials for counting. These samples along with samples of the initial protein solution were counted for 10 minutes. Using the method of solution depletion, the adsorption of protein on the glass beads (without rinsing) was calculated.

It should be noted at this point that although most of the equilibrating buffer is removed after centrifugation, allowances in the calculations must be made for the trapped fluid in the volume between the particles. The trapped buffer, in itself, will result in a decrease in the radioactivity of the labeled protein solution that is added to the glass beads. Although the volume of trapped fluid was small (i.e. <3% of the volume added) it could have a significant affect on the results if not taken into account when depletion of protein in the bulk solution is small.

In some experiments the glass beads, following adsorption and centrifugation, were extensively rinsed with isotonic Tris buffer. The

radioactivity of the rinse was monitored, and when the level approached background, the rinsing was stopped. The glass beads were then placed in scintillation vials and counted. The adsorption of fibrinogen on the glass beads after rinsing was then calculated. The glass beads contained in the Eppendorf tubes were exposed subsequently to a measured amount of 2% SDS overnight with the shaker in continuous operation. The glass beads were again centrifuged and samples of the SDS solution were counted. The amount of protein thus eluted from the glass beads was determined, and compared to the adsorption value obtained by counting the beads.

3.3.10 Real Time In Situ Adsorption Experiments

As with the off-line experiments using glass beads, the cell, connecting glass tubing and a measured quantity of glass beads were equilibrated overnight in isotonic Tris buffer prior to an experiment. In order to prevent adsorption of protein on the cell and the glass tubing surfaces, these components underwent a surface treatment procedure as follows.

Thermal Treatment Procedure

The glass cell (see Figure 20) having an effective volume of 14.6 mL, and a 20 cm length of 1 mm I.D. glass tubing were exposed to an unlabeled 1 mg/mL fibrinogen solution for two hours at room temperature. They were then placed, in the presence of fibrinogen solution, in an air oven for ten minutes at 70°C. The cell and tubing were subsequently rinsed extensively with isotonic Tris buffer and stored in isotonic Tris until needed.

This treatment minimized protein adsorption on the walls of the cell and glass tubing during adsorption experiments. It was particularly important to minimize adsorption on the glass tubing that was placed directly in front of the

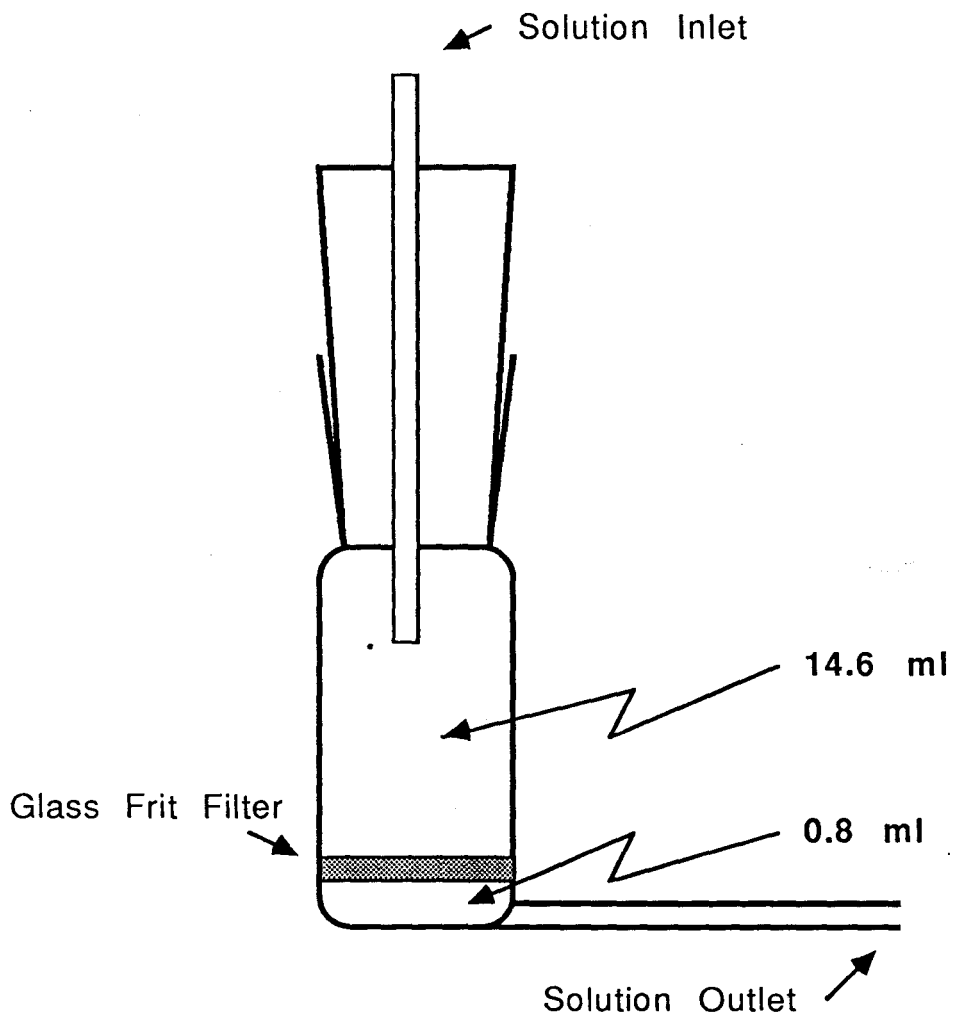

Figure 20. Glass cell used in the real time analysis of protein adsorption.

detectors to obtain a continuous measurement of the radioactivity in the solution leaving the cell during an in situ adsorption experiment. Any adsorption onto the walls of this tubing would interfere with the determination of solution radioactivity. The adsorption cell underwent thermal treatment, as did the glass frit filter contained in it. The frit with its large surface area would, if left untreated, contribute significantly to solution depletion in the cell thus interfering with the measurement of adsorption to the particles placed in the cell.

Real Time In Situ Adsorption Experimental Set-up

The overall experimental arrangement is shown in Figure 21. Tygon tubing (0.08 cm I.D., 0.23 cm O.D.) was attached to the inlet and outlet of the thermally treated reaction cell. The tygon tubing at the outlet of the cell was attached to a 20 cm length of 1.0 mm I.D. thermally treated glass tubing. The glass tubing was secured in a lead holder and placed between the two detectors, as shown in Figure 22a. Tygon tubing was attached to the outlet of the glass tubing leaving the detector area and led to a waste beaker. The two detectors were placed directly in contact with the glass tubing and shielded on all sides by approximately 5.5 cm of lead (see Figure 22b).

Each detector consisted of a monoline crystal assembly which included a high resolution NaI(Tl) crystal, a photomultiplier tube, an internal light shield and a chrome plated aluminum housing. The assembly was attached to a tube base and coupled to a high voltage power supply and multichannel analyzer.

The output voltage on the high voltage power supply (Canberra model 3002), was adjustable over the full range from 0 to ±3000V by means of two calibrated front panel voltage controls. Most photomultipliers, such as the one used in this work, are operated in the range of 900 to 1000 volts. Preliminary

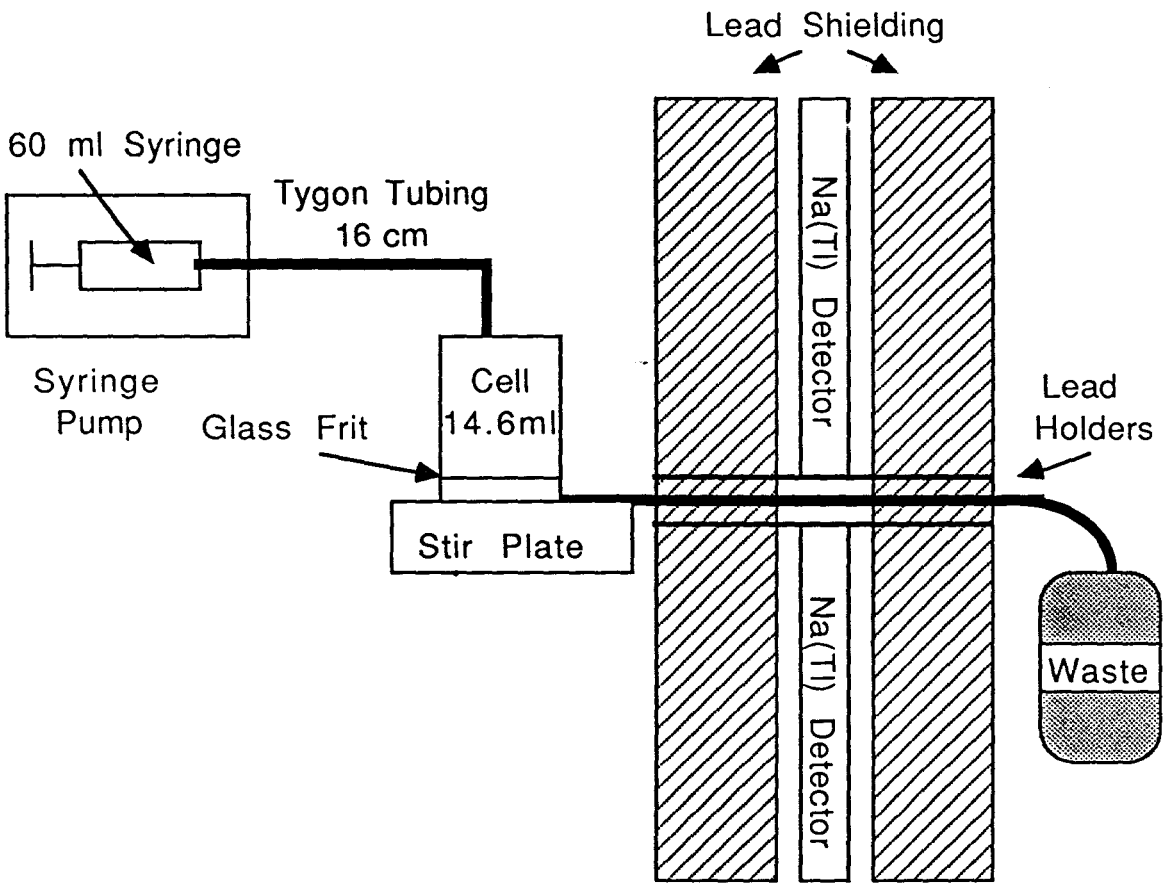

Figure 21. Experimental set-up used in the real time analysis of protein adsorption.

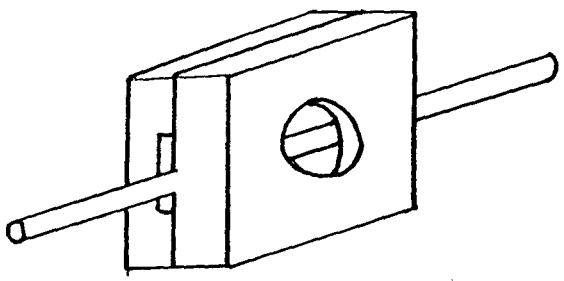

Figure 22a. Lead holders used to secure glass tubing.

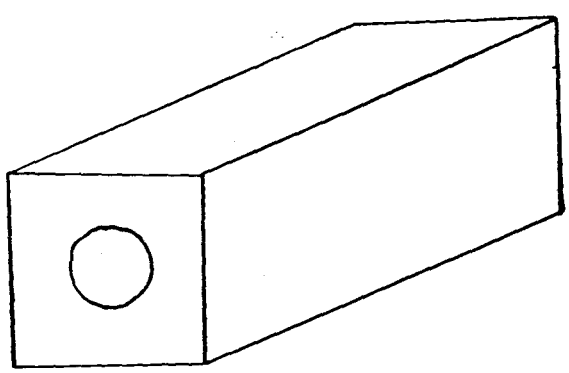

Figure 22b. Lead blocks used to shield detectors.

experiments performed to establish the integral spectrum of the photomultiplier tube indicated that the level of high voltage supply could not exceed 1000 volts. Beyond this level, a significant number of noise pulses were detected. The operating voltage generally used was 900 volts. The amplification of the photomultiplier, as emphasized in the discussion above, is strongly dependent on the high voltage; thus the voltage supply must be very stable. A meter was used to monitor the output voltage, and in general no fluctuations were noted over the course of a typical experiment. The multichannel analyzer, operated in the multichannel scaling mode, provided the essential function of collecting and storing radioactivity data for the solution leaving the cell as a function of time. The multichannel analyzer also provided a means of visual monitoring. Figure 23 shows a schematic of the system set-up.

After the detectors were placed in position, the high voltage power supply and multichannel analyzer (MCA) were turned on. A system initialization procedure was performed on the MCA, and the dwell time (count accumulation time) set to 30 seconds. The high voltage supply was then set to 900 volts. Radioactivity data for the solution leaving the adsorption cell were collected in the MCA and later analyzed on a microcomputer. This procedure is discussed in more detail in the following sections.

Determination of Background Radiation Level

The reaction cell and tubing were filled with isotonic Tris buffer before placement of the glass tubing into the lead holder. A syringe, containing buffer, was placed in the adapter of a Harvard syringe pump and attached to the tygon tubing at the inlet to the reaction cell. The pump and data collection on the multichannel analyzer were started simultaneously. The background radiation

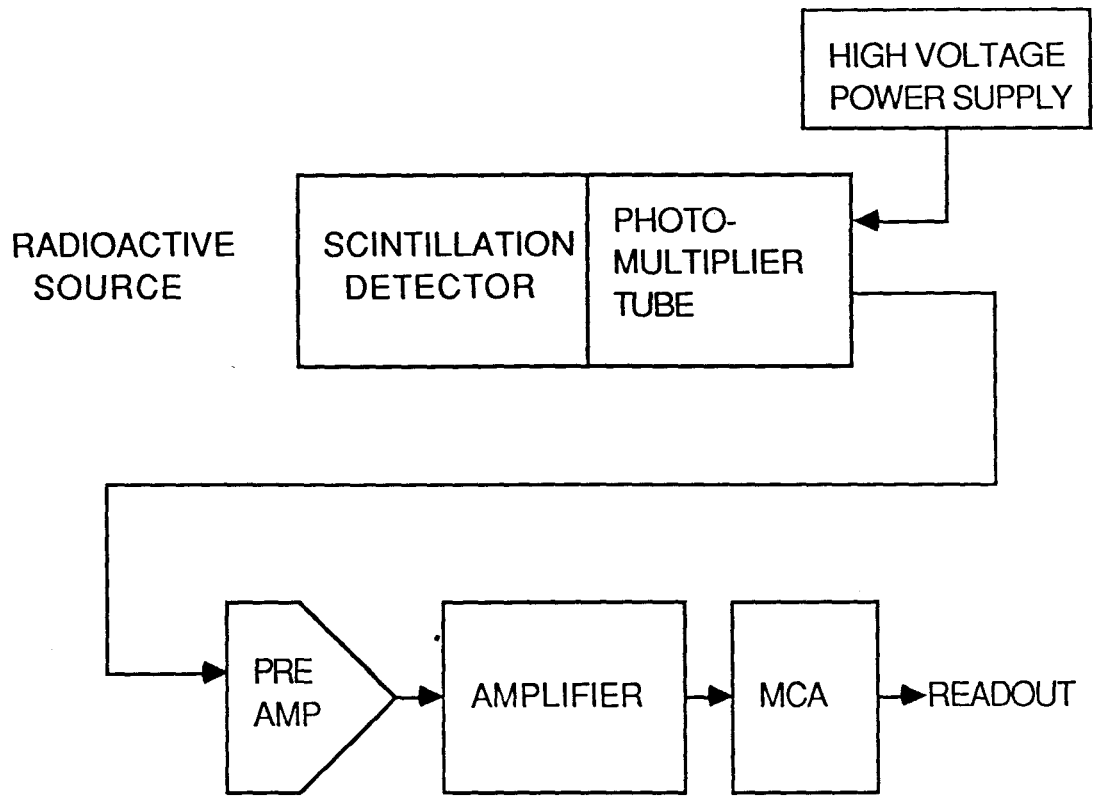

Figure 23. Schematic representation of the detection equipment used in the real time analysis of protein adsorption.

level was monitored for a minimum of 10 minutes during which 20 separate 30 second counts were taken. Care was taken to ensure that there were no air bubbles in any portion of the experimental apparatus.

Control Run

In general, two runs were made for each set of experimental conditions; a control run and an adsorption run. The control run refers to the experiment performed in the absence of any particulate adsorption surface in the cell. This run serves to monitor the variation in cell effluent radioactivity over the course of time due simply to displacement of the starting buffer from the cell. The adsorption run was carried out in a manner similar to the control run, but with the adsorbing surface under study (i.e. glass beads) present in the cell.

A syringe containing the radioactively labeled protein solution under study was placed in the adapter of the Harvard adjustable speed syringe pump. The pump was started and allowed to run until solution appeared at the needle tip. This was done in order to ensure that there was no air in the syringe tip. The pump was then stopped and the syringe connected to the tygon tubing at the inlet of the cell. The amount of radioactive fluid in the syringe was recorded. The stir plate beneath the cell was then turned on and the pump and data collection on the MCA were started simultaneously .

The run was allowed to continue for 90 minutes. The pump was then stopped, the volume of solution in the syringe was again recorded, and the waste volume measured.

The cell was then detached from the experimental apparatus and rinsed extensively. Tris solution was injected into the glass tubing, and the count rate checked to ensure that the background radiation level had remained

unchanged and thus that no adsorption had occurred on the walls of the glass tubing during the run.

The data collected in the MCA during the run were transferred to a microcomputer for analysis.

Adsorption Run

The glass bead run was carried out in the same manner as the control run, except that the adsorbing surface under study was present in the cell, as a suspension of particles in isotonic Tris. Again, isotonic Tris was pumped through the system, and care was taken to ensure that there were no air bubbles present in either the tubing or reaction cell.

A syringe containing the radioactively labeled solution under study was placed in the adapter of the pump as was done for the control run. The pump was started and allowed to run until radioactive fluid was present at the needle tip. The pump was then turned off and the syringe attached to the tygon tubing at the inlet of the cell.

The volume of radioactive fluid in the syringe was recorded. The stir plate was then turned on, the pump was started, and data collection on the MCA was begun. The run was allowed to continue for a minimum of 90 minutes, at which point the pump was shut off, the volume of fluid contained in the syringe was again recorded, and the waste volume measured. As with the control run, the experimental cell was rinsed extensively.

The glass tubing passing through the detectors was rinsed with 20 volumes isotonic Tris and several 30 second counts taken to ensure that no adsorption of radioactive material onto the walls had occurred.

A solution count used to calibrate the in situ radioactivity data in terms of mass of protein was obtained by injecting the starting radiolabeled protein solution directly into the tubing passing through the detector. Data were collected for a minimum of 10 minutes (i.e. 20 counts of 30 seconds), and then transferred to the microcomputer. These data provide a means of determining the quantity of radioactivity associated with a predetermined amount of protein.

3.3.11 Systems Studied

Experiments were carried out on both single component fibrinogen solutions and on plasma containing labeled fibrinogen, IgG and albumin.

Fibrinogen Solutions

Numerous experiments were conducted on pure fibrinogen in isotonic Tris buffer, pH 7.35 (the single component system). The concentration of fibrinogen was determined by measuring UV absorbance at a wavelength of 280 nm. The absorbance reading was converted to concentration in mg/mL using an extinction coefficient of 1.55 for fibrinogen. Experiments were carried out over a range of concentrations from 40 μg/mL to 300 μg/mL. Also, the effect of flow rate was studied at a given fibrinogen concentration.

Plasma

Flow experiments were run using plasma diluted to varying extents in Tris buffer. These experiments were all carried out using the same plasma pool. This plasma pool had a fibrinogen concentration of 2.7 mg/mL as determined by clotting with thrombin, digestion of the clot and biuret analysis of the resulting solution. A measured amount of radiolabeled fibrinogen (approximately 1 to 8% of the existing fibrinogen concentration) was added to

the plasma. Tris buffer was again used to obtain the desired plasma dilution. Plasma concentrations studied ranged from 1% to 20% of normal.

The effect of flow-rate on the adsorption and subsequent desorption of labeled fibrinogen from plasma was studied at a designated plasma concentration.

The adsorption from diluted plasma of two other proteins, namely IgG and albumin, were briefly studied. The plasma pool used was the same as that used for the fibrinogen studies. This plasma pool had an IgG concentration of 7.84 mg/mL and an albumin concentration of 34.7 mg/mL. IgG in plasma was determined by the single radial immunodiffusion method. Albumin was determined by formation of a colour complex with bromcresol green. Measured amounts of radioactively labeled protein (either IgG or albumin) were added to the plasma. Tris buffer was again used to obtain the desired dilution. Plasma concentrations studied were 0.1% and 1% for IgG, and 1% for albumin.

4.0 Data Analysis

A brief overview of the data analysis procedures, used to obtain a measure of adsorbed amount of protein, is given in this section of the thesis. Both the static adsorption experiments on glass tubing as well as the adsorption experiments on glass beads both off-line and in real time are discussed.

4.1 Static Adsorption Experiments

The fibrinogen concentration, C_f, of the solutions used in the experiments was determined from UV absorbance using a spectrophotometer at a wavelength of 280 nm. The calculation is based on Beer's law assuming a 1 cm path length:

$$C_f = \frac{A}{\varepsilon} \quad . \qquad [14]$$

Where

C_f = concentration of fibrinogen (mg/mL)

A = absorbance

ε = extinction coefficient (mL/mg)

The calculation of quantity of protein adsorbed per unit area of tube surface was based on an assumed average area per measured tubing segment of 5 cm length. The internal diameter was measured for several of the tubes and averaged. A simple calculation was then carried out to determine the average area (S):

$$S = \pi(I.D._{avg})L \qquad [15]$$

Generally, a 10 minute count of each of the 5 cm lengths of tubing was performed in order to assure sufficiently high counts. The counts obtained were divided by the length of the counting interval (i.e. usually 10 minutes) to obtain the counting rate.

A count of the radioactive solution used was taken for each experiment, generally for a 0.1 mL sample. As with the tubing, counts were obtained for 10 minute intervals. However, the Beckman Gamma counting system used for these measurements does not count past 1,000,000 counts in any specified counting interval. Thus, for highly radioactive solutions, the length of the counting interval was reduced to the range of 2 to 3 minutes. It should also be noted that the Beckman counting system does not count effectively at rates greater than 600,000 counts per minute (CPM). Above this count rate, significant losses are incurred. Thus, when solution counts exceeded 600,000 CPM, the volume of radioactive fluid measured was decreased, and the counting repeated. The counting rates per mL of radioactive solution were determined by the following calculation:

$$A_o = \frac{\text{Solution Count}}{tV} \qquad [16]$$

Where

A_o = solution counting rate (counts / min mL)
t = time interval
V = Volume of radioactive fluid counted (mL)

The surface concentration of protein on the tubing surface was calculated according to Equation 17.

$$\Gamma = \frac{C_f A_S}{A_o S} \qquad [17]$$

Where

Γ = Fibrinogen surface concentration ($\mu g/cm^2$)

C_f = Fibrinogen solution concentration in ($\mu g/mL$)

A_S = Counts per minute of radioactive material adsorbed

S = Area (cm^2) (see Equation 15)

A_o = Solution counts (counts per minute per mL solution)

The adsorption data obtained for off-line experiments performed on glass tubing are generally based on four samples and are reported (in Section 5.2) as average adsorption value ± standard deviation. The four samples refer to four-5 cm pieces of tubing originating from a single 20 cm length of tubing. Thus, the standard deviation reported refers to the variation in surface concentration (i.e. within an experiment) along the glass tube. It should be emphasized here that the results are generally reported for a single experiment unless otherwise noted. However, experiments were repeated in order to check reproducibility.

4.2 Off-line Equilibrium Adsorption Experiments on Glass Beads

The equilibrium adsorption of protein in-situ on the glass beads was determined by the method of solution depletion. An initial solution count of the labeled protein solution was obtained before each experiment. Generally, a 10

minute count was taken and the count rate per minute per mL of solution was calculated by Equation 16.

After equilibration of the glass beads and radioactive protein solution, a count of the supernatant solution was obtained. The adsorption of protein on the glass beads (before rinsing) was calculated according to Equation 18.

$$\Gamma = \frac{(A_o V_o - AV)\, C_f}{A_o S} \qquad [18]$$

Where

A_o = initial solution count (counts / min mL)

A = supernatant count (counts / min mL)

V_o = initial volume of protein solution exposed (mL)

V = initial volume of protein solution exposed + trapped fluid (mL)

C_f = fibrinogen concentration (μg / mL)

S = Area (cm^2)

In some experiments, extensive rinsing of the glass beads was carried out. The rinsed beads along with the initial solutions were counted, and adsorption after rinsing calculated according to Equation 19.

$$\Gamma = \frac{A_s C_f}{A_o S} \qquad [19]$$

Where

A_s = glass bead count (counts / minute)

A_o = initial solution counts (counts / min mL)

C_f = fibrinogen concentration (μg / mL)

S = surface area of beads (cm^2)

Some experiments also involved the removal of the adsorbed protein using 2% SDS solutions, following an extensive rinse. Samples of the SDS solution were counted and the adsorption of protein onto glass beads after rinsing was calculated according to Equation 20. These data provide an alternative method of determining the adsorption of protein to the beads after rinsing.

$$\Gamma = \frac{AVC_f}{A_o S} \qquad [20]$$

The equilibrium adsorption data on glass beads are reported as average ± standard deviation, under a given set of experimental conditions for 4 samples. However, as mentioned previously, experiments were repeated in order to ensure reproducibility.

The off-line experiments performed on the glass beads, as discussed above, gave an indication of the adsorption values to expect on-line under flow conditions. The off-line studies also demonstrated the importance of the effect of rinsing.

4.3 Real Time In Situ Adsorption Experiments

As indicated previously, two runs were generally carried out for each set of experimental conditions; a control run and an adsorption run. The control run refers to the run made in the absence of any adsorbing material. Under these

conditions, a simple differential radioactivity balance on the cell can be written as follows:

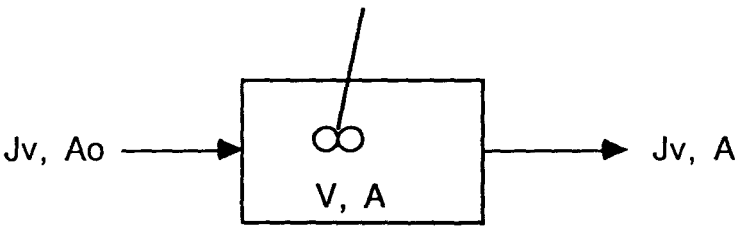

Accumulation in the Cell	=	Inflow to Cell	-	Outflow from Cell

$$V\frac{dA}{dt} = J_V A_o - J_V A \qquad [21]$$

Where

J_V = Flow-rate (mL / min)

V = Cell volume (mL)

A_o = Radioactivity of solution entering the cell (counts / min mL)

A = Radioactivity of solution exiting the cell (counts / min mL)

t = Time (min)

The above analysis implies that the cell is well mixed so that the radioactivity within the cell is identical to that in the exit stream. The solution to Equation 21 is given by Equation 22:

$$A = A_o\left(1 - \exp\left(\frac{-J_V t}{V}\right)\right) \qquad [22]$$

The value of A as a function of time was calculated for each control experiment from Equation 22, and was compared to the experimental data, thus providing a check that the system was behaving as expected.

Following the control run, the same experiment was carried out in the presence of glass beads. Based on the data collected from this experiment, the amount of radioactivity on the surface of the beads could be calculated from the radioactivity balance,equation 21, modified to include a term for adsorption to the glass beads:

Accumulation in the Cell (bulk solution)	=	Inflow to Cell	-	Outflow from Cell	-	Surface Bound Radioactivity

$$VA(t) = J_V A_o t - J_V \int_0^t A(t)dt - SA_S(t) \qquad [23]$$

$$SA_S(t) = J_V A_o t - VA(t) - J_V \int_0^t A(t)dt \qquad [24]$$

Where

S = surface area of glass beads (cm^2)

$A_S(t)$ = surface radioactivity at time t (counts / min cm^2)

J_V = flow-rate (mL/min)

A_o = radioactivity of solution injected (counts / min mL)

V = cell volume (mL)

$A(t)$ = radioactivity at cell outlet at time t (counts / min mL)

Equation 24 enables the variation in surface radioactivity to be determined over the course of time based on the A(t) data obtained from the adsorption run. Knowledge of the surface radioactivity and the appropriate calibrating solutions enabled the surface concentration of adsorbed material, Γ, to be calculated according to equation 25.

$$\Gamma(t) = \frac{A_S(t)C_f}{A_o} \qquad [25]$$

Where

$A_S(t)$ = surface radioactivity at time t (counts / min cm^2)

C_f = fibrinogen concentration (μg/mL)

A_o = radioactivity of solution injected (counts / min mL)

It should be noted here that the radioactivity of solution passing through the detectors that is counted in any specified interval (A or A_o) has the units of CP x mL. The exact volume of solution counted (x) is not important as the geometry of the system does not change over the course of experiments and the volume of solution counted does not vary. Thus the calculation of adsorption can be carried out as follows:

$$\Gamma = \frac{\left(J_v A_o t - VA(t) - J_v \int_0^t A(t)dt \right) C_f}{SA_o} \qquad [26]$$

It is apparent from the above equation that the adsorption, Γ, is independent of the volume of radioactive solution counted since A (or A_o) appear in each term in the numerator and denominator. Thus if a volume of 0.1 mL of solution were

counted (i.e. x = 0.1 ml) the right hand side of Equation [26] would be multiplied by (10/10) or 1. This is a convenient advantage of the current experimental set-up.

5.0 Results and Discussion

This section of the report presents and discusses the results obtained relating to the thermal treatment of surfaces. This is followed by a more detailed discussion of off-line equilibrium studies, and real time in situ studies.

5.1 Preliminary Experiments

A number of preliminary experiments were performed in order to test the feasibility of the in situ method for measuring adsorption proposed herein, and to become familiar with the experimental procedures involved in the iodine-125 labeling of proteins. During this time experience was also gained in the operation of equipment used in gamma ray detection.

The preliminary experiments involved a system utilizing a closed cell which consisted of a 10 mL conical flask. The radioactive protein solution was injected through a side arm, and exited through a glass tube placed in a single holed stopper at the neck of the flask. The glass beads used as the adsorbing surface were prevented from leaving the cell by a glass wool filter placed at the cell exit. The fluid in the cell (i.e. flask) was vigorously stirred by a magnetic stir bar and it was assumed that the radioactivity per mL of solution at the exit of the cell was equal to the solution radioactivity in the cell. Thus application of a radioactivity balance across the cell, along with continuous measurement of the exit radioactivity, allowed determination of the kinetics of adsorption in situ and in real time.

Numerous experiments were performed using this set-up to establish the feasibility of the solution depletion/serum replacement approach to studying protein adsorption and to find optimum conditions of cell volume, flowrate, stirring, and surface to volume ratio. Results from these experiments indicated

that the adsorption from a single component protein system could be monitored with little difficulty. Typical data for a cell volume of 11.5 mL, a flowrate of 0.15 mL/min, a fibrinogen concentration (isotonic Tris buffer pH 7.35) of 40 μg/mL, and an initial in situ count rate of about 6500 CP1/2M are shown in Figure 24. The data are shown as the level of effluent radioactivity, for a counting interval of 30 seconds, plotted against time for both the control run and the glass bead run. As can be seen from Figure 24, significant differences between the control run (carried out in the absence of adsorbing surface) and the adsorption run were observed, indicating that adsorption can readily be detected.

Experiments were performed to determine if the solution flowrate was constant over the time period of a typical experiment. The flowrate is a particularly important variable that must be carefully controlled in order to ensure valid and reproducible results. Unknown fluctuations in flowrate could have a significant effect on the calculated adsorption (see Equation [26]). To verify that flowrate was constant over time a solution was injected into the closed cell system described above, and aliquots were collected at the cell exit into pre-weighed test tubes. The test tubes were then re-weighed and the weight of the liquid aliquot determined. Knowledge of the density of the fluid enabled the volumetric flowrate to be calculated. It was established that the injected flowrate was constant over the time periods studied, typical of an on-line experiment, as is shown in Figure 25.

During the course of the preliminary experiments, significant fluctuations in background radioactivity were noted. This was due to the close proximity of radioactive sources, other than that under study, to the detectors. It was

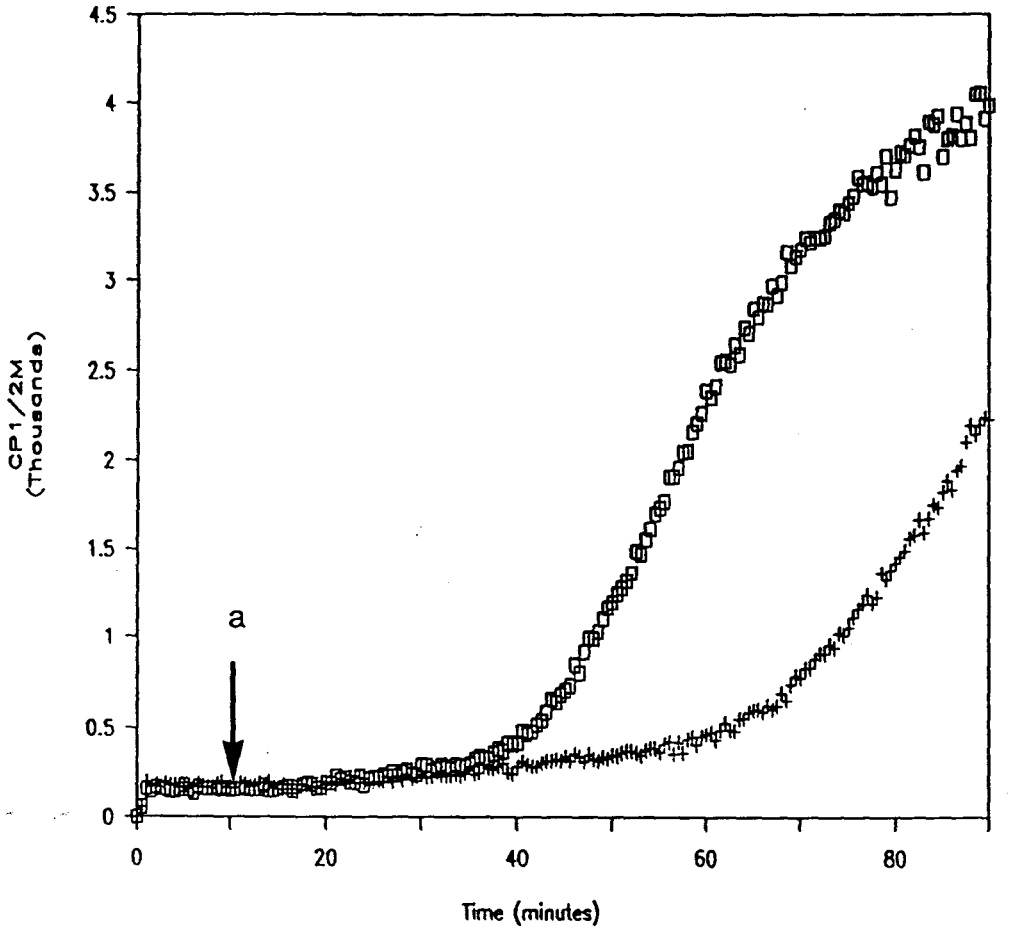

Figure 24. Variation of the radioactivity of the cell effluent as a function of time. (C_f = 40 µg/mL, J_v = 0.15 mL/min, V = 11.5 mL, S= 685 cm^2, A_o = 10473 CP1/2M) (□) Activity recorded in the absence of glass beads. (+) Activity recorded in the presence of glass beads. (a) Calculated time when radioactive material should reach the detector.

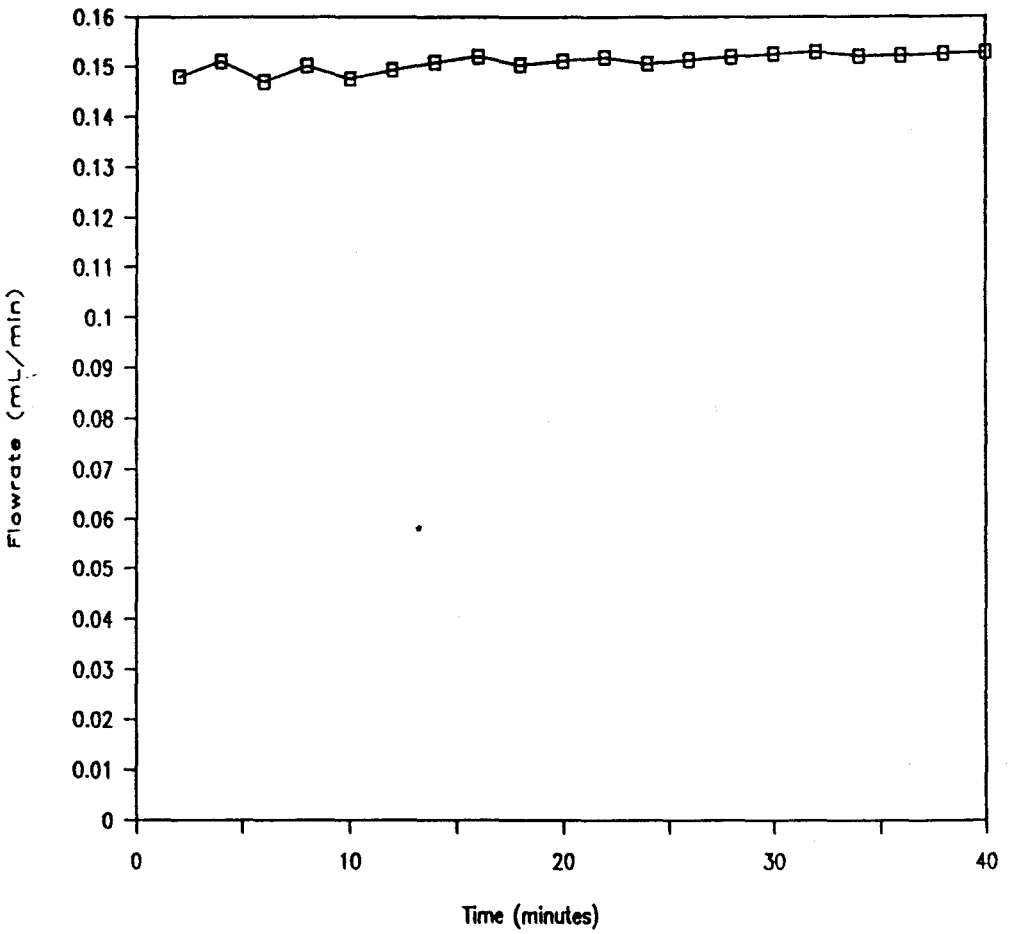

Figure 25. Variation in flowrate over time.

particularly important that the detectors be shielded from the radioactive solution at the exit of the flow system, and the radioactive material contained in the syringe at the inlet. Also, a Beckman Gamma Counter used extensively by other researchers for counting radioactive material was relatively close (4 feet) to the detectors. This further emphasized that the detectors required shielding from the various radioactive sources in the laboratory in order that accurate results be obtained. To this end, lead block shields were designed to enclose each detector such that the detectors were shielded on all sides by approximately 5.5 cm of lead as shown previously in Figure 22b. This shielding arrangement resulted in a significantly reduced and constant level of background radiation at the detectors, of the order of 80 - 180 CP1/2M.

In initial experiments it was noted that the first detectable increase in radioactivity occurred substantially later during the control run than would be expected from the known system dead volume and flowrate (see Figure 24). It was hypothesized that this delay might be the result of adsorption of protein on the glass wool filter, and on the walls of the cell itself. Following the completion of a run, the glass tubing segment passing through the detectors was rinsed with isotonic Tris. It was noted that the level of radioactivity on the tubing was significantly higher (10X) than the background radiation level due to adsorption of radioactive protein to the tubing.

In order that an accurate determination of adsorption to the particles under study be made, it was essential that adsorption to the cell walls, filter, and glass tubing be eliminated. Extensive development work was carried out to this end, and a procedure was defined that minimized adsorption on the cell, filter,

and tubing during flow experiments. This procedure is discussed in some detail in Section 5.2.

The results obtained from the preliminary experiments involving the use of lead shielding to minimize background radiation, and a surface treatment procedure to minimize adsorption on the cell, filter, and tubing appeared promising. On the basis of these preliminary data a suitable adsorption cell was designed and constructed (see Figure 20). The glass cell had a fixed volume of 14.6 mL and contained a glass frit filter to retain the particles under study in the cell during an experiment. The results obtained using this cell are discussed in detail in a later section.

The preliminary experiments performed, as discussed above, uncovered problems such as the fluctuation in background radiation, and the necessity of minimizing adsorption on the cell, filter, and tubing surfaces. With the solution to these problems in hand the potential of the system for the real time analysis of protein adsorption appeared both feasible and promising.

5.2 Thermal Treatment Of Surfaces to Minimize Adsorption

During the preliminary experiments, as discussed above, it became apparent that protein adsorption on the cell walls, cell filter, and glass tubing needed to be minimized. The glass frit filter, used to prevent the adsorbing particles from leaving the cell with the cell effluent, had a high surface area and thus would itself cause significant solution depletion if adsorption occurred on its surface. Also, any adsorption onto the glass tubing passing through the detectors would interfere with the determination of protein concentration in the bulk fluid, upon which determination of adsorption depends. Thus, it was important that the adsorption of protein be minimized on these surfaces.

Recent work by Voegel et al suggested the possibility of forming a thermally treated layer of fibrinogen on solid substrate surfaces that is non-adsorbing for a variety of proteins (45). Using this approach extensive experiments were performed to develop a surface treatment procedure which would minimize protein adsorption. These are now described.

5.2.1 Effect of Solution Composition During Treatment on Adsorption to Thermally Treated Fibrinogen Layers

Experiments were performed in which the fluid contained in the tubes during heating of the adsorbed fibrinogen layer was varied. The adsorbed layer was established by exposing tubes to a 1 mg/mL unlabeled fibrinogen solution for a minimum of 2 hours at room temperature, then heating in a forced air oven at a designated temperature and time. The tubes were then rinsed and subsequently exposed to an ^{125}I-labeled protein solution (1 mg/mL, 2 h exposure) to determine if additional adsorption or exchange of adsorbed and bulk proteins took place. The results obtained for an oven temperature of 70° C and a time of 10 minutes are shown in Table 7.

It should be noted that tubes exposed only to labeled fibrinogen (1 mg/mL, 2h) with no prior thermal treatment gave an average adsorption of 0.511 ± 0.033 μg/cm^2. A tube exposed to unlabeled fibrinogen for two hours with no thermal treatment, then to labeled fibrinogen resulted in accumulation of radioactivity corresponding to 0.156 ± 0.009 μg/cm^2 of fibrinogen. Assuming that equilibrium was reached in the initial adsorption, it may be concluded that approximately 30% of the initially adsorbed fibrinogen exchanged with solution fibrinogen in the second exposure. These results are consistent with data obtained by Chan and Brash (44) indicating that under these conditions the

fraction of the adsorbed layer that can be exchanged is of the order of 30%; the remaining 70% is unexchangeable.

Table 7

Effect of Fluid Contained in Tubing During Heating on the Adsorption of Fibrinogen onto a Thermally Treated Fibrinogen Layer (Temperature, 70°C; Time, 10 min)

Fluid in Tubing During Heating	Fibrinogen * Adsorption ($\mu g/cm^2$)
Air	0.209±0.021
Isotonic Tris Buffer (pH 7.4)	0.147±0.022
Fibrinogen Solution	0.030±0.000

* 1 mg/mL solution in isotonic Tris, 2h exposure.

As seen in Table 7, adsorption to the layer formed by heating in air was slightly higher than to the same layer with no thermal treatment as discussed above (0.209 versus 0.156 $\mu g/cm^2$). In these experiments it is unclear whether the protein in the bulk solution exchanges with fibrinogen on the surface, or additional adsorption onto the preadsorbed layer occurs. If necessary, to investigate this further, one could use a double labeling technique in which both protein populations are labeled using different isotopes.

Adsorption to (or exchange with) the layer formed by heating in the presence of buffer was significantly less than to the layer heated in air. However, when heating was done in the presence of fibrinogen solution the subsequent adsorption (or exchange) of fibrinogen was virtually eliminated. Thus it appeared that the composition of the fluid contained in the tube during thermal treatment significantly affected the protein adsorption capacity of the

layer. The layer formed by heating in the presence of fibrinogen solution gave the least adsorptive surface. Based on these results, the thermal treatment procedure was routinely carried out in the presence of fibrinogen solution.

5.2.2 Effect of Treatment Temperature on Adsorption to Thermally Treated Fibrinogen Layer

Experiments were performed to study the effect of temperature and time of heating on the subsequent adsorption of labeled protein onto a thermally treated fibrinogen layer. These experiments were necessary in order to determine conditions that would minimize adsorption onto the experimental apparatus during flow experiments.

Tubes were exposed to an unlabeled fibrinogen solution at a concentration of 1 mg/mL for two hours. The tubes filled with fibrinogen solution were then placed in the oven at designated temperatures for specific lengths of time. They were then rinsed and exposed to a labeled fibrinogen solution (1 mg/mL, 2 h) to determine the amount of fibrinogen adsorbed onto, or exchanged with, the thermally treated surface. A summary of the results is shown in Table 8 and Figure 26.

It appeared, based on Table 8, that increasing the temperature resulted in less adsorption (or exchange) of protein onto the thermally treated layer. However, time of heating up to 10 minutes appeared to have little effect on the subsequent adsorption. Other heating times (i.e. 15 and 20 minutes) were studied, but again appeared to have little effect on the adsorption of fibrinogen onto the thermally treated layer.

Experiments were performed at temperatures above 70°C to determine if a further increase in temperature would result in a decrease of adsorption onto

the thermally treated layer. It was found that the adsorption onto the thermally treated layer could not be reduced to levels less than those obtained at 70°C.

Table 8

Effect of Treatment Temperature on the Adsorption of Fibrinogen onto a Thermally Treated Fibrinogen Layer

Time (minutes)	Temperature (°C)	Fibrinogen * Adsorption (μg/cm^2)
5	50	0.0573±0.007
10	50	0.0551±0.010
5	60	0.0237±0.002
10	60	0.0263±0.004
5	70	0.0197±0.001
10	70	0.0210±0.003

* 1 mg/mL solution in isotonic Tris, 2 h exposure.

It has been reported previously (45) that the adsorption of fibrinogen to glass is partly reversible below 70°C. This could explain the higher apparent adsorption onto the thermally treated layer below 70°C (see Table 8) if it is postulated that below 70°C some of the fibrinogen adsorbed on the surface exchanges with fibrinogen in the bulk solution. However, it appeared that the dense layer that was obtained at 70°C was essentially irreversibly bound, and did not exchange with fibrinogen in the bulk solution. This finding is consistent with the results obtained by Voegel et al (45). Based on the data presented above, it appeared that heating at 70°C for 10 min would provide a minimally adsorptive surface.

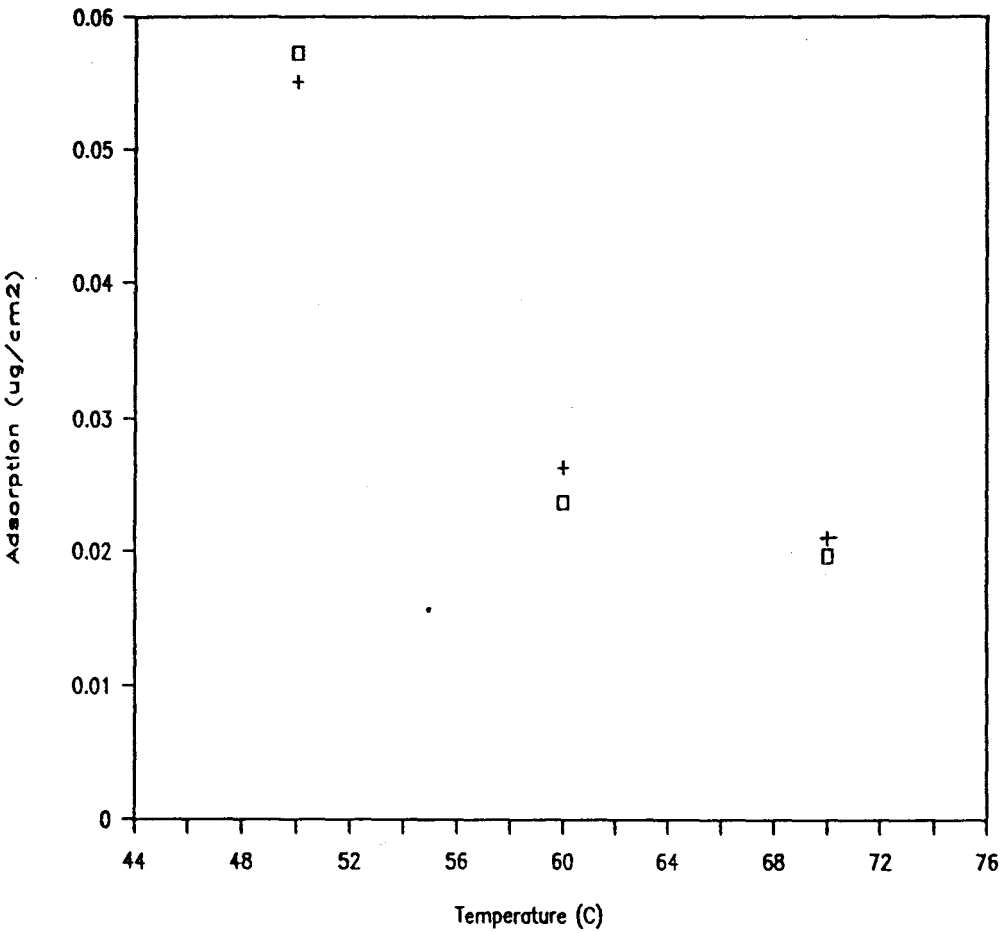

Figure 26. Adsorption of fibrinogen to a preadsorbed, thermally treated fibrinogen layer vs. temperature during thermal treatment. (□) 5 min heating time. (+) 10 min heating time.

5.2.3 Effect of Treatment Temperature on Quantity of Fibrinogen in Thermal Layer

In relation to the thermal treatment process further investigations were made in order to better understand the effect of elevated temperatures on the adsorption of fibrinogen to glass. Tubes were exposed to a 1 mg/mL fibrinogen solution containing ^{125}I-labeled protein at room temperature for a period of two hours. The tubes filled with fibrinogen solution were then placed in an oven at a designated temperature for a period of 10 minutes. The effect of oven temperature on the surface concentration of adsorbed fibrinogen is shown in Table 9 and Figure 27. The data show that secondary heating at temperatures between 50°C and 85°C results in a large increase in adsorption. Adsorption was higher at 50°C and decreased at higher temperatures, suggesting the existence of a maximum between room temperature and 50°C (see Figure 27).

Table 9

Effect of Temperature on the Adsorption of Fibrinogen to Glass *

Oven Temperature (°C)	Adsorption (μg/cm^2)
Room temp. (20°C)	0.411
50	3.853
60	2.997
70	1.774
80	1.639
85	1.357

* Adsorption in two steps: (1) 1 mg/mL, 2h, room temperature; (2) 1 mg/mL, 10 min, variable temperature as shown.

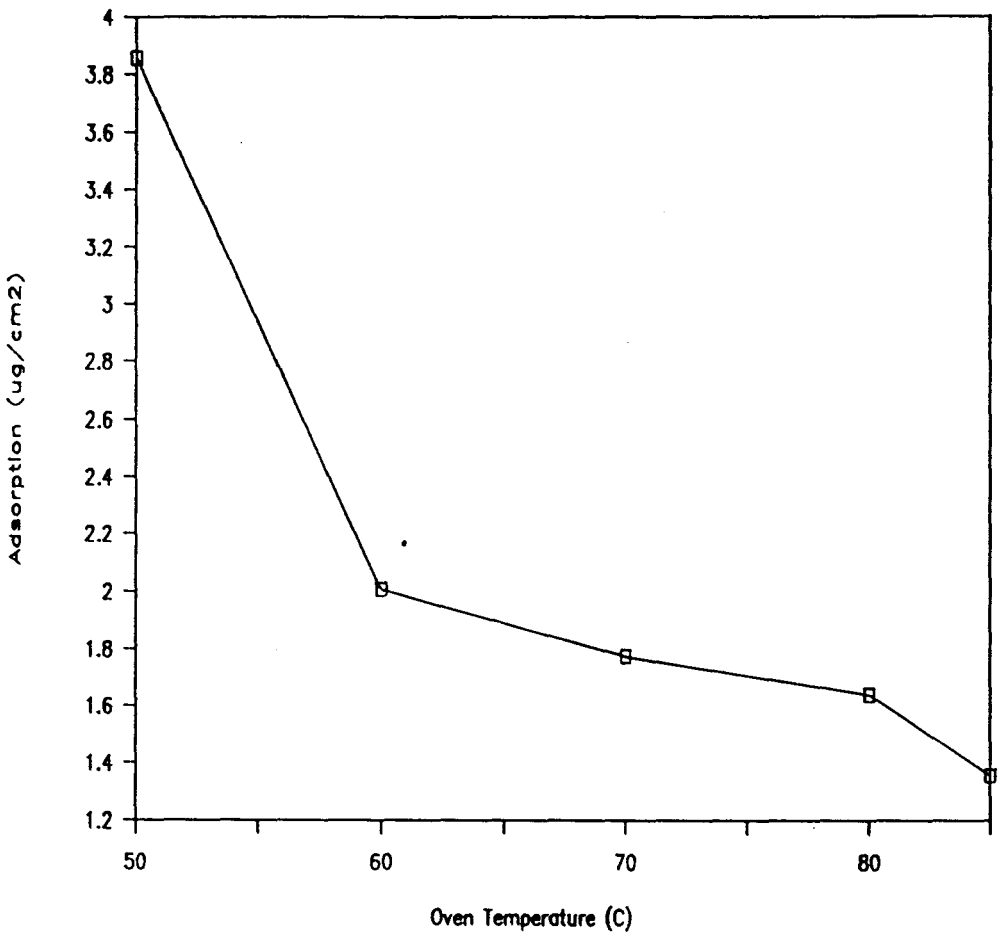

Figure 27. Adsorption of fibrinogen onto glass vs. temperature during thermal treatment . Adsorption in two steps: (1) 1 mg/mL, 2h, room temperature; (2) 1 mg/mL, 10 min, variable temperature as shown.

It should be noted that the data in Table 9 at elevated temperatures represent very high adsorption values. Experiments by other researchers, discussed earlier, indicated that the limiting capacity of glass for fibrinogen adsorption at pH 7.4 is about 0.7 $\mu g/cm^2$. In addition it may be shown that surface concentrations corresponding to a close-packed monolayer of fibrinogen vary from 0.2 to 1.8 $\mu g/cm^2$ depending on molecular orientation in the layer. Thus adsorption values between 1 $\mu g/cm^2$ and 4 $\mu g/cm^2$ suggest multi-layering. These multilayers formed at elevated temperatures must result from fibrinogen in the bulk solution interacting with fibrinogen adsorbed initially at room temperature. Experiments were performed to investigate the possibility that fibrinogen in solution was binding to adsorbed fibrinogen. Studies using SDS-polyacrylamide gel electrophoresis (both reduced and non reduced) suggested that such binding was not occurring.

Subsequently, it was found that increasing the volume of the rinse solution used following thermal treatment significantly reduced the level of adsorption, suggesting that the heating process resulted in additional protein being loosely bound to the surface. Using a rinse volume of 60mL lower adsorption values were obtained of the order of 1.1 ± 0.2 $\mu g/cm^2$ at 70°C.

The interactions of this thermally treated layer with fibrinogen in solution were extensively investigated to determine if exchange between solution and surface molecules occurred, or if the thermally treated layer was stable. These experiments are discussed in the following sections.

5.2.4 Stability of Thermal Layer in Contact with Various Solutions

Although initial experiments indicated that the heated fibrinogen layer adsorbed on the surface did not exchange with the protein in the bulk solution,

several additional experiments were performed to confirm that this was indeed true. Tubes were exposed to a labeled fibrinogen solution at a concentration of 1 mg/mL for two hours at room temperature and then placed in the oven at 70°C for 10 min. They were subsequently exposed to an unlabeled fibrinogen solution or to plasma for a minimum of two hours at room temperature and rinsed extensively. Typical data are shown in Table 10. It should also be noted that the surface fibrinogen concentration of the thermally treated layer is significantly less than shown in Table 9. This is due, as discussed earlier, to the substantial increase in rinse volume used in the later experiments. The data show that there was no loss of radioactivity from the surface on exposure to an unlabeled fibrinogen solution and it may be inferred that neither desorption nor exchange was occurring.

Table 10

Exchange or Removal of Thermally Treated Fibrinogen Layer on Glass by Exposure to Fibrinogen Solution or Plasma*

	Solution Incubated with Thermal Layer	Surface Fibrinogen Concentration of Thermal Layer Following Incubation ($\mu g/cm^2$)
Expt 1	Buffer (Tris)	0.907±0.052
	Fibrinogen (1mg/mL)	0.912±0.064
	Plasma (100% normal)	0.843±0.032
Expt 2	Buffer(Tris)	0.923±0.021
	Fibrinogen (1mg/mL)	1.003±0.051
	Plasma (100% normal)	1.090±0.180

* Thermal layer exposed for 2h, room temperature.

Although the data for plasma are somewhat more scattered it is concluded that little or none of the thermally treated fibrinogen layer was removed or exchanged on exposure to plasma. It should be noted that under similar conditions, adsorbed fibrinogen layers that are not thermally treated undergo significant exchange with fibrinogen in solution or desorption in contact with plasma. Recent work by Voegel et al indicated that no loss or exchange of an adsorbed fibrinogen layer, which had previously been maintained for 15 minutes at 75°C, occurred on exposure to unlabeled fibrinogen and albumin solutions (45). Thus, the results obtained here (Table 10) are consistent with those of Voegel's group.

The above experiments were carried out under static conditions. Further experiments were carried out on the stability of the thermally treated layer under flow conditions to determine whether the thermally treated layer was shear sensitive. Tubes were exposed to a 1 mg/mL fibrinogen solution containing labeled fibrinogen for two hours. They were then thermally treated at 70°C for ten minutes. The tubes were subsequently rinsed and exposed to either buffer, fibrinogen solution, or plasma at differing flow rates. The surface radioactivity was monitored continuously. The results obtained for plasma at flow rates of 1.8 mL/min and 8 mL/min in 1 mm inner diameter glass tubing are shown in Figure 28. As can be seen from the data no significant quantity of the thermally treated layer was removed on exposure to plasma at shear rates up to 1400 sec^{-1}.

As shown above exposure of the thermally treated layer to isotonic Tris buffer, fibrinogen solution or plasma under static and flow conditions did not cause removal of the layer. However earlier work in this laboratory showed that

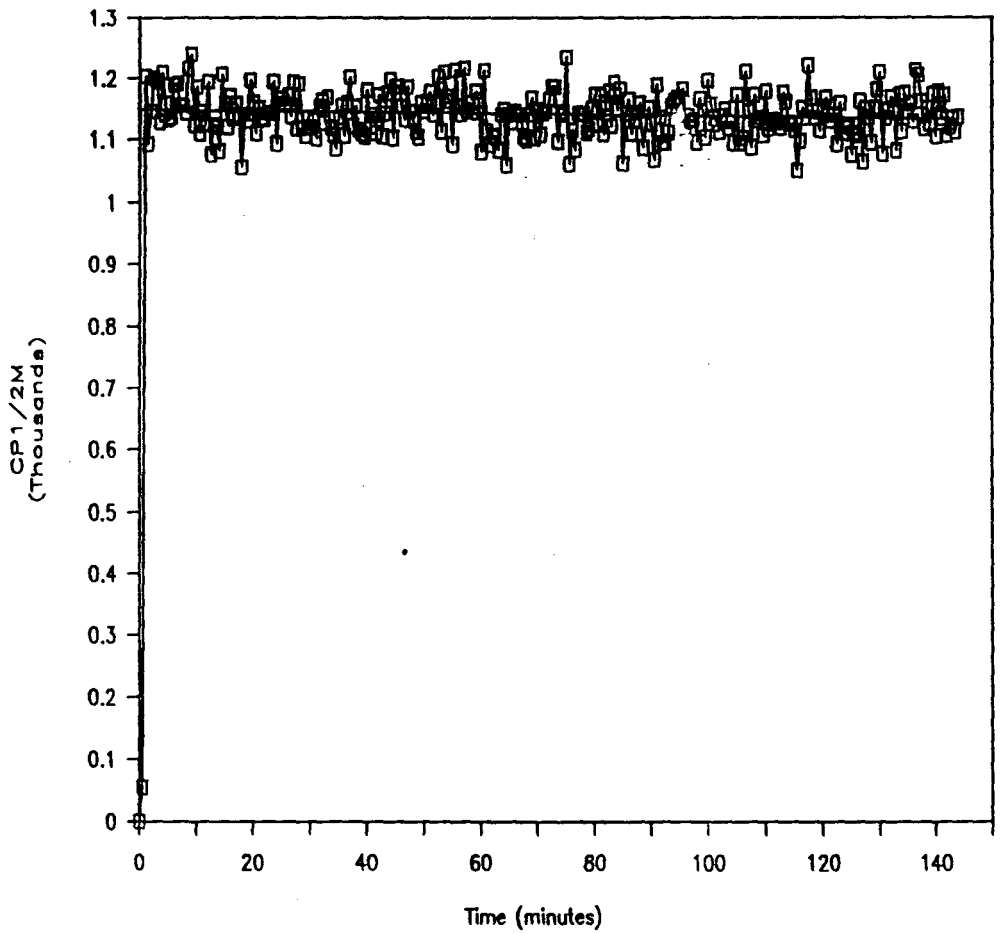

Figure 28. Surface radioactivity vs. time following exposure of a labeled, thermally treated fibrinogen layer adsorbed on glass to plasma. (Plasma flowrate: t = 0 - 60 min, 1.8 mL/min; t = 60 - 125 min, 8 mL/min; t = 125 - 140 min, rinse isotonic Tris buffer.)

desorption of up to 80% of an adsorbed fibrinogen layer (not thermally treated) on glass into solutions of increasing Tris-NaCl concentrations takes place. Therefore the effect of salt on the stability of the thermally treated layer was investigated. Tubes were exposed to a labeled fibrinogen solution (1 mg/mL) for 2 hours, and thermally treated for 10 minutes at 70 °C. They were then exposed to buffers of varying salt concentration for 2 hours and the residual protein adsorption measured. The data are shown in Table 11 and indicate that the exposure of the thermally treated layer to salt solutions up to 1 M had no effect. Thus, the thermally treated layer remained intact even on exposure to high salt concentrations.

Table 11

Effect of Salt Concentration on the Thermally Treated Fibrinogen Layer*

	Solution Composition	Residual Fibrinogen ($\mu g/cm^2$)
Expt 1	Isotonic Tris	1.222±0.100
	Tris-NaCl (0.5M)	1.262±0.146
	Tris-NaCl (1.0M)	1.240±0.026
Expt 2	Isotonic Tris	1.235±0.163
	Tris-NaCl (0.5M)	1.140±0.043
	Tris-NaCl (1.0M)	1.233±0.015

* Layers exposed to salt solutions for 2 h.

As a final check on the layer stability, experiments were performed using sodium dodecyl sulphate (SDS) to determine if the fibrinogen layer could be removed. SDS is a powerful negatively charged detergent which has been used extensively as a protein eluent (44).

Tubes were exposed to a labeled fibrinogen solution for 2 hours and thermally treated at 70 °C for 10 minutes. They were then exposed to a 2% SDS solution for either 2 hours or overnight. The results are shown in Table 12. As can be seen exposure to a 2% SDS solution for 2 hours removes approximately 90% of the adsorbed protein. An exposure time of 24 hours results in the removal of 95% of the layer.

Table 12

Effect of SDS on Thermally Treated Fibrinogen Layers on Glass*

Solution Composition	Residual Fibrinogen ($\mu g/cm^2$)
Isotonic Tris-2h	1.221±0.117
SDS-2h	0.151±0.009
SDS-24h	0.069±0.005

* Layers exposed to Tris or 2% SDS.

To summarize, a glass surface treatment procedure was developed that resulted in minimal adsorption of protein to the treated surface. This procedure consisted of exposure of the glass surface to a 1 mg/mL fibrinogen solution for a minimum of 2 hours. The surface was then heated at 70 °C for 10 minutes in the presence of the fibrinogen solution. This procedure resulted in a non-adsorbing fibrinogen layer that appeared from extensive experiments to be strongly attached to the surface. It was not removed in contact with buffer, plasma, fibrinogen solutions or strong salt solutions.

5.3 In Situ Equilibrium Adsorption Experiments on Glass Beads

A number of in situ experiments to study the adsorption characteristics of the glass beads at equilibrium were performed off-line. It was important that these experiments be carried out to obtain an indication of the adsorption levels

to expect so that a suitable on-line, serum replacement experiment could be designed. The chemical and physical properties of the glass beads were discussed earlier and are outlined in Table 6 (Section 3.3.9). Studies performed by the Ontario Research Foundation Fine Particle Laboratory indicated that the glass beads had a mean diameter of 41.06 ± 1.16 μm and a surface area of 611.56 cm^2/g.

5.3.1 Effect of Iodine Labeling on Adsorption of Fibrinogen to Glass Beads

In the on-line experiments with glass beads, the fraction of labeled protein in the solution studied was variable due to the physical limitations on the quantity of protein that could be labeled. It has been documented previously (89-91), that the labeling procedure may affect the adsorption behaviour of the protein due to the presence of the iodine itself, or the alteration of the protein by iodination. In this regard it has been recommended (91) that the effect of labeling be checked for each protein-surface pair studied.

In order to investigate the effects of labeling on the adsorption of fibrinogen to glass beads, a series of experiments using solutions having the same total concentrations but varying proportions of labeled and unlabeled protein was carried out. Fibrinogen was labeled using the ICI labeling technique. Glass beads were exposed (off-line) for 2 h to 0.5 mg/mL fibrinogen solutions (isotonic Tris buffer, pH 7.35) containing different amounts of labeled protein. Solution counts were obtained before and after adsorption and from the solution depletion (see Section 4.2), the quantity of protein adsorbed to the beads was determined. Table 13 shows the results obtained for fibrinogen in the range of 0.1 to 10 percent labeled protein. As is shown in the table, there

appears to be, within experimental error, no dependence of quantity adsorbed on percent label. Experiments were also performed with fibrinogen solutions containing greater proportions of labeled protein; namely 50 and 100 percent. Again, the adsorption results showed no dependence on percent label.

Table 13

Effect of Iodine Labeling on Equilibrium Adsorption of Fibrinogen to Glass Beads (off-line experiment)*

Percent Labeled Fibrinogen	Surface Concentration of Fibrinogen ($\mu g/cm^2$)
10	1.116 ± 0.191
5	0.910 ± 0.117
1	1.180 ± 0.051
0.1	0.917 ± 0.080

* Solution concentration, 0.5 mg/mL in isotonic Tris buffer, pH 7.35; exposure time, 2h.

It should be noted that possible degradation of the fibrinogen before and after labeling was investigated by SDS polyacrylamide gel electrophoresis. There was no evidence of any alteration in banding pattern of the labeled compared to the unlabeled protein.

The experiments discussed above indicate that adsorption in the fibrinogen-glass bead system is independent of the ratio of labeled to unlabeled protein. Thus, no preferential adsorption of either labeled or unlabeled protein onto the glass bead surface occurred. In addition, studies using gel electrophoresis indicated no protein degradation due to labeling.

5.3.2 Effect of Rinsing on Adsorption of Protein onto Glass Beads

Work by other researchers (44) has shown that a maximum surface concentration of 0.7 $\mu g/cm^2$ is obtained on exposure of pyrex glass tubing to fibrinogen solutions (0.05M Tris buffer, pH 7.35) for two hours under static conditions. The value of 0.7 $\mu g/cm^2$ may be assumed to represent the limiting capacity of glass for fibrinogen under these conditions. However equilibrium adsorption data obtained in situ on glass beads in the present work indicates significantly greater adsorption (see Table 13). It was hypothesized that the greater adsorption was due to the fact that in contrast to the method used to study tubing, the solution depletion procedure used for glass beads does not require that the surface be rinsed free of solution. Clearly rinsing could cause the desorption of loosely bound protein.

In order to investigate the effect of rinsing on adsorption, glass beads were exposed for 3 hours to ^{125}I-labeled fibrinogen solutions of various concentrations. Adsorption was determined without rinsing using the method of solution depletion, as described above. The glass beads were then extensively rinsed and adsorption after rinsing was determined both by counting the radioactivity bound to the glass beads, and by eluting the adsorbed protein using sodium dodecyl sulphate (SDS). Solution counts of the resulting detergent solution were then obtained, and the adsorption determined.

The results obtained for the adsorption of fibrinogen in the range of concentration of 40 $\mu g/mL$ to 500 $\mu g/mL$, before and after rinsing are shown in Table 14 and Figure 29. From these data, it is apparent that rinsing has a significant effect on the adsorption values obtained. The surface concentrations before rinsing, based on the method of solution depletion, are significantly

greater than those after rinsing. Thus, it appears that rinsing may indeed cause the removal of loosely bound protein from the surface of the glass beads.

Table 14

Effect of Rinsing on the Equilibrium Adsorption of Fibrinogen onto Glass Beads (off-line)*

Concentration (μg/mL)	Adsorption Before Rinsing (μg/cm^2)	Adsorption After Rinse (μg/cm^2)	
		Bead Count	Elution
500	1.199 ± 0.172	0.821 ± 0.014	0.925 ± .053
300	1.198 ± 0.194	0.786 ± 0.005	0.843 ± .020
225	1.124 ± 0.093	0.764 ± 0.006	0.807 ± .002
150	1.064 ± 0.066	0.714 ± 0.007	0.762 ± .018
75	0.892 ± 0.033	0.651 ± 0.009	0.668 ± .042
40	0.798 ± 0.006	0.587 ± 0.006	0.596 ± .015

* Adsorption from isotonic Tris buffer, pH 7.35; exposure time 3h.

It should be noted that at the higher solution concentrations, adsorption even after rinsing is greater than 0.7 μg/cm^2 obtained by others(45). It is possible that this discrepancy is due to the fact that rinsing of glass beads is more gentle than for the tubing segments used in previous work. Another, and possibly more likely explanation, is that the surface properties of the glass beads may differ from those of pyrex glass tubing, thus resulting in intrinsic differences in adsorption behaviour.

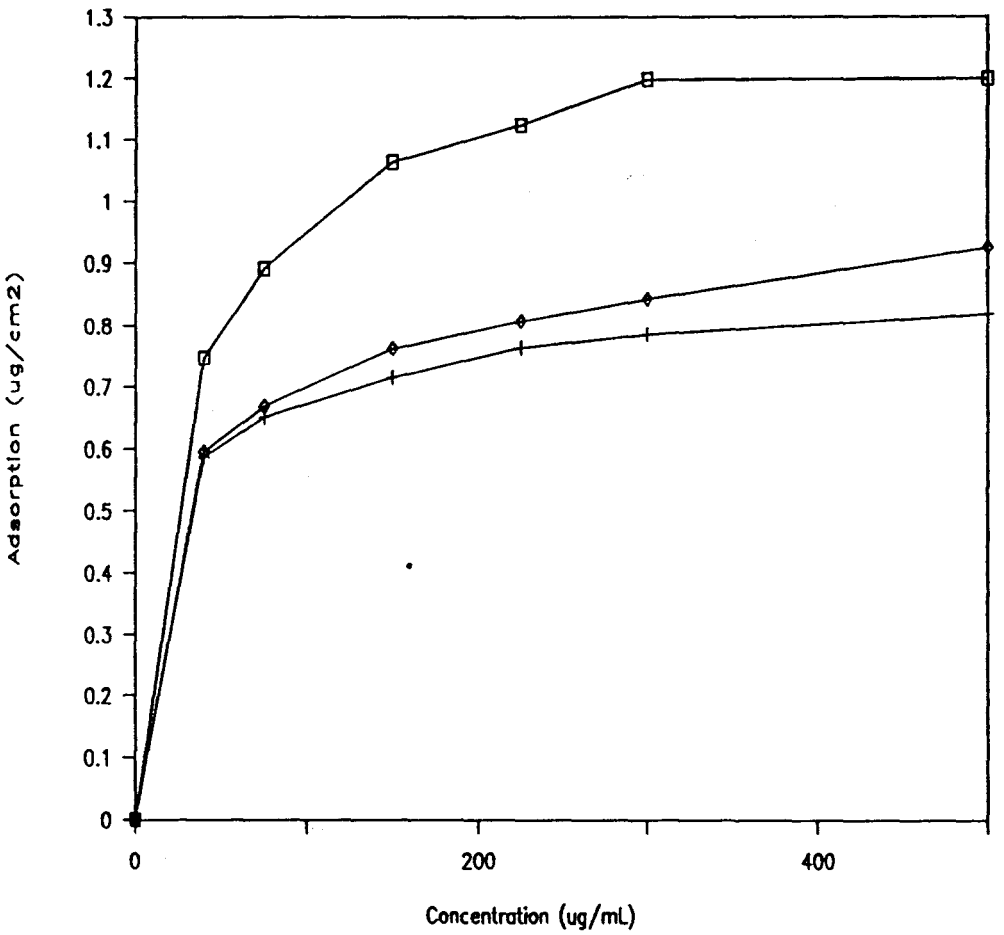

Figure 29. Adsorption isotherms of fibrinogen from isotonic Tris buffer, pH 7.35, to glass beads (3 hr data). (□) Adsorption before rinsing. (◊) Adsorption after rinsing (by elution). (+) Adsorption after rinsing (by direct counting of glass beads).

5.3.3 Adsorption of Fibrinogen to Glass Beads From Plasma: Effect of Plasma Concentration

Solution depletion experiments were performed to investigate the equilibrium adsorption in situ of fibrinogen onto glass beads from plasma. Glass beads were exposed to diluted plasma containing ^{125}I labeled fibrinogen for a minimum of two hours. Plasma was diluted with isotonic Tris buffer and concentrations ranged from 0.1 to 5 percent normal plasma. It was important that these experiments with plasma be carried out to provide an indication of the adsorption values to expect during real time kinetic experiments. In this way experimental variables could be optimally chosen (e.g. labeled protein concentration and surface to volume ratio). Fibrinogen adsorption data before and after rinsing, for a 2 hour exposure, are shown in Table 15 and Figure 30.

The data shown in Table 15 and Figure 30 clearly indicate that adsorption of fibrinogen from plasma passes through a maxima as a function of plasma concentration thus indicating that the Vroman effect is observable by solution depletion as well as by direct measurement. The Vroman effect, as discussed earlier (Section 2.2.4), is the transient adsorption of proteins (particularly fibrinogen) from plasma; it is manifested also as a maximum in adsorption as a function of plasma dilution. Figure 30 shows the quantity of fibrinogen adsorbed from plasma plotted against the bulk concentration for two hour adsorption times. The bulk concentration is expressed as percent of normal plasma concentration, and 100 percent plasma corresponds to a fibrinogen concentration of 2.7 mg/mL. Up to a plasma concentration of approximately 0.5 percent, the surface is presumably filling with protein. At

plasma concentrations greater than 0.5 percent competitive effects among proteins begin to dominate, and the fibrinogen is displaced.

Table 15

Equilibrium Adsorption of Fibrinogen to Glass Beads from Plasma*

Percent Plasma	Adsorption Before Rinsing ($\mu g/cm^2$)	Adsorption After Rinsing	
		Glass Beads ($\mu g/cm^2$)	Elution ($\mu g/cm^2$)
5	-------	0.077 ± 0.001	0.082 ± .001
2	0.168 ± 0.030	0.111 ± 0.000	0.115 ± .002
1	0.193 ± 0.010	0.134 ± 0.001	0.143 ± .006
0.5	0.221 ± 0.011	0.163 ± 0.001	0.163 ± .006
0.2	0.125 ± 0.001	0.113 ± 0.004	0.116 ± .006
0.1	0.064 ± 0.000	0.054 ± 0.000	0.056 ± .002

* ^{125}I labeled fibrinogen added to plasma; exposure time, 2h.

Figure 30 also reemphasizes that rinsing has a strong effect on the measurement of protein adsorption. The adsorption data obtained before rinsing are significantly greater than those obtained after rinsing. Thus it appears, as mentioned earlier, that rinsing removes some of the loosely bound protein adsorbed to the glass beads.

Shear conditions during rinsing may also influence protein adsorption measurements. Using the Labquake shaker, as was done for these experiments, the rinsing is performed under very gentle conditions. However, adsorption experiments performed in glass tubing are exposed to fairly high shear rates during rinsing. These shear rates may result in the removal of more of the loosely adsorbed protein. This could be the reason why adsorption in the

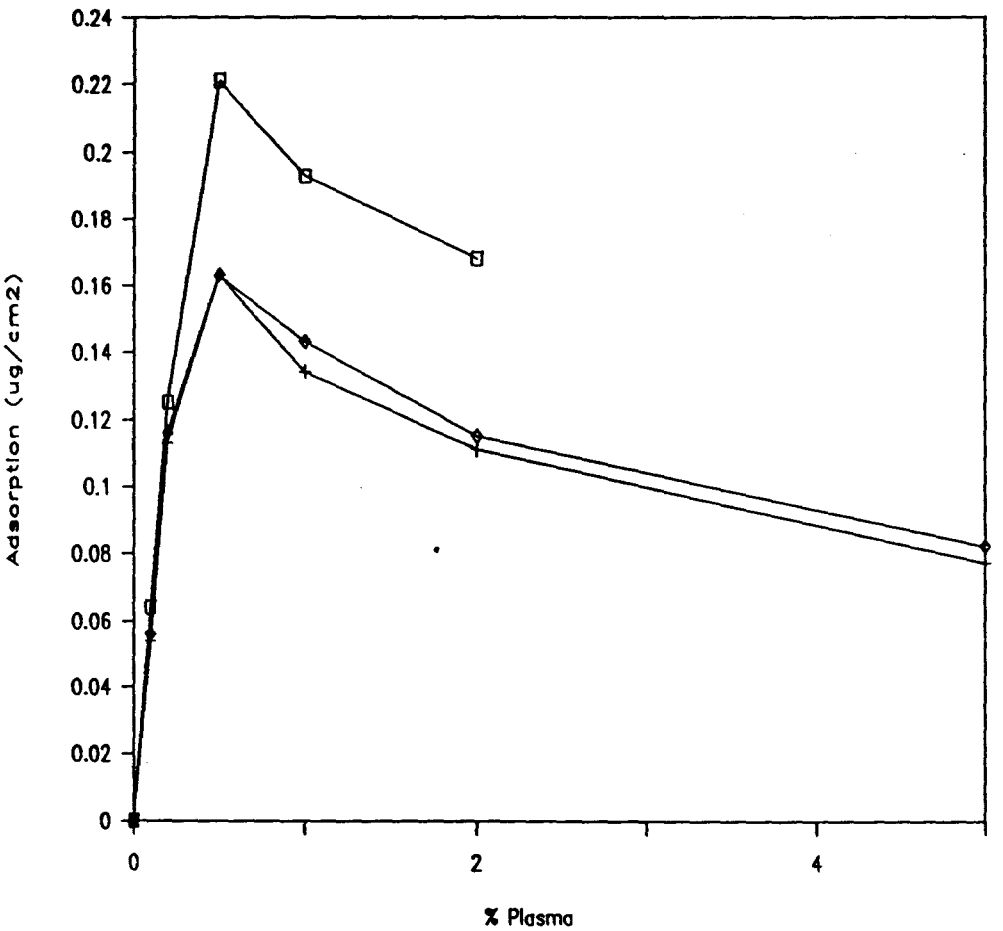

Figure 30. Adsorption of fibrinogen from diluted plasma onto glass beads vs. bulk plasma concentration (2 hr exposure). (□) before rinsing. (◊) after rinsing (by elution). (+) after rinsing (by direct counting of beads).

present experiments even after rinsing, was higher than in tubing experiments reported previously (44).

5.3.4 Adsorption of IgG onto Glass Beads from Plasma: Effect of Plasma Concentration

Experiments were performed to investigate the equilibrium adsorption of IgG onto glass beads from plasma by solution depletion. Glass beads were exposed to diluted plasma containing ^{125}I-labeled IgG for two hours. Plasma dilutions ranged from 10:1 to 100:1 . The data obtained after rinsing are shown in Table 16, and Figure 31.

The data obtained before rinsing are not presented since they showed a high degree of scatter and provided little useful information. This scatter is likely due to the very small extent of depletion of protein in the bulk solution. The data in

Table 16

Adsorption of IgG to Glass Beads from Plasma*

Percent Plasma**	IgG Adsorption After Rinsing ($\mu g/cm^2$)
10	0.022
5	0.026
2	0.029
1	0.035
0.5	0.039
0.2	0.058
0.1	0.061
0.05	0.014
0.02	0.007
0.01	0.005

* 2h solution depletion experiment.
** Plasma diluted with isotonic Tris buffer, pH 7.35.

Table 16 and Figure 31 clearly indicate that that a Vroman effect is occurring for IgG adsorption from plasma.

Figure 31 shows the surface concentration of IgG adsorbed plotted against bulk concentration for two hour adsorption times. The bulk concentration is expressed as percent of normal plasma concentration, and 100 percent plasma corresponds to an IgG concentration of 7.84 mg/mL. A maximum in adsorption occurs at about 0.1% plasma. At plasma concentrations greater than 0.1%, the competitive effects of other proteins apparently become important and the IgG is displaced. These data clearly indicate that IgG undergoes the Vroman effect and are in agreement with those of Breemhaar et al (71).

It should be emphasized that the peak in IgG adsorption (i.e. the Vroman effect) occurs at a lower plasma concentration than for fibrinogen. Thus for a 2 hour adsorption time fibrinogen adsorption on glass peaks at about 0.5% (Figure 30) where as IgG peaks at about 0.1%. This is in general agreement with recent work by Vroman (65) suggesting that adsorption in plasma is sequential with more abundant proteins being adsorbed initially and then replaced by less abundant proteins. However, whether IgG is displaced directly by fibrinogen cannot be ascertained from the present data.

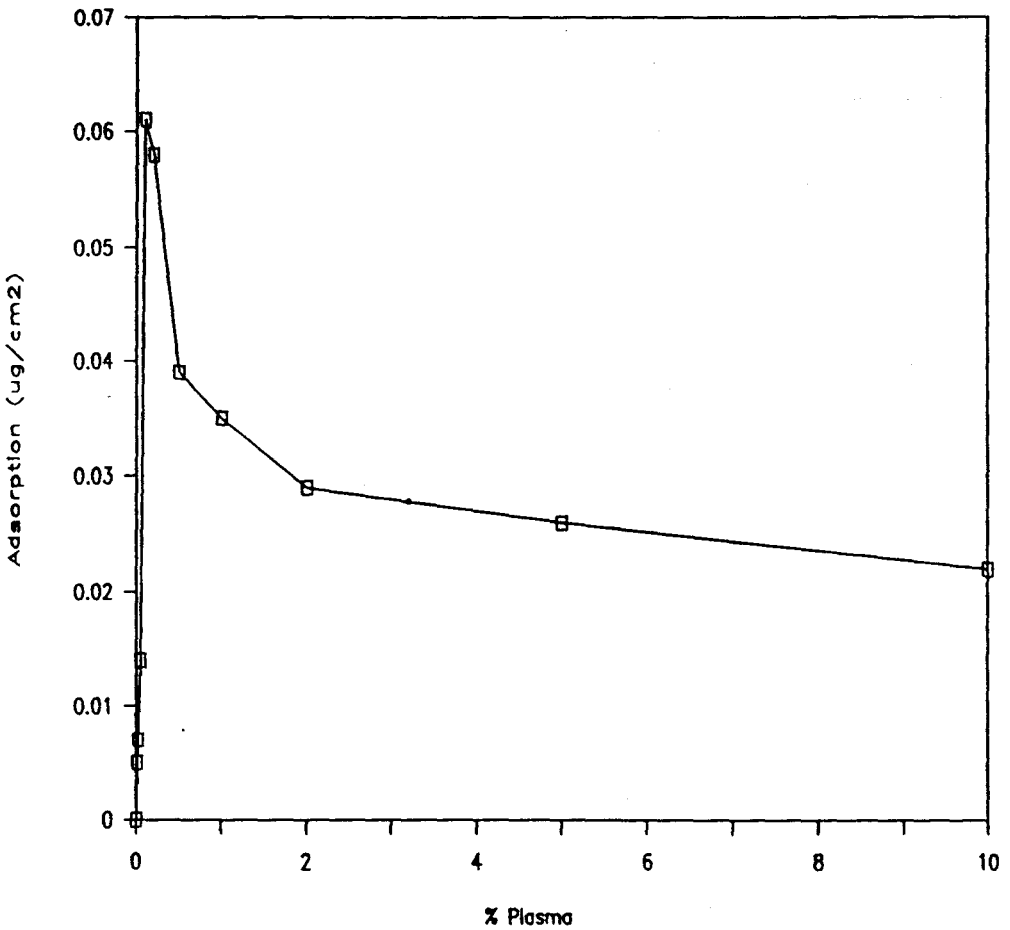

Figure 31. Adsorption of IgG after rinsing from diluted plasma onto glass beads vs. bulk plasma concentration (2h exposure).

5.4 Real Time Analysis of Fibrinogen Adsorption From a Single Component System

For these studies fibrinogen was labeled with ^{125}I using the ICl method, and solutions for adsorption experiments were made using isotonic Tris buffer, pH 7.35. The radiolabeled protein solution was injected at a flowrate of 0.15 mL/min into the adsorption cell (Figure 20) which had a volume of 14.6 mL. As discussed earlier, two runs were made for each experiment; the control run and the adsorption run. From continuous measurement of the radioactivity of the solution at the cell exit, the kinetics of protein adsorption onto the glass beads could be determined in situ.

Figure 32 shows the experimental data obtained at an injected protein concentration of 40 μg/mL. The effluent radioactivity determined over 30 second intervals is plotted against time for both the control run and the adsorption run. The theoretical curve for the control run, calculated from Equation 22, is also shown, and within experimental error is the same as the experimental data. The flat portion of the curve showing zero effluent radioactivity during the early part of the control run is due to the dead volume of the circuit which delays detection of radioactivity at the detectors after the nominal beginning of an experiment.

There is a significant difference between the control run and the adsorption run, as depicted in Figure 32 indicating that substantial adsorption to the glass beads had occurred (Figure 33). The concentration of the injected protein solution for a given surface to volume ratio has a strong effect on the "difference" between the control run and the adsorption run. Figure 34 shows data for the same surface to volume ratio at an injected concentration of 150

μg/mL and as can be seen the "difference" between the control and adsorption runs is much reduced. Although substantial adsorption is still taking place, the relative depletion of protein in the bulk solution is less. At still higher concentrations (e.g. >1000 μg/mL) adsorption occurs very quickly and the depletion of protein in the bulk solution, at the chosen surface/volume ratio, cannot be clearly seen. If data at this level of concentration were required, the volume of the reaction cell could be decreased, and/or the amount of surface area increased so that depletion in the bulk solution would be significant.

Figures 32 and 34 also demonstrate that rinsing of the circuit at the end of either the control or adsorption run reduced the radioactivity on the tubing passing through the detectors to background levels thus providing confirmation that no adsorption to the tubing surface had occurred, and that the surface thermal treatment procedure is effective.

As indicated in Chapter 4, the effluent radioactivity data may be converted to adsorption data by application of a radioactivity balance, Equation 24, across the cell. A knowledge of the area of the beads allows calculation of the surface concentration of adsorbed protein (Equation 26). Figures 33 and 35 show fibrinogen adsorption to the glass beads at an injected concentration of 40 μg/mL and 150 μg/ml respectively. As can be seen from these figures, the rates of adsorption were constant up to a surface concentration of about 0.5 $\mu g/cm^2$ in both experiments. Although adsorption was still continuing beyond this level, the rate was significantly decreased. Thus, it is apparent that at least two adsorption regimes exist; an initial phase in which the surface is only sparsely covered and the adsorption rate is relatively high and constant, and a

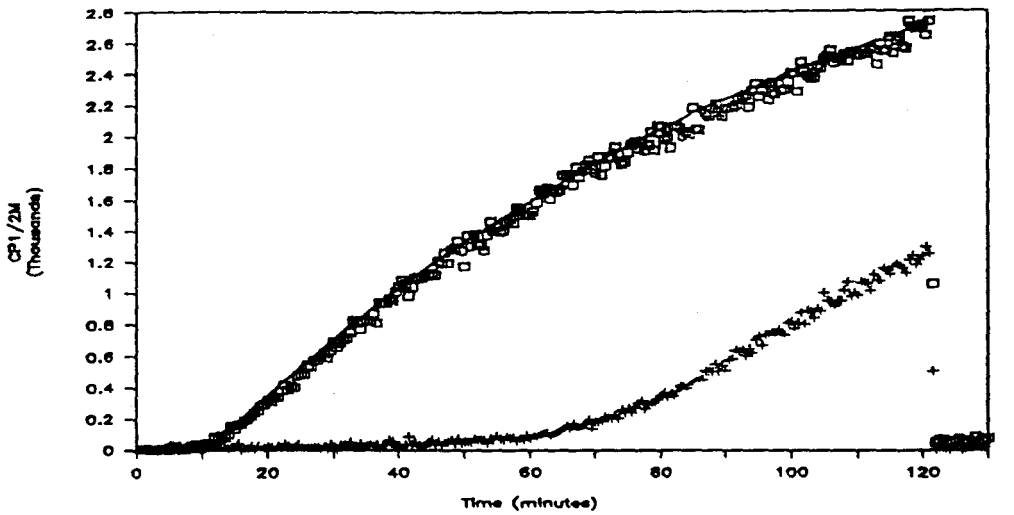

Figure 32. Variation of the radioactivity of the cell effluent as a function of time (C_f = 40 µg/mL, J_v = 0.15 mL/min, V = 14.6 mL/min, S = 685 cm^2, A_o = 4138 CP1/2M). (-) calculated from Equation 22. (¤) radioactivity recorded in the absence of glass beads. (+) radioactivity recorded in the presence of glass beads. Tubing rinsed with buffer at 120 min.

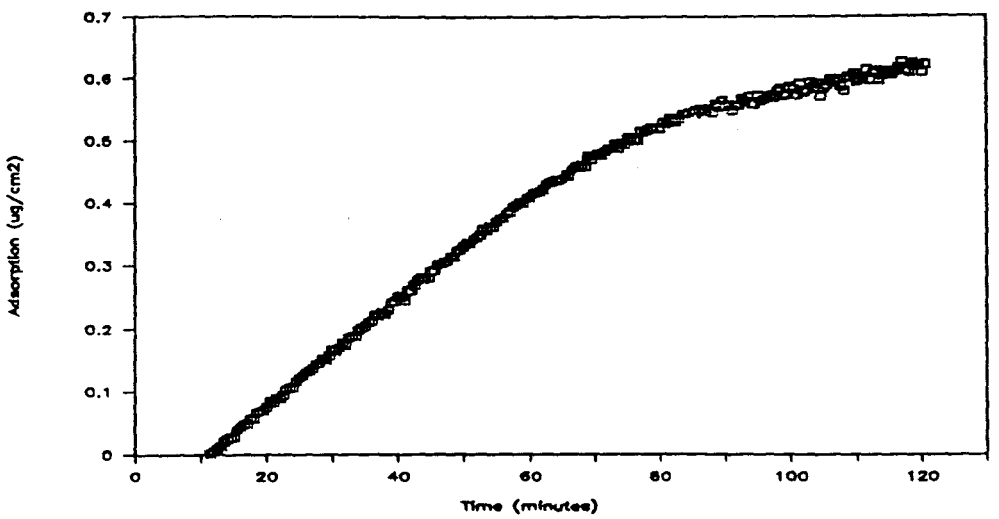

Figure 33. Fibrinogen adsorption from isotonic Tris buffer, onto glass beads as a function of time (C_f = 40 µg/mL, J_v = 0.15 mL/min, V = 14.6 mL/min, S = 685 cm^2, A_o = 4138 CP1/2M).

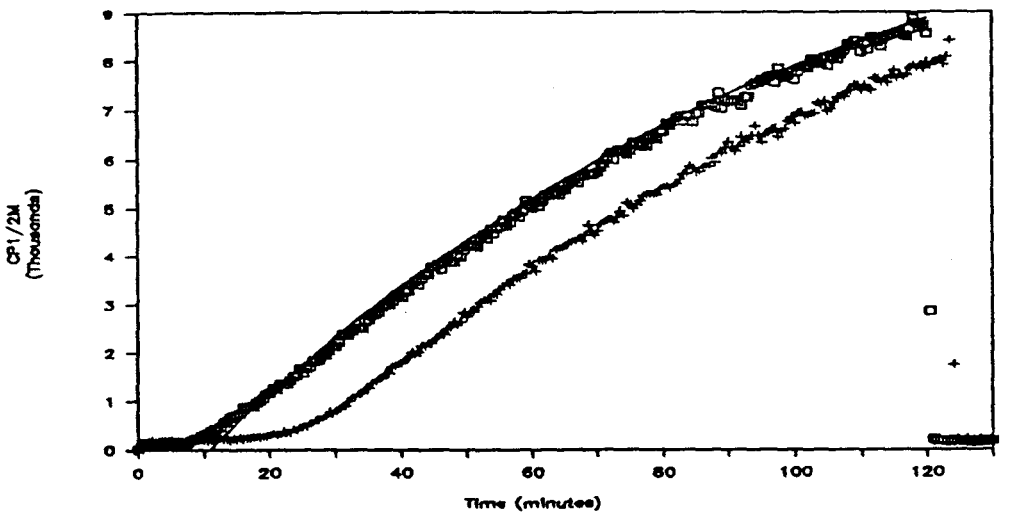

Figure 34. Variation of the Radioactivity of the Cell Effluent as a Function of Time (C_f = 150 µg/mL, J_V = 0.15 mL/min, V = 14.6 mL/min, S = 685 cm^2, A_0 = 13163 CP1/2M). (-) calculated from Equation 22. (▫) radioactivity recorded in the absence of glass beads. (+) radioactivity recorded in the presence of glass beads. Tubing rinsed with buffer at 120 min.

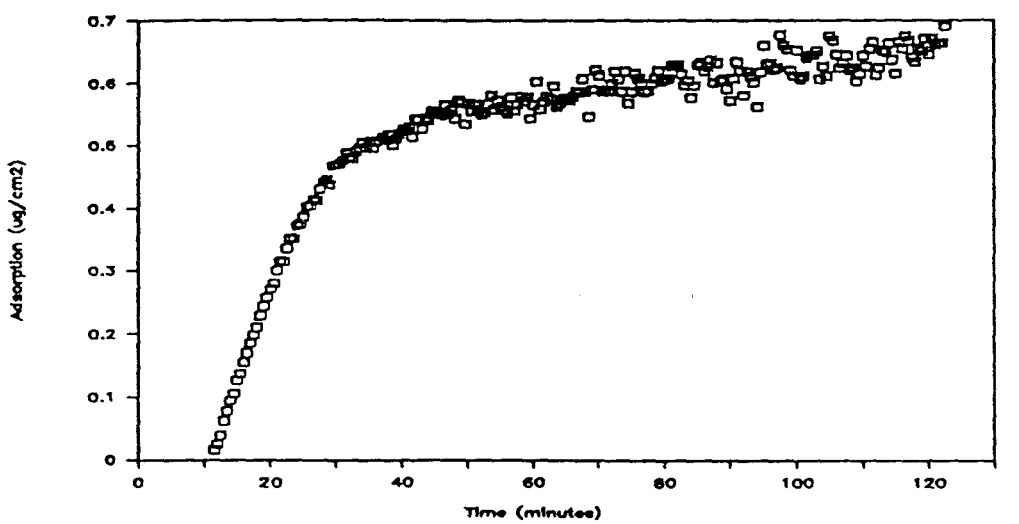

Figure 35. Fibrinogen adsorption onto glass beads as a function of time (C_f = 150 µg/mL, J_V = 0.15 mL/min, V = 14.6 mL/min, S = 685 cm^2, A_0 = 13163 CP1/2M).

second phase where the surface is probably almost completely covered and the rate is considerably slowed and decreasing.

Figure 36, shows adsorption data obtained for a range of injected fibrinogen concentrations from 40 µg/mL to 300 µg/mL at a flowrate of 0.15 mL/min with the same surface to volume ratio. As can be seen from Figure 36, the same two phase adsorption kinetics occurs at all concentrations. The initial rate increases with increasing fibrinogen concentration and the period of the initial constant rate phase decreases with increasing concentration. At longer times, the curves in Figure 36 appear to be leveling off at the same surface concentration of about 0.64 µg/cm^2.

The initial rate of fibrinogen adsorption from isotonic Tris, pH 7.35, onto glass beads is linearly related to injected protein concentration at a flowrate of 0.15 mL/min as is shown in Table 17 and Figure 37. This results from the fact that under the conditions studied, the initial adsorption of fibrinogen to the surface is "supply" limited as indicated in Figures 32 and 34 showing virtually complete solution depletion (i.e. zero effluent radioactivity) at short times. It is likely that the intrinsic rate of adsorption is greater than the rate determined by the present method.

Under conditions of complete solution depletion, the protein mass balance, equation 24 reduces to:

$$S\, A_{S(t)} = J_V A_0 t \qquad [27]$$

and adsorption , Γ, is given by:

$$\Gamma = \left(\frac{J_V\, t}{S}\right) C_f \qquad [28]$$

The rate of adsorption is then:

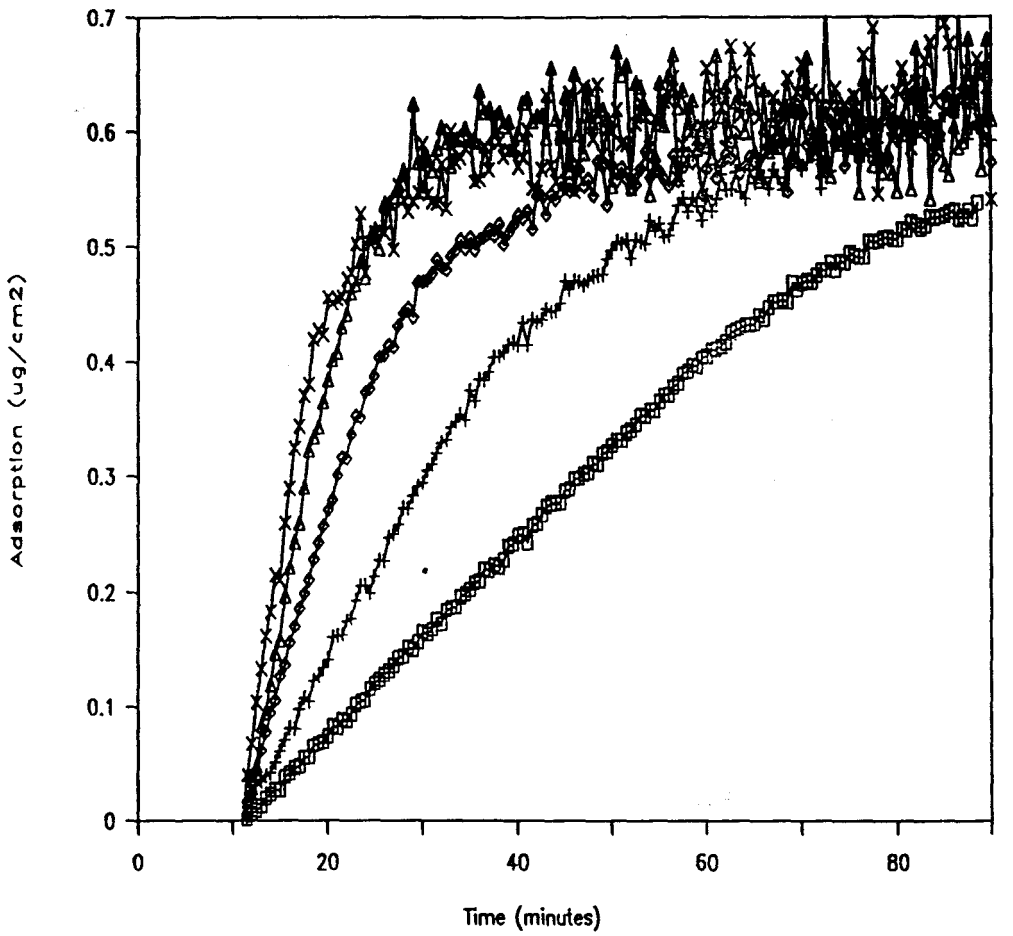

Figure 36. Fibrinogen adsorption as a function of time at various injected protein concentrations. (□) 40 μg/mL, (+) 75 μg/mL, (◊) 150 μg/mL, (Δ) 225 μg/mL, (x) 300 μg/mL. (J_v = 0.15 mL/min, V = 14.6 mL, S = 685 cm^2)

$$\frac{d\Gamma}{dt} = \left(\frac{J_v}{S}\right) C_f \qquad [29]$$

i.e. $$\frac{d\Gamma}{dt} = K_1 C_f \qquad [30]$$

Where $K_1 = J_v/S$ is constant for the experiments in Table 17 and Figure 37.

It should be emphasized that the flowrate and surface area are under the control of the experimenter. Thus if one or both of these values is altered, the apparent initial rate of adsorption (really the rate of supply of protein to the cell) would change. For example, if the flowrate were increased, the apparent rate of adsorption would increase in proportion. However, a point would eventually be reached where the initial adsorption rate would no longer be supply limited. Only then would the true initial rate of adsorption be observed.

Table 17 shows the initial rate of adsorption as calculated by linear regression of the adsorption data, and the relationship discussed previously (i.e. Equation 30). As is apparent from the values presented in the table, there is a slight difference between the two calculated rates at each injected protein concentration, and this difference increases with increasing concentration. This is partially due to the fact that although the solution is virtually depleted of protein during the initial stage, there is some measurable radioactivity, thus the last two terms in Equation 26 are small positive values.

Using the real time in situ technique, the effect of protein solution flowrate on the adsorption of fibrinogen from a single component system was briefly studied. Figure 38 shows the adsorption kinetics of fibrinogen at an injected protein concentration of 40 μg/mL for flowrates of 0.15 mL/min and 0.285 mL/min. In this situation the injected protein concentration and the surface area were held constant, and the effect of flowrate on the rate of adsorption studied.

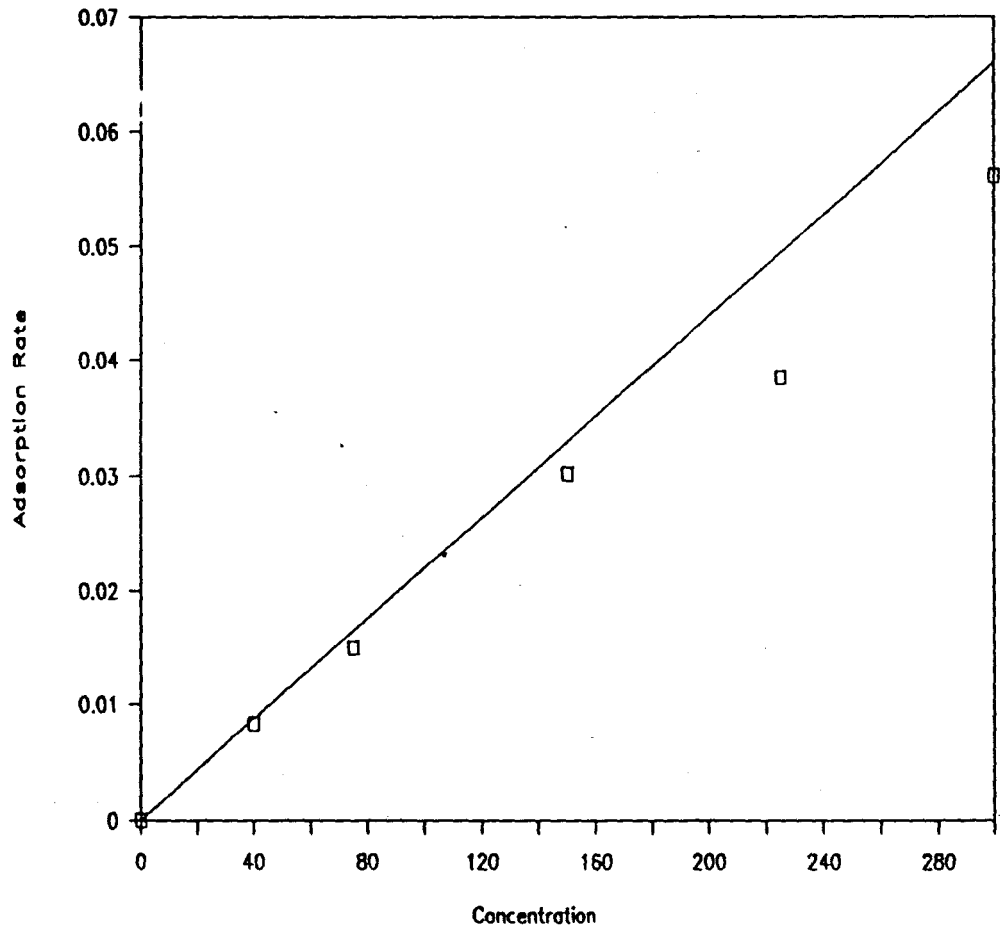

Figure 37. Initial rate of fibrinogen adsorption from isotonic Tris (pH 7.4) onto glass beads as a function of injected protein concentration. (J_V = 0.15 mL/min, S = 685 cm^2, V = 14.6 mL)

Table 17

Initial Rate of Fibrinogen Adsorption on Glass Beads (J_V = 0.15 mL/min) as a Function of Injected Protein Concentration

Injected Protein Concentration (μg/mL)	Initial Rate of Adsorption (μg/cm^2 min)	K_1C_f
40	0.0083	0.0087
75	0.0150	0.0164
150	0.0302	0.0329
225	0.0385	0.0427
300	0.0562	0.0659

Providing the initial adsorption is still supply limited, an increase in flowrate should result in a corresponding increase in the rate of adsorption according to Equation 28. The adsorption rates as determined by this relationship are very similar to the rate determined by linear regression of the adsorption data (see Table 18). However, further flowrates investigations should be performed to establish at what point the initial adsorption rate changes from being transport controlled to being kinetic controlled.

It was reported previously, that the limiting capacity of glass for fibrinogen (0.05M Tris buffer, pH 7.35) is about 0.7 μg/cm^2. In the present work using the same in situ method, adsorption of fibrinogen from isotonic Tris buffer on glass tubing was generally in the range of 0.45 to 0.55 μg/cm^2. Thus the real time in situ data , even at the low injected concentration of 40 μg/mL give higher adsorption than the non in situ data involving rinsing.

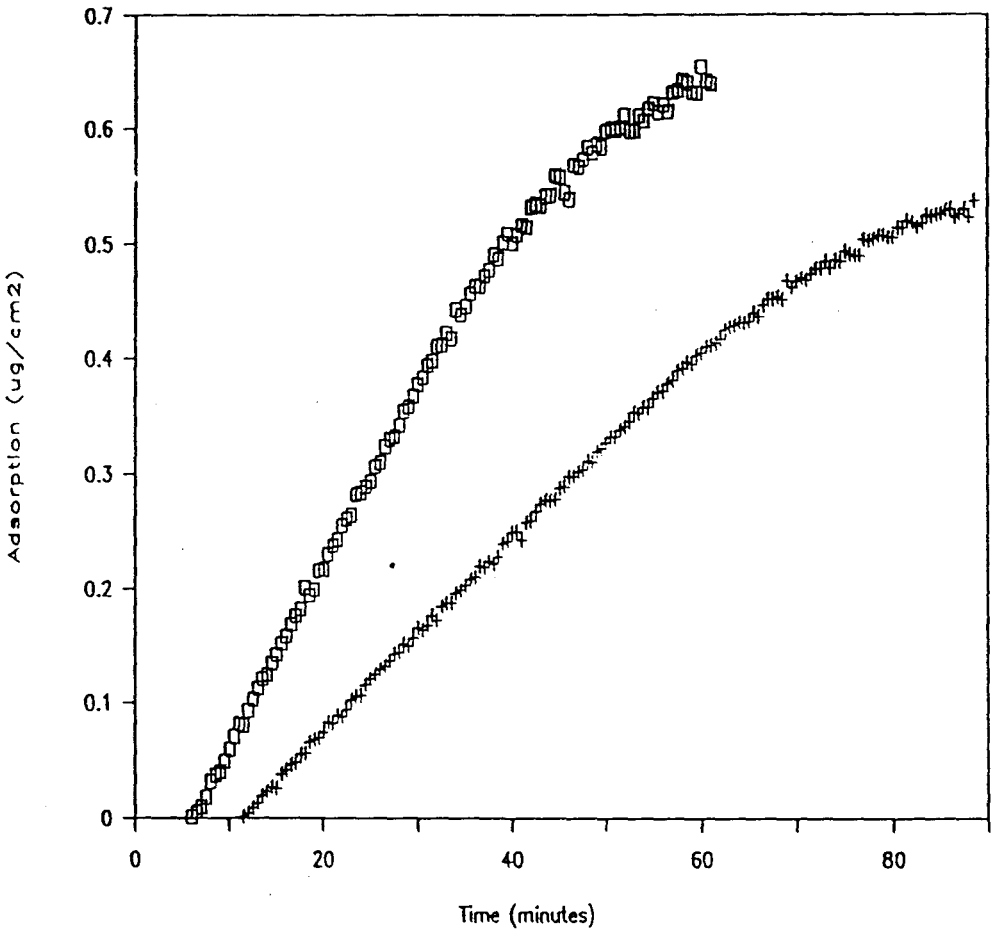

Figure 38. Fibrinogen adsorption onto glass beads as a function of time for two experiments at different flowrates (C_f = 40 µg/mL, V = 14.6 mL, S = 684 cm^2). (+) 0.15 mL/min, (▫) 0.285 mL/min

Table 18

Initial Rate of Fibrinogen Adsorption on Glass Beads (C_f = 40 μg/cm^2) as a Function of Injected Protein Concentration

Flowrate (mL/min)	Initial Rate of Adsorption (μg/cm^2 min)	$C_f J_v CS$
0.15	0.0083	0.0087
0.285	0.0157	0.0166

Perhaps a more valid comparison is between the real time in situ and equilibrium in situ data on the glass beads. The equilibrium in situ data obtained off-line, as reported previously in Table 14, were for a three hour exposure time and adsorption values ranged from 0.798 μg/cm^2 (40 μg/mL) to 1.199 μg/cm^2 (500 μg/mL). The long time in situ data obtained on-line under flow conditions as depicted in Figure 36 are seen to be of the same order of magnitude. However, consideration must be given to the fact that in the on-line experiments the glass beads experience an increasing bulk solution concentration over the course of the experiment. For example, in an experiment at 0.15 mL/min with a cell volume of 14.6 mL, the concentration in the cell starts at zero, and reaches 56% of the injected concentration at 80 min, and 71 % at 120 min. Thus, a direct comparison of on-line and off-line results is not possible since concentration conditions can never be the same. However, the off-line results do give an indication of the order of magnitude of surface concentrations to be expected on-line.

In order to check the reproducibility of the data, on-line experiments were repeated up to 4 times. Figure 39 shows the results obtained from two

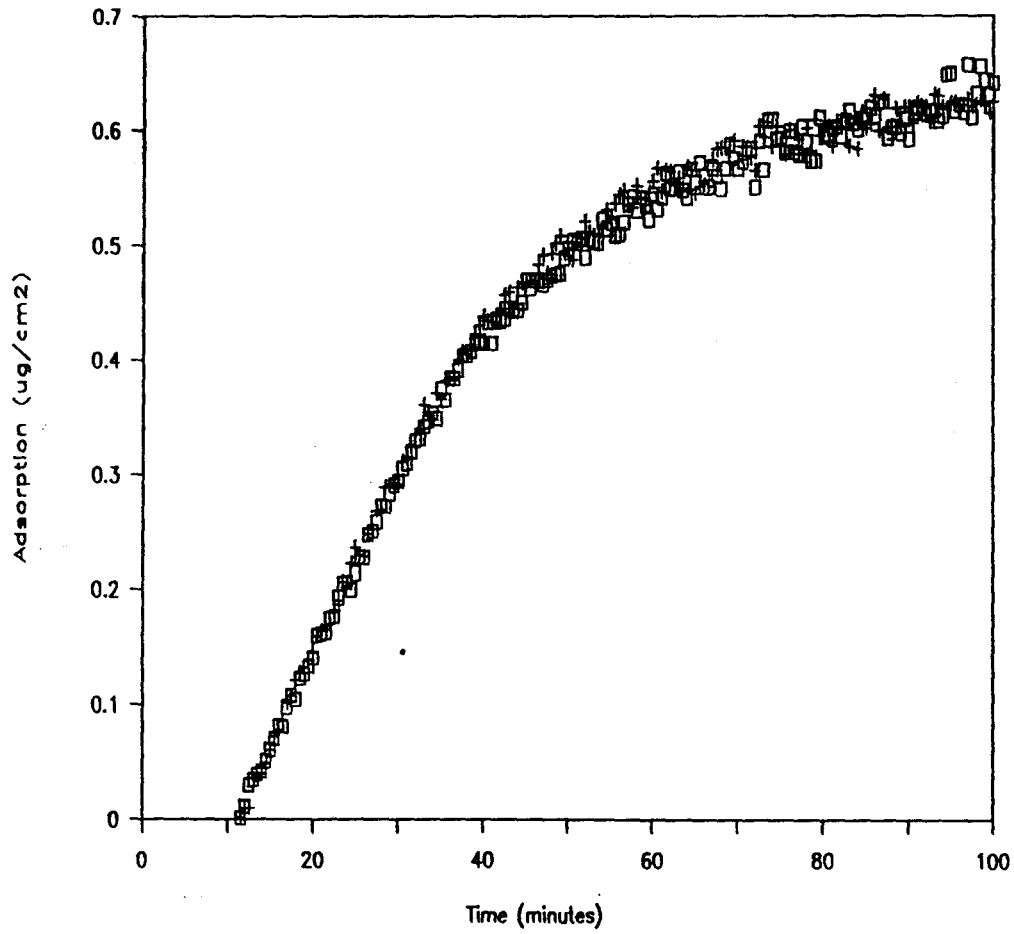

Figure 39. Fibrinogen adsorption onto glass beads as a function of time for two identical experiments demonstrating reproducibility of data under the same experimental conditions (C_f = 75 µg/mL, 0.15 mL/min, V = 14.6 mL, S = 685 cm^2, A_o = 7857, 7011 CP1/2M).

experiments carried out at an injected protein concentration of 75 μg/mL. It can be seen from Figure 39 that the data, in general, were highly reproducible.

5.5 Real Time Kinetic Analysis of Fibrinogen Adsorption From Plasma

In the initial experiments performed to study the adsorption of fibrinogen from plasma, approximately 10% to 15% of the quantity of fibrinogen in the plasma was added as ^{125}I labeled fibrinogen (ICI technique). However, it was found that the low specific activity of the protein obtained using the ICI technique resulted in relatively low count rates for the effluent and a large amount of scatter in the experimental data. In subsequent experiments, therefore, in order to achieve a higher specific activity of the labeled protein, lactoperoxidase labeling was used. With this method the specific activity of the labeled fibrinogen was sufficiently high that addition of only a few percent of the quantity of fibrinogen in the plasma as labeled protein gave sufficiently high solution count rates to provide good adsorption data.

Generally 1% to 8% of the fibrinogen in the plasma was added as labeled protein. Figure 40 shows the effluent radioactivity plotted against time at a flowrate of 0.15 mL/min, and an injected plasma concentration of 1% normal. The cell volume was 14.6 mL and the surface area was 684 cm^2. The corresponding adsorption data at an injected plasma concentration of 1%, as well as at concentrations of 2.5%, and 5% are shown in Figure 41. The data obtained at an injected plasma concentration of 1% normal indicate that adsorption of fibrinogen was linear up to about 50 min. Thereafter, the rate of adsorption decreased and appeared to reach zero at a surface concentration of 0.36 $\mu g/cm^2$ and a time of 90 min. However a slight decrease in surface

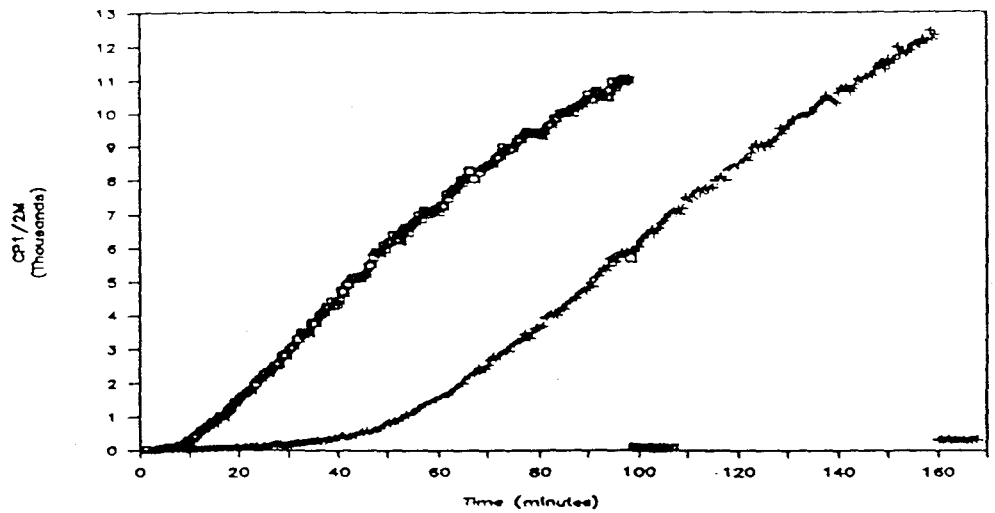

Figure 40. Variation of the radioactivity of the cell effluent as a function of time (1% plasma, J_V = 0.15 mL/min, V = 14.6 mL/min, S = 685 cm^2, A_0 = 18151 CP1/2M). (-) calculated from Equation 22. (□) radioactivity recorded in the absence of glass beads. (+) radioactivity recorded in the presence of glass beads.

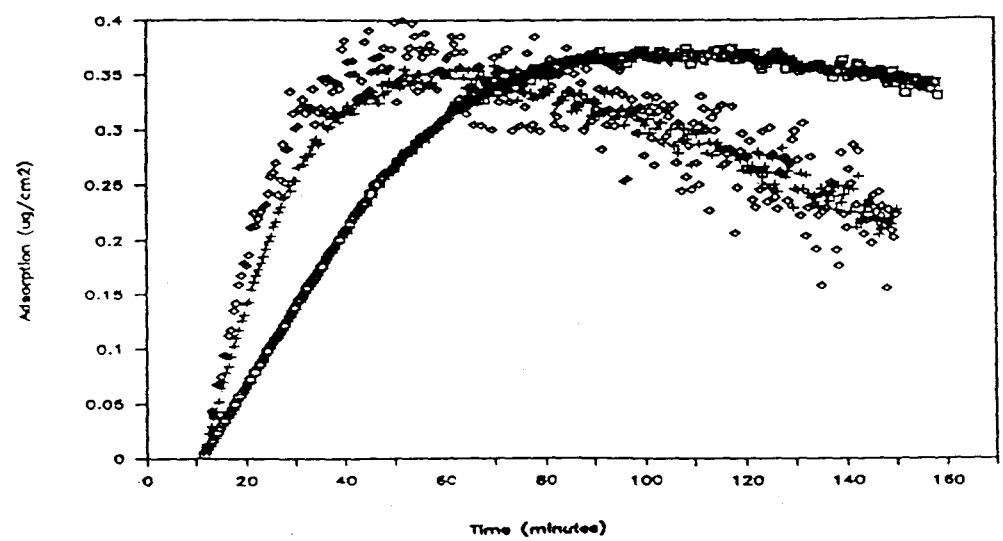

Figure 41. Fibrinogen adsorption from diluted plasma onto glass beads as a function of time (J_V = 0.15 mL/min, V = 14.6 mL/min, S = 685 cm^2). (□) 1% plasma, (+) 2.5% plasma, (◊) 5% plasma.

concentration actually occurred at longer times. At a plasma concentration of 2.5% normal, the initial rate of fibrinogen adsorption was greater than at 1 % plasma. In this case the data show a well-defined maximum at about 60 min and a surface concentration of about 0.35 $\mu g/cm^2$. A further increase in the plasma concentration to 5% normal again resulted in an increase in the initial rate of adsorption of fibrinogen. After about 25 min the rate decreased and became zero at about 45 min at a surface concentration of 0.35 $\mu g/cm^2$. Desorption of fibrinogen then occurred.

The data at the higher injected plasma concentrations, showing maxima in fibrinogen adsorption are consistent with the concepts proposed by Vroman that high concentration proteins dominate the surface at short time intervals, while at longer times exchange processes occur, and proteins with lower concentrations and higher adsorption affinities can displace the initially adsorbed proteins. At high dilutions the competitiveness of lower concentration proteins is less important and the fibrinogen is displaced much more slowly. This probably accounts for the absence of a peak at an injected plasma concentration of 1%.

The adsorption of fibrinogen from plasma has been extensively studied "off-line" (with rinsing) by several groups and Vroman effects have been observed on many surfaces. Generally adsorption is studied as a function of time at a constant plasma concentration, or as a function of plasma concentration at a constant time, referred to as the time domain and the concentration domain respectively. In the present experiments, concentration and time are varying together and the domain may be referred to as mixed. Because of this fundamental difference in experimental design, it is not possible

to compare the present data with those in the literature at least from a quantitative stand-point. Thus adsorption peak heights and positions cannot be compared.

It may be noted nonetheless that the maximum adsorption in these experiments (i.e. 0.35 $\mu g/cm^2$) is significantly higher (factor of 3) than in off-line experiments with rinsing on glass tubing. For example a peak height of about 0.10 $\mu g/cm^2$ was obtained off-line whether in the time or concentration domain (44). The peak height off-line has also generally been found to be independent of surface type. The increase in peak height is probably due to the elimination of the rinsing step in the real time in situ experiments, resulting in measurement of both the irreversibly and reversibly adsorbed proteins. It is also possible that the surface properties of the glass beads versus the glass tubing are different. However, the off-line in situ data on the glass beads appear to support the idea that a significant amount of protein is removed by rinsing (see Section 5.3.3). Thus, it appears that the higher peak height may be due to the elimination of the rinsing step.

It is also of interest to note that the broadness of the peak obtained during on-line experiments is considerably more emphasized than off-line. On-line results indicate that significant adsorption of fibrinogen occurs within a 30 minute time period (i.e. at an injected plasma of 5% normal). This contact or residence time on-line may be sufficient for the protein to orientate and conformationally adjust to the interface leading to a stronger binding and greater irreversibility, thus resulting in a broader peak than is obtained off-line.

Figure 42 shows results obtained at higher plasma concentrations, namely 10 and 20 percent normal. It should be noted that, due to the higher

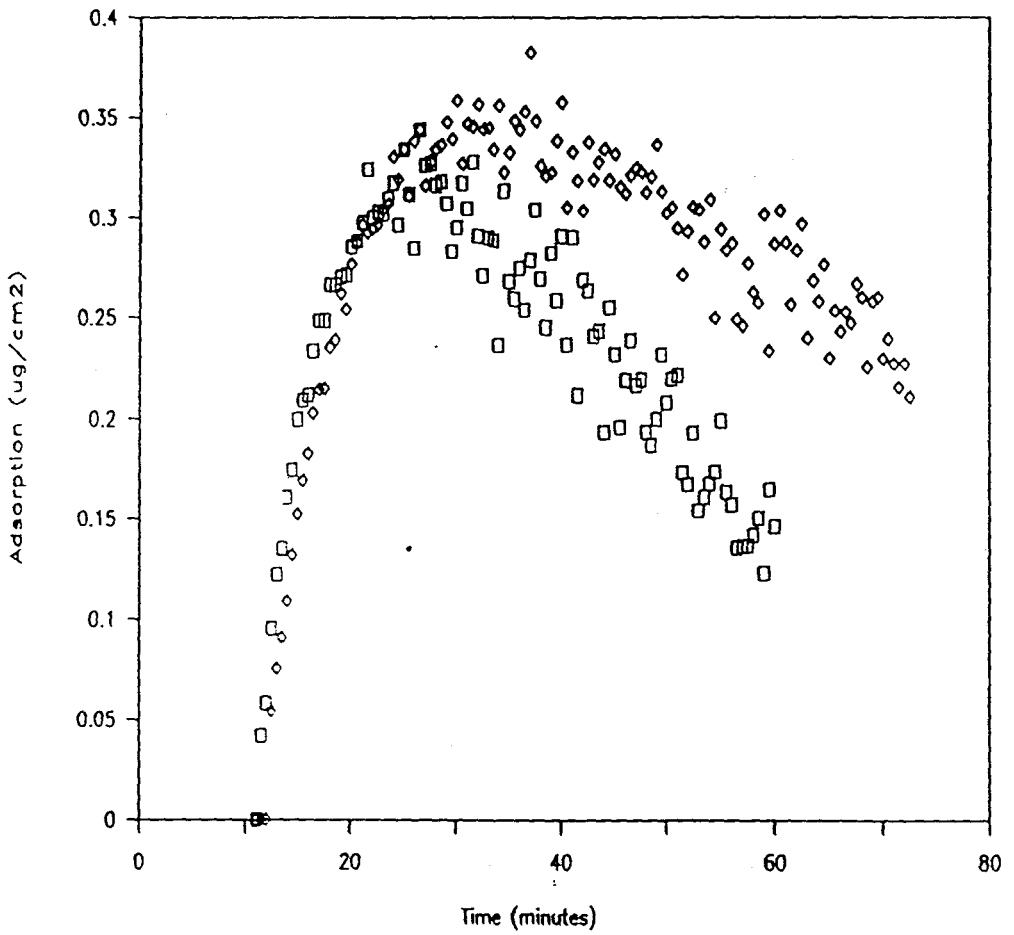

Figure 42. Fibrinogen adsorption onto glass beads from diluted plasma as a function of time (J_V = 0.15 mL/min, V = 14.6 mL, S = 685 cm^2). (◊) 10% plasma, (▫) 20% plasma

concentrations of fibrinogen in the injected plasma, the initial rate of fibrinogen adsorption is significantly greater than that obtained at the lower plasma concentrations. Also, the desorption rate of proteins is significantly greater than at the lower plasma concentrations. This effect also is presumably due to the higher concentrations of displacing proteins in the more concentrated plasma.

A comparison of the initial adsorption rate determined by regression of the adsorption data and Equation 30, for a pure protein system indicated that the system was supply limited. However linear regression of the data obtained from the plasma experiments had very poor correlation coefficients (< 0.7). In addition, only the 1 % plasma experiment had virtually a complete depletion of protein in the bulk solution (i.e. zero effluent radioactivity). At the higher injected plasma concentrations, the bulk solution was not totally depleted, indicating that the adsorption is not supply limited.

The effect of flowrate on the adsorption of fibrinogen from plasma at an injected plasma concentration of 2.5 % of normal was studied. Figure 43 shows the results obtained at flowrates of 0.158, 0.202, and 0.302 mL/min. The effect of increasing the flowrate as seen in Figure 43, is to increase the rate of adsorption of fibrinogen from the plasma. However, the increase in protein adsorption is not proportional to the increase in flowrate. Thus, re-emphasizing that the system is not supply limited under these experimental conditions. The desorption rate did not appear to be significantly affected by the increased flowrate.

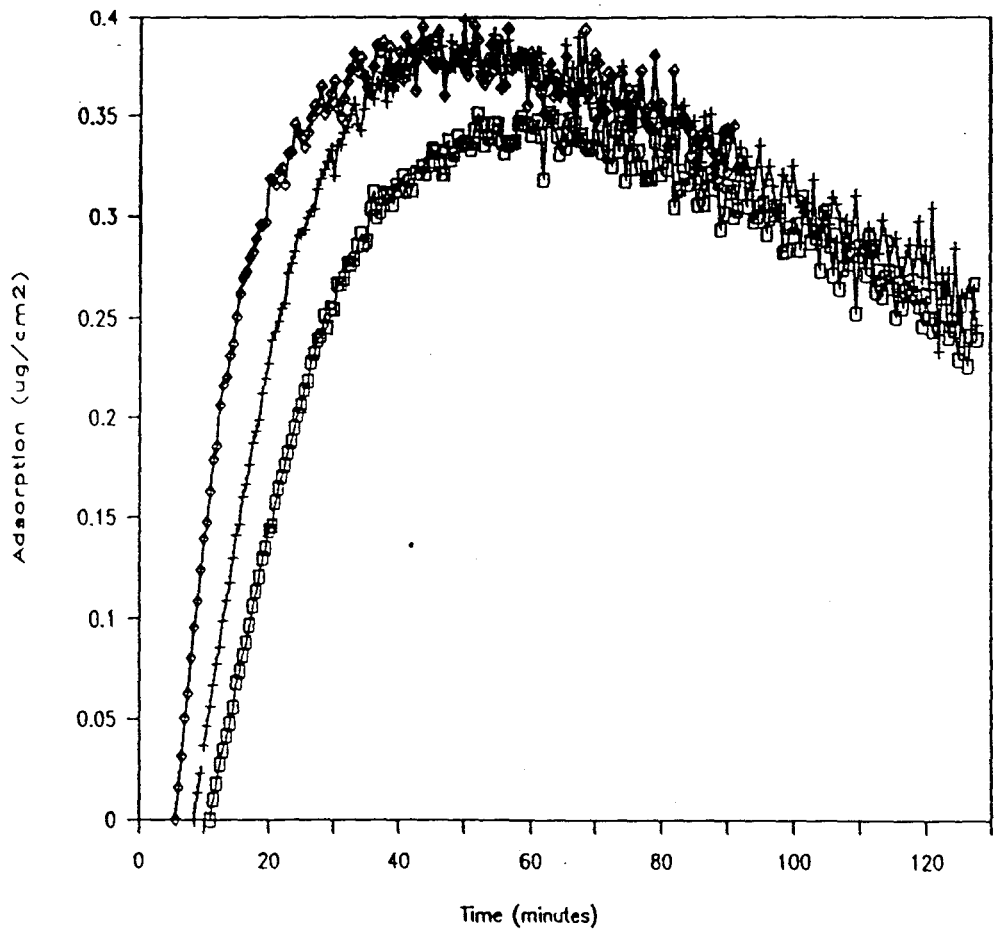

Figure 43. Fibrinogen adsorption onto glass beads from diluted plasma as a function of time (2.5% plasma, V = 14.6 mL, S = 685 cm^2). Effect of flowrate. (□) 0.158 mL/min, (+) 0.202 mL/min, (◊) 0.303 mL/min.

5.6 Real Time Analysis of IgG Adsorption From Plasma

Experiments to study the adsorption of IgG from diluted plasma to glass beads were also performed. The main objective was to determine whether adsorption of this protein is also transient as predicted by Vroman (65). IgG was labeled with ^{125}I using the lactoperoxidase technique. The labeled protein was added to plasma (about 5% of quantity of IgG in plasma added as labeled IgG) and the plasma mixed with isotonic Tris buffer to obtain the desired dilution. Adsorption data for at an injected plasma concentration of 1% are shown in Figure 44. In this experiment the cell volume was 14.6 mL, the flowrate 0.15 mL/min, and the surface area of the beads 684 cm^2. The data indicate that adsorption of IgG occurs up to a surface concentration of 0.07 $\mu g/cm^2$ at about 35 minutes. Significant desorption then takes place as for fibrinogen, presumably also due to the competitive effects of low concentration, high affinity proteins in the plasma. The scatter in the data is considerably greater than for fibrinogen since the effluent radioactivity levels are relatively low. It should be noted that the peak height is again significantly higher than that obtained off-line. This difference is believed to be at least partially due to the elimination of the rinsing step in the on-line experiments, as discussed earlier. It should be noted that the levels of adsorption, up to about 0.06 $\mu g/cm^2$, are similar in the on-line and off-line in situ experiments in the present work (i.e. when rinsing was not performed).

IgG adsorption experiments were performed using 0.1% plasma. It was hypothesized that at such a low plasma concentration, adsorption of IgG would still be significant but the competitive effects of the low concentration proteins would be attenuated to the extent that little or no IgG displacement would occur.

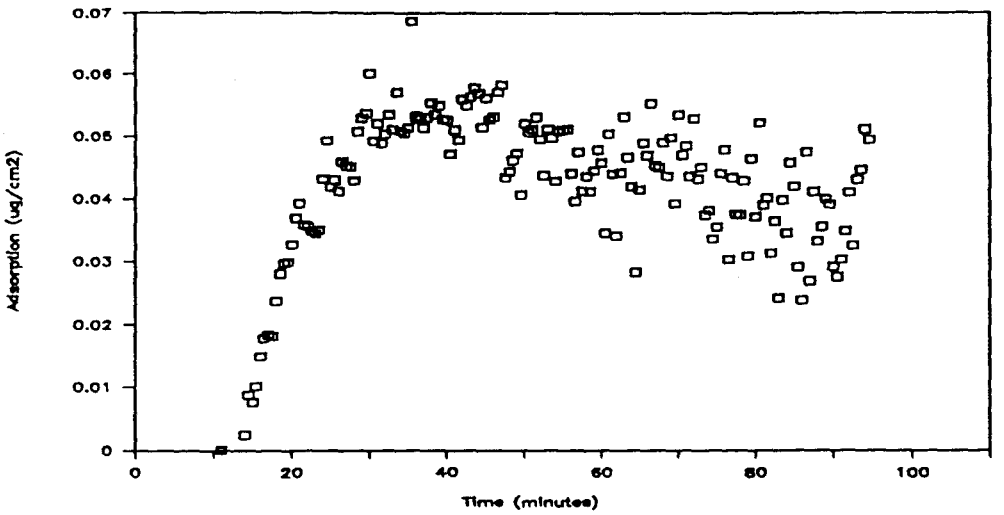

Figure 44. IgG adsorption from diluted plasma onto glass beads as a function of time (1% plasma, J_V = 0.15 mL/min, V = 14.6 mL/min, S = 685 cm^2).

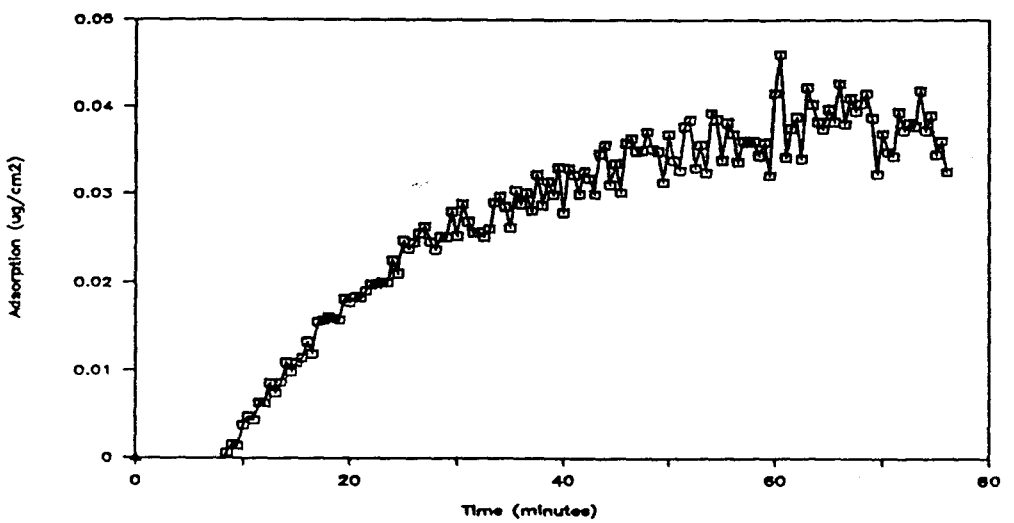

Figure 45. IgG adsorption from diluted plasma onto glass beads as a function of time (0.1 % plasma, J_V = 0.15 mL/min, V = 14.6 mL/min, S = 685 cm^2).

Figure 45 shows a plot of IgG adsorption versus time for an injected plasma concentration of 0.1%, and shows as anticipated a relatively low adsorption rate, a low plateau adsorption, and no desorption.

The real time in situ experimental method developed in this work to study protein adsorption was useful in the study of IgG adsorption from plasma at plasma concentrations up to 1.0% of normal. However, the adsorption of IgG from higher concentrations of plasma could not be studied with the surface/volume ratios typically used. IgG is present in normal plasma at high concentrations (i.e. 7.86 mg/mL) so that even at relatively high dilutions (e.g. 20:1 or 5% normal plasma concentration), the adsorption could not be monitored since there was not sufficient depletion of protein in the bulk solution. Thus in order to monitor the adsorption of IgG from higher concentrations of plasma, the surface to volume ratio would need to be significantly increased to achieve adequate depletion of protein in the bulk solution.

5.7 Real Time Analysis of Albumin Adsorption from Plasma

Experiments were also performed to study albumin adsorption from diluted plasmas. Albumin was labeled using the lactoperoxidase technique and the labeled protein then added to plasma (approximately 1% of the quantity of albumin in plasma added as labeled albumin) diluted to the desired concentration with isotonic Tris.

Adsorption studies performed at 1% normal plasma indicated virtually no difference between the control run and the adsorption run and calculation of surface concentration from the adsorption run data indicated that no adsorption was taking place. However it has been reported by other researchers (71) that albumin adsorption from plasma does occur and indeed does undergo the

Vroman effect. This apparent discrepancy may be explained in that the present experimental conditions are such that albumin adsorption cannot be detected even at relatively low plasma concentrations (i.e. 1%). The albumin concentration of the plasma pool used in these studies was 34.7 mg/mL. Thus, although adsorption of albumin may occur, it could not detected in the present system due to insufficient depletion of the bulk solution. Adsorption studies of albumin from diluted plasma may be carried out using the present method if the surface area to volume ratio is sufficiently increased that depletion of the protein in the bulk solution is significant and measurable.

6.0 Summary and Conclusions

The method of serum replacement/solution depletion to study protein adsorption in real time and in situ using ^{125}I labeled proteins has been successfully developed and implemented. Extensive preliminary studies were performed which overcame several problems. These problems included fluctuations in background radioactivity and unwanted adsorption onto the cell, cell filter, and connecting tubing material. Background fluctuations were largely eliminated by appropriate shielding of the detector, and unwanted adsorption was greatly reduced by surface treatment. The latter involved thermal treatment of a monolayer of adsorbed fibrinogen for 10 minutes at 70 °C in the presence of fibrinogen solution. Also a series of experiments designed to check for preferential adsorption of ^{125}I labeled fibrinogen onto the surface under study were performed and indicated no significant difference between labeled and unlabeled protein. In addition, the fibrinogen was examined by SDS-PAGE before and after labeling. No evidence of molecular degradation as a result of labeling was found.

To measure protein adsorption kinetics in real time, solutions containing ^{125}I labeled proteins were injected at a constant flowrate into a specially designed cell containing the surface under study in particle form. The adsorption was determined by continuous measurement of depletion of protein in the bulk solution.

The adsorption of fibrinogen from isotonic Tris buffer was studied in some detail. The concentration of protein in the injected solution had a strong effect on the rate of adsorption onto glass beads. An increase in the concentration of

the protein injected, resulted in a corresponding increase in the initial rate of adsorption. Two adsorption regimes were found to exist: an initial phase where the adsorption rate was high, and a second phase where the surface is almost completely covered and the rate decreases to zero. Under the conditions of surface-volume ratio, flow rates and concentration, the actual initial rates were supply limited, and lower than the true adsorption rate.

Adsorption of fibrinogen to glass beads from plasma diluted to various extents was also studied. The plasma concentration was found to have a significant effect on the kinetics of adsorption of fibrinogen to glass beads. At relatively low injected plasma concentrations (e.g. 1% normal plasma) adsorption was similar to that from buffer. An initial constant rate period was followed by a decreasing rate period, and a constant "saturation" adsorption was ultimately reached.. However, at higher plasma concentrations the constant and decreasing rate periods were followed by desorption. These findings represent a manifestation of the generalized Vroman effect whereby at short time intervals, high concentration proteins dominate the surface due to transport effects while at longer times surface-solution exchange processes occur,and proteins of low concentration but high adsorption affinity may enter the adsorbed layer, thereby displacing the initially adsorbed proteins. The Vroman hypothesis therefore predicts a sequence of protein adsorption from plasma in which more abundant proteins are adsorbed initially and later replaced by less abundant proteins. A given protein undergoing the Vroman effect will thus exhibit adsorption kinetics showing a maximum. At low plasma concentrations (i.e. 1%) the competitive effects of the other proteins are less important and the fibrinogen is displaced more slowly.

The adsorption of IgG from diluted plasma to glass beads was also briefly studied and the plasma concentration was found to have a significant effect. At very low plasma concentrations (i.e. 0.1%), adsorption increased linearly with time then slowed, and eventually a plateau value was reached. However, at a plasma concentration of 1% the adsorption kinetics showed a maximum, and adsorption was followed by desorption. Thus, at this plasma concentration the competitive effects of low concentration, high affinity, proteins are significant, and the Vroman effect is observed for IgG also. It should be emphasized that the desorption of IgG(i.e. the Vroman effect), occurs at a much lower plasma concentration, than it does for fibrinogen, again in support of the generalized Vroman effect. Whether IgG is displaced directly by fibrinogen remains to be determined.

Attempts to study albumin adsorption from diluted plasmas were unsuccessful since within the constraints of the current experimental design, insufficient depletion of albumin, the most abundant plasma protein, in the bulk plasma occurred to allow the observation of adsorption.

In summary, the experimental method designed, developed, and implemented in this work has proved useful in the study of protein adsorption kinetics from single component systems, or complex fluids such as plasma. The method is particularly useful in the study of the transient adsorption of proteins from plasma, known as the Vroman effect.

7.0 Suggestions for Future Work

The experimental method employed to study the adsorption of proteins in real time has been relatively successful, but has not by any means been fully exploited in the present investigations. A number of recommendations regarding future work can be made. These recommendations fall into two main categories: (1) improvements of the experimental method and design, and (2) research areas for exploration.

7.1 Improvements of the Experimental Method and Design

1. A new cell design with the glass frit filter in the tubing at the outlet of the cell, rather than in the body of the cell should be attempted. This would significantly reduce the system dead volume and the area of the frit surface.

2. The surface to volume ratio was not varied in the present study. It was found, in some cases, that insufficient depletion of protein in the bulk solution occurred so that adsorption of the protein could not be detected. It is suggested that , in such cases,the surface to volume ratio be increased so that sufficient protein depletion occurs.

7.2 Research Areas for Exploration

1. Experiments on single protein systems, other than fibrinogen, should be implemented to study the real time adsorption of these proteins.

2. Experiments on mixtures containing two or three proteins should be performed to elucidate the competitive effects between proteins in relatively simple mixtures. Such data would constitute a test of the Vroman concepts of competitive adsorption.

3. More experiments involving the adsorption of different proteins from plasma should be done to determine their relative importance in the Vroman effect.

4. Experiments involving deficient plasmas should be done to determine the effect of various protein deficiencies on the adsorption of fibrinogen, IgG, and albumin from plasma.

5. Further experiments should be done to determine the effect of flowrate and stirring rate on protein adsorption kinetics using the system developed in this thesis.

References

1) Andrade J.D., Hlady V., Pol Sci, 79 (1986)

2) Baier R.E., Dutton R.C., J. Biomed Mater Res, 3, 191 (1969)

3) Brash J.L., Lyman D.J., 3, 175 (1969)

4) Brash J.L., Ann NY Acad Sci, 516, 206 (1987)

5) Hirsh J., Brain E.A., "Hemostasis and Thrombosis: A Conceptual Approach", New York, 1979 (revised edition 1983)

6) Chanarin I., Brozovic M., Tidmarsh E., Waters D., "Blood and its Diseases", Churchill Livingstone, New York, 1976 (revised edition 1984)

7) Allen P., Kaplan M.D., Prog Haem Thromb, 4, 127 (1978)

8) Ogston D., Bennett B., Brit Med Bull, 34, 107 (1978)

9) Dyson R., "Cell Biology: A Molecular Approach", Boston, 1974

10) Dickerson R.E., Geis I., "Structure and Action of Proteins", R.E Dickerson and Irving Geis 1969

11) Creighton T.E., "Proteins: Structure and Molecular Properties", WH Freeman and Company, 1983

12) McGiveny R.W. "Biochemistry: A Functional Approach", WB Saunders Company, 1970

13) Pauling L., Corey R.B., Branson H. R., Proc Natl Acad Sci US, 37, 205 (1951)

14) King J., " Protein and Nucleic Acid Structure and Dynamics", Benjamin/Cummings Publishing Company Incorporated, 1985

15) Alberts B., Bray D., Lewis O., Raff M., Roberts K., Watson J., "Molecular Biology of the Cell", Garland Publishing Company Incorporated, 114, 1983

16) Doolittle R.F., Sci Amer, 245, 126 (1981)

17) Privalov P.L., J. Mol Biol, 159, 665 (1982)

18) Henschen A., Luttspeich F., Kehl M., Southan C., Ann NY Acad Sci, 408, 28 (1983)

19) Neuberger A., Van Deenen, "Blood Coagulation", Elsevier Science Publishers B.V., 1986

20) Doolittle R.F., Nature, 280, 464 (1979)

21) Gardlund B., Hessel B., Marguerie G., Murano G., Blomback B., Eur J. Biochem, 77, 595 (1977) .

22) Doolitle R.F., Ann NY Acad Sci, 408, 13 (1983)

23) Doolittle R.F., Goldbaum D.M., Doolittle L.R., J. Mol Biol, 120, 311 (1978)

24) Cohen C., Szent-Gyorgyi A.G., J. Amer Chem Soc, 79, 248 (1957)

25) Mihalyi E., Biochim Biophys Acta, 102, 487 (1965)

26) Chan B.M.C., Brash J.L., J. Colloid Interface Sci, 84, 263, (1981)

27) Hall C.E., Slater H.S., J. Biophys Biochem Cytol, 5, 11 (1959)

28) Fowler W., Erickson H., J. Mol Biol, 134, 241 (1979)

29) Norton P., Slayter H., Proc Natl Acad Sci, 78, 1661 (1981)

30) Mosesson M., Hainfeld J., Wall J., Haschemeyer R., J. Mol Biol, 153, 695 (1981)

31) Adamson A.W., "Physical Chemistry of Surfaces", New York: Wiley 1983 (4th edition)

32) Kipling J.J., " Adsorption from Solutions of Non electrolytes, New York: Academic Press 1965

33) Brash J.L., Davidson V.J., Thromb Res, 9, 249 (1976)

34) Lundstrom I., J. Theor Biol, 110, 195 (1984)

35) Beissinger R.L., Leonard E.F., J. Colloid Interface Sci, 85, 521 (1982)

36) Sevastianov V.I., Tseytlina E.A., Volkov A.V., Shumakov V.I., Trans Am Soc Artif Intern Organs, 30, 137 (1984)

37) Koutsoukos P., Norde W., Lyklema J., J. Colloid Interface Sci, 71, 350 (1979)

38) Koutsoukos P., Norde W., Lyklema J., J. Colloid Interface Sci, 95, 385 (1983)

39) Koutsoukos P., Norde W., Lyklema J., J. Colloid Interface Sci, 112, 447 (1986)

40) Grannis G.F., Clin Chem, 16, 486 (1970)

41) Nielsen H., Weeke, Clin Chim Acta, 35, 281 (1971)

42) Putnam F.W., "The Plasma Proteins, Vol 2", Academic Press London, 1975

43) Chan B.M.C., Thesis, McMaster University, 1979

44) Chan B.M.C., Brash J.L., J. Colloid Interface Sci, 82 (1981)

45) Voegel J.C., Dejardin Ph., Strasser C., De Baillou N., Schmitt A., Coll Surf, 25, 139 (1987)

46) Donovan J.W., Mihalyi E., Proc Nat Acad Sci, 71, 4125 (1974)

47) Medved L.V., Gorkun O.V., Privalov P.L., FEBS Lett, 161, 291 (1983)

48) Privalov P.L., Adv Prot Chem, 33, 167 (1979)

49) Tanford C., Adv Prot Chem, 23, 218 (1968)

50) Thompson J.M., "Blood Coagulation and Haemostasis", Longman Grosys Limited 1985

51) Mandle R. Jr., Colman R.W., Kaplan A.P., Proc Natl Acad Sci, 73, 4179 (1976)

52) Scott C., Colman R.W., J. Clin Invest, 65, 413 (1980)

53) Schmaier A.H., Silver L., Adams A.L., Fischer G.C., Munoz P.C., Vroman L., Colman R.W., Thromb Res, 33, 51 (1984)

54) Jacobsen S., Kriz M., J. Pharmacol, 29, 25 (1967)

55) Kato H., Nagasawa S., Iwanaga S., Meth Enzymol, 80, 172 (1981)

56) Kerbiriou D.M., Griffin J.H., J. Biol Chem, 254, 12020 (1979)

57) Eylar E.H., J. Theor Biol, 10, 89 (1965)

58) Cohn E.J., Hughes W.L. Jr., Weare J.H., J. Am Chem Soc, 69, 1753 (1947)

59) Brown J.R., Fed Proc Amer Soc Exp Biol, 33, 1389 (1974)

60) Peters T. Jr., Adv Clin Chem, 13, 137 (1970)

61) Brash J.L., Thibodeau J.A., J. Biomed Mat Res, 20, 1263 (1986)

62) Pruzanski W., Ogryzlo M.A., Adv Clin Chem, 13, 342

63) Vroman L., Adams A., Fischer G., Munoz P., Blood, 55, 156 (1980)

64) Vroman L., Adams A.L., J. Biomed Mat Res, 3, 43 (1969)

65) Vroman L., Adams A.L., J. Colloid Interface Sci ,111, 391 (1986)

66) Uniyal S., Brash J.L., Thromb Haem, 47, 285 (1982)

67) Brash J.L., ten Hove P., Thromb Haem, 51, 326 (1984)

68) Horbett T.A., Thromb Haem, 51, 174 (1984)

69) Wojciechowski P., ten Hove P., Brash J.L., J. Colloid Interface Sci, 111, 455 (1986)

70) Grinnell F., Feld M.K., J. Biol Chem, 257, 4888 (1982)

71) Breemhaar W., Brinkman E., Biomat, 5, 269 (1984)

72) Cooper P.N., "Introduction to Nuclear Radiation Detectors", Cambridge University Press 1986

73) Chase G.D., "Principles of Radioisotope Methodology", 1962 by Grafton D., Chase

74) Snell A., "Nuclear Instruments and their Uses", John Wiley and Sons 1962

75) Birks J.B., "Scintillation Counters", London Pergamon Press Limited 1953

76) Krane K.S., "Introductory Nuclear Physics", John Wiley and Sons 1988

77) McFarlane A.S., J. Clin Invest, 42, 346 (1963)

78)Harwig, J. Nucl Med, 16, 757 (1975)

79) Ardaillou M.J., Larrieu M.J., 5, 327 (1974)

80) Contreras M.A., Bale W.F., Spar I.L., Meth Enzymol, 92, 277 (1983)

81) Doran D.M., Spar I.L., J. Immun Meth, 39, 155 (1980)

82) Marchalonis J.J., Biochem J., 113, 299 (1969)

83) Thorell J.I., Johansson B.G., Biochim Biophys Acta, 251, 363 (1971)

84) Regoeczi E., "Iodine-Labeled Plasma Proteins, Vol 1 CRC Press", CRC Press Incorporated 1984

85) Baszkin A., Deyme M., Perez E., Proust J., Am Chem Soc Symp Series (1987)

86) Pefferkorn E., Nabzar L., Carroy A., J. Colloid Interface Sci, 106, 94 (1985)

87) Aptel J.D., Thomann J.M., Voegel J.D., Schmitt A., Bres E.F., Coll Surf, 32, 159 (1988)

89) Grant W.H., Smith L.E., Stromberg R.R., J. Biomed Mater Sci, 11, 33 (1977)

90) Van Der Scheer A., Feijen J., Elhorst J.K., Krugers-Dagnea P., Smolders C.A., J. Colloid Interfac Sci, 66, 136 (1978)

91) Horbett T.A., J. Biomed Mater Res, 15, 673 (1981)